

Study of Solitons and Vortex Formation in Dense Quantum Plasmas



By

Shahida Nargis

Department of Mathematics
Quaid-i-Azam University, Islamabad
PAKISTAN
(2011)

Study of Solitons and Vortex Formation in Dense Quantum Plasmas



By

Shahida Nargis

Supervised by

Prof. Dr. Muhammad Ayub

Department of Mathematics
Quaid-i-Azam University, Islamabad
PAKISTAN
(2011)

Study of Solitons and Vortex Formation in Dense Quantum Plasmas

By

Shahida Nargis

A Thesis

Submitted in the Partial Fulfillment of the
Requirements for the Degree of

**DOCTOR OF PHILOSOPHY
IN
MATHEMATICS**

Supervised by

Prof. Dr. Muhammad Ayub

Department of Mathematics
Quaid-i-Azam University, Islamabad
PAKISTAN
(2011)

DECLARATION

I **Miss. Shahida Nargis** D/O **Mr. Abdul Ghafur Mirza** Registration No. 03140613001, a student of Doctor of Philosophy at Quaid-i-Azam University, Islamabad Pakistan, do hereby solemnly declare that the thesis entitled “**Study of Solitons and Vortex Formation in Dense Quantum Plasmas**” submitted by me in partial fulfillment of the requirements for Doctor of Philosophy degree in Mathematics is my original work and has not been submitted and shall not, in future, be submitted by me for obtaining any degree from this or any other University or Institution.

Date: _____

Signature: _____
(Shahida Nargis)

FORWARDING SHEET

The thesis titled **“Study of Solitons and Vortex Formation in Dense Quantum Plasmas”** submitted by **Miss. Shahida Nargis** in partial fulfillment of the requirement for the Ph.D. degree in Mathematics has been completed under my guidance and supervision. I am entirely satisfied with the quality of the research work done by the student.

Date: _____

Signature: _____.

Prof. Dr. M. Ayub (Supervisor)
Chairman
Department of Mathematics,
Quaid-i-Azam, University,
Islamabad, Pakistan.

**Dedicated
to
My Beloved Mother
“Syeda Nargis Parveen”
and
My Respected Father
“Abdul Ghafur Mirza”**

List of Publications

- 1) Ion-acoustic Vortices in a Nonuniform, Dissipative Quantum Magnetoplasma with Sheared Ion Flows
Physics of Plasmas, **15**, 122305 (2008)
(W. Masood, A. M. Mirza and **Shahida Nargis**)
- 2) Dust-acoustic Vortices in an Inhomogeneous Quantum Plasma with Dissipation and Sheared Dust-Flows
Physics of Plasmas, **15**, 103703 (2008)
(W. Masood, A. M. Mirza, and **Shahida Nargis**)
- 3) Ion-acoustic Vortices in Inhomogeneous and Dissipative Electron-Positron-Ion Quantum Plasmas
Physics of Plasmas, **16**, 042308 (2009)
(W. Masood, A. M. Mirza, **Shahida Nargis** and M. Ayub)
- 4) Propagation and Stability of Quantum Dust-Ion-Acoustic Shock Waves in Planar and Nonplanar Geometry
Physics of Plasmas, **16**, 013705 (2009)
(W. Masood, S. Siddiq, **Shahida Nargis** and A. M. Mirza)
- 5) Revisiting Coupled Shukla-Varma and Convective Cell Modes in Classical and Quantum Dusty Magnetoplasma
J. Plasma Physics, **76**, 547 (2010)
(W. Masood, A. M. Mirza and **Shahida Nargis**)
- 6) Electron-Acoustic Vortices in Multicomponent Magnetoplasma
Physics of Plasmas, **17**, 054505 (2010)
(Q. Haque, Arshad M. Mirza and **Shahida Nargis**)

Publication in Conferences Proceedings

- 7) National Symposium on Frontiers in Physics, February (2011) at GCU, Lahore, Pakistan, Invited talk on “Ion-acoustic Vortex Formation in Dense Magnetoplasma”, by **Shahida Nargis**, W. Masood and A. M. Mirza.

Acknowledgements

All praises to **Almighty Allah**, the benevolent and most merciful, who enabled me to complete this research work successfully. I offer Salaam to the **Holy Prophet Hazrat Muhammad (S.A.W.W)** who is a blessing for the world.

First and foremost, I want to express my deepest gratitude to my respectable teacher and supervisor **Prof. Dr. M. Ayub**, the Chairman Mathematics Department, for providing me invaluable guidance during the research work. His sympathetic attitude encourages me to complete this work.

Very special thanks to Dr. W. Masood, Theoretical Plasma Physics Division, Nilore, Pakistan and Dr. A. M. Mirza, Physics Department, Quaid-i-Azam University, Islamabad for their cooperation. My heartiest thanks to Dr. Babur, who helped me very sincerely. My immense gratitude goes to Drs. Sikandar, Nasir and Anwar.

My deepest gratitude to all my teachers for their valuable guidance throughout my coursework. I am very thankful to my teacher Madam Gal-e-Farazana, for her guidance to reach this goal.

Finally, my deepest sense of acknowledgement goes to my loving sisters Nadia, Farah, Mona and my brother Imran, who always prayed for my success in every aspects of life. Finally, I am very thankful to my university friends Naela and Javed for their moral support and encouragement which enabled me to complete this work.

(Shahida Nargis)

ABSTRACT

By employing quantum hydrodynamic model, the nonlinear dynamics of ion-acoustic waves in a collisional, nonuniform quantum magnetoplasma is investigated in the presence of ion sheared flow. It is shown that the parallel ion shear flow can drive the quantum ion-acoustic wave unstable, in the linear case. Whereas, in the nonlinear case, possible stationary solutions of the nonlinear set of equations is obtained in the form of various types of vortices. It is shown that the inclusion of the quantum statistical and Bohm potential terms significantly modify the scale-lengths of nonlinear structures. It is pointed out that this investigation can be applicable to dense astrophysical and laboratory plasmas where the quantum effects would play significant role.

It is shown that large amplitude ion-acoustic waves in a nonuniform electron-positron-ion plasma can give rise to monopolar, dipolar and vortex street type structures in dense quantum plasma with sheared ion flows.

Linear and nonlinear properties of quantum dust-acoustic waves are also studied in the presence parallel dust sheared flow for inhomogeneous dissipative dust-contaminated magnetoplasma. It is shown that in the linear case, the shear dust flow parallel to the external magnetic field can drive the quantum dust-acoustic wave unstable provided it has a negative slope. On the other hand, in the nonlinear case, stationary solutions of the nonlinear mode coupling equations which govern the dynamics of quantum dust-acoustic waves can be represented in the form of various types of nonlinear vortex structures. Again, in this case, we found that the inclusion of quantum statistical and Bohm potential terms significantly modify the scale-lengths of the vortex structures.

We have also revisited the coupled Shukla-Varma and convective cell mode for classical and quantum dusty magnetoplasma. We found that the inclusion of electron thermal effects modify the classical coupled Shukla-Varma and convective cell mode. We also discuss how the quantum statistical and Bohm potential terms can be incorporated in the said mode.

The dust-ion-acoustic solitons and shock waves are also investigated in a nonuniform quantum dusty plasma case by employing the quantum hydrodynamic model. By using the small amplitude perturbation expansion method, KdV and KdVB types of equations are derived. The dissipation is introduced by taking into account the kinematic viscosity among the plasma constituents. Our numerical results show that the strength of

the quantum dust-ion-acoustic shock wave is maximum for spherical, intermediate for cylindrical and minimum for the planar geometry case. The effects of quantum Bohm potential, dust concentration and kinematic viscosity on the quantum dust-ion-acoustic shock structure are also investigated. Finally, the temporal evolution of dust-ion-acoustic KdV solitons and Burger shocks are also investigated by putting the dissipative and dispersive coefficients equal to zero. The effects of quantum Bohm potential on the stability of dust-ion-acoustic shock is also investigated. It is pointed out that the relevance of present investigation might be in microelectronic devices as well as in dense astrophysical plasmas.

Contents

1	Introduction	5
1.1	Characteristics of Dense Plasmas	8
1.2	Layout of the Thesis	16
2	Model Equations for Quantum Plasmas	18
2.1	Schrödinger-Poisson Model	18
2.2	Wigner-Poisson Model	20
2.3	Drift-Approximation	22
3	Quantum Ion-Acoustic Vortices in a Nonuniform Electron-Ion Plasma	25
3.1	Introduction	25
3.2	Nonlinear Equations	28
3.2.1	Linear dispersion relation	31
3.2.2	Nonlinear analysis	32
3.3	Summary	38
4	Quantum Ion-Acoustic Vortices in Electron-Positron-Ion Plasmas	39
4.1	Introduction	39
4.2	Governing Nonlinear Equations	41
4.2.1	Linear analysis	45
4.2.2	Nonlinear solutions	46

4.3	Summary	50
5	Dust-Acoustic Vortices and Shukla-Varma Mode in Quantum Plasma	52
5.1	Introduction to Dusty Plasma	53
5.1.1	A simple derivation of dust-acoustic mode	56
5.1.2	Dust ion-acoustic mode	57
5.2	Nonlinear Model for Quantum Dust-Acoustic Waves	59
5.2.1	Dispersion relation	61
5.2.2	Nonlinear analysis	62
5.2.3	Summary	67
5.3	Shukla-Varma and Convective Cell Mode in Quantum Dusty Plasma . .	68
5.3.1	Introduction	68
5.3.2	Shukla-Varma and convective cell mode: classical case	70
5.3.3	Shukla-Varma and convective cell modes: for quantum plasmas .	73
5.3.4	Summary	74
6	Quantum DIA Shock and Solitons in Planar and Nonplanar Cases	76
6.1	Introduction	77
6.2	Dust-Acoustic Solitary Waves	78
6.3	Dust Acoustic Solitary Waves in Cylindrical and Spherical Geometry . .	81
6.4	Model Equations for Planar Geometry Case	83
6.5	KdV Equation for Plane Geometry Case	85
6.6	KdVB Equation for Plane Geometry Case	86
6.7	Model Equations for Nonplanar Geometry Case	88
6.8	KdVB and KdV Equations for Nonplanar Geometry	88
6.9	Results	90
6.10	Stability Condition of DIA Shocks	94
6.11	Summary	95

List of Figures

1-1	Phase diagram of plasma in thermodynamic equilibrium in space and laboratory plasmas.	10
3-1	A vortex chain type solution obtained by solving equation (3.19) for a uniform density and dense astrophysical plasma case.	34
3-2	3-D vortex profile obtained by solving equation (3.19) by using the parameters as used in Fig. (3-1).	35
3-3	Two dimensional contour plot of Φ by solving equations (3.23) and (3.24) for some typical plasma parameters as given in the text.	37
4-1	Plot of vortex chains profile obtained from Eq. (4.20) for some dense astrophysical parameters in e-p-i plasmas.	48
4-2	3-D vortex profile obtained by solving equation (4.20) for the parameters used in Fig. (4-1).	48
4-3	Two dimensional view of Φ obtained by solving equations (4.24) and (4.25) for the same plasma parameters as taken in Fig. (4-1).	50
5-1	Carbon grains grown in a plasma having size of the order of 10nm to $1\mu\text{m}$ [94].	54
5-2	A vortex chain profile is plotted by solving equation (5.27) for dense astrophysical plasma parameters.	64
5-3	Two dimensional contour plot of Φ obtained by solving equations (5.31) and (5.32) for the same parameters as given in the text.	66

5-4	Variation of the normalized growth rate as a function of k_y of coupled SV and convective cell mode for $n_{i0} = 1.43 \times 10^{26} \text{ cm}^{-3}$, $n_{d0} = 0.43 \times 10^{26} \text{ cm}^{-3}$, $Z_d = 10^3$, the external magnetic field $B_0 = 10^{13} \text{ Gauss}$ $k_{ne} = 10^4 \text{ cm}^{-1}$ and $k_d = 10 k_{ne}$ with $k_z = 0.1 k_{ne}$, where $k_{ne}(k_d)$ represents the electron (dust) scale-length.	75
6-1	Numerical results by solving equation (6.38) for different values of ν , with $H_e = 0.5$, $p = 0.7$, and $\eta_0 = 0.5$	90
6-2	Solution of equation (6.38) numerically for different positron concentrations: $p = 0.5-0.7$, where $\nu = 2$, $H_e = 0.5$, and $\eta_0 = 0.5$	91
6-3	Numerical solution of (6.38) for various values of $H_e = 0.05$ and 0.5 , where $\nu = 2$, $p = 0.7$ and $\eta_0 = 0.5$	92
6-4	Solution of equation (6.38) numerically for various values of $H_e = 0.05$ and 0.5 , where $\nu = 2$, $p = 0.7$ and $\eta_0 = 0.5$	92
6-5	Solution of Eq. (6.38) for $\nu = 2$ and for various time scale $\tau = -9, -6, -3$, and $H_e = 0.5$, $p = 0.7$ with $\eta_0 = 0.5$	93
6-6	Formation of dust-ion-acoustic solitons for various time scale as a function of ξ for $\nu = 2$ by taking $C = 0$ in Eq. (6.38) for time $\tau = -9, -6, -3$, and $H_e = 0.5$, and $p = 0.7$	93
6-7	The solution of quantum DIA Burgers equation (6.38) for various time scale: $\tau = -9, -6, -3$ and by taking $B = 0$ in spherical case ($\nu = 2$), with $H_e = 0.5$, $p = 0.7$ and $\eta_0 = 0.5$	94

Chapter 1

Introduction

A plasma can be defined as a quasineutral gas of charged and neutral particles exhibiting collective behavior. The charged particles interact with one another through the long-range Coulomb type force. Classical plasmas are characterized by high temperature and low densities which can be found in interplanetary or interstellar media as well as in laboratory produced plasmas. One of the fundamental characteristics of plasma is its ability to shield out electric potential that is applied to it. The shielding distance is known as electron Debye length $\lambda_{De} \equiv \sqrt{k_B T_e / 4\pi n_{e0} e^2}$ in an electron-ion plasma, where $T_e(n_{e0})$ is the electron temperature (number density), and k_B is the Boltzmann constant. On the other hand, dense quantum plasmas consist of high density and low-temperature plasmas with pressures in excess of a megabars. Classical plasmas switches to a dense plasma as soon as plasma condenses at sufficiently low-temperatures such that the average distance between the two nearest neighbors become comparable or smaller than their de Broglie's wavelength. In quantum plasmas, the degenerate plasma particles such as ions and electrons follow Fermi-Dirac type distribution. The plasma particles occupy all the available energy levels, from the ground state to the higher energy levels such that in each energy state no more than two Fermions can occupy the same state. This is due to the Pauli exclusion principle. The high-density, low-temperature quantum plasmas obeying the Fermi-Dirac distribution are quite different from the so called classical low-density,

high-temperature plasmas which obeys Maxwell-Boltzmann type distribution. Classical plasmas usually deals with a low-density and high-temperature plasmas, wherein the quantum effects are not significant. On the other hand, for low-temperatures and high-density case, the quantum effects begin to play important role. In this case, an additional scalelength is introduced, which is known as the de Broglie wavelength $\lambda_{Bj} = h/(2\pi m_j v_j)$, where j represents species index. It represents the wavelength associated with the plasma particle, the quantum effects would be more significant for large wavelengths compared to the interparticle spacing. There is a lot of interest in quantum plasma study during the last few years due to its applications in various fields namely in microelectronic device [1], in dense astrophysical environments [2, 3] (e.g., in the interior of Jovian planets, in white dwarfs, and in neutron stars), free electrons in metals [4], highly compressed plasma produced due to launching of strong shock waves through matter, dense pinch plasmas and in inertial confinement fusion produced plasmas due to the interaction of high power lasers or ion beams on solid targets can acquire densities of the order of 10^{26} cm^{-3} as well as in dusty plasmas [5, 6, 7]. It has also applications in spintronics, nanotubes, quantum wells and quantum dots etc.

There are two well-known mathematical formulations in quantum plasmas, namely the Wigner-Poisson and the Schrödinger-Poisson. These two approaches are generally employed to describe the statistical and hydrodynamic behavior of charged species at quantum scales in dense plasmas. These two approaches are the quantum analogue of kinetic and fluid treatments of classical plasmas, respectively. The two approaches have been elaborated at length by Manfredi [8]. The quantum hydrodynamic (QHD) model is based on the Schrödinger-Poisson formulation, which includes the quantum statistical pressure and quantum force term essentially representing quantum tunneling effect of electrons through the Bohm potential. Number of linear dispersion relations are derived and analyzed for quantum plasmas [6, 7, 9, 10]. The QHD models are simple, numerical efficient, in these models one uses directly the macroscopic variables of interest alongwith appropriate boundary conditions for a given problem. However, one

of the shortcoming of QHD model is that wave particle interaction or simply the Landau damping cannot be explained using QHD model equations which are derived from the Wigner [11] distribution function.

For better understanding of quantum plasmas and its applications, it is worthwhile to first briefly review the historical developments. More than four decades ago, Kilimonovich & Silin [12] and Bohm and Pines [13, 14] has studied the dynamics of quantum plasma and presented dispersion relation of electron plasma oscillations in a dense quantum plasma. The electrons, ions and holes are assumed degenerate (obeying Fermi-Dirac distribution), whereas the ions are assumed to be cold and classical (obeying Maxwell-Boltzmann distribution). Electromagnetic properties of electron gas for quantized magnetic field has been discussed for dense quantum electron plasma with a background of fixed ions [15, 16]. By employing, many particle kinetic model, the quantum electrodynamic properties of cold plasma [17] has been investigated. Using covariant Wigner function, relativistic properties of quantum plasmas were investigated [18].

The non-relativistic quantum plasmas can be studied with the help of Schrödinger description whereas, collective behavior of relativistic quantum plasmas can be investigated with the help of quantum field theory [19]. Manfredi [8] has developed quantum hydrodynamic model for the electron gas which consists of electron continuity and momentum balance equations. In the electron momentum conservation equation or simply the equation of motion of electron fluid, the quantum effects appears in the form of Bohm potential term. The quantum statistical and quantum Bohm potential introduces new type of pressure effects which has pure quantum origin. Several authors have found new modes and instabilities by using quantum hydrodynamic model and highlighted the importance of Bohm potential and quantum statistical pressure in dense plasma systems [20, 21, 22]. Furthermore, quantum magnetohydrodynamic (QMHD) model has also been proposed in recent years [23, 24]. Apart from linear waves, some nonlinear properties has also been investigated such as the vortex and soliton and shock wave formation in quantum plasmas [25], trapping in quantum plasmas, the wave particle interaction for dense

quantum plasmas [26, 27] etc. It is found that electrostatic and electromagnetic waves are significantly modified in the presence of external magnetic field. Several new modes and instabilities found to exist due to electron spin magnetic moment and quantized Landau energy levels of highly degenerate fermions in the presence of strong background magnetic field [28, 29].

By employing Pauli equation, a multifluid model for Fermionic electron plasma has been derived so as to investigate the spin and quantum electrodynamic effects on quantum plasma using Maxwell equations [30, 31]. Various limits are identified wherein the Bohm potential, Fermi statistical pressure, spin and quantum electrodynamic effects play important role. New dispersion relation for Alfvén waves has been derived by considering spin-up and spin-down electrons as two different types of electron fluids [32]. Quantum effects are also recognized in solid state systems such as in dense metallic systems, nanostructures, quantum dots, quantum wires, quantum wells, quantum diodes, nanotubes, and in quantum optics [33, 34, 35] etc.

1.1 Characteristics of Dense Plasmas

As discussed earlier in the introduction that the quantum mechanical effects becomes relevant when the de Broglie wavelength becomes comparable to the average distance between the particles $\langle r \rangle = (r_k - r_l) \propto n^{3/2}$, where n represents the number density of plasma particles and $r_k (r_l)$ is the position of $k(l)$ -th particle. The thermal de Broglie wavelength of the charged particles can be written as

$$\lambda_{Bj} = \frac{h}{\sqrt{2\pi m_j k_B T_j}} \quad (1.1)$$

where h is the Planck's constant, j is the species index (j equals to e for electrons, and i for ions) and m_j is the mass of j -th species. It is evident from the above expression that the quantum effects would be more pronounced for lighter particles namely the electrons as compared to massive ones such as ions. Due to this reason, the ions would be treated

classically in most of calculations of electron-ion dense quantum plasmas. The condition for which quantum effects would be important if the temperature of the system (T) is less than the Fermi temperature T_{Fj} [8], where

$$T_{Fj} \equiv \frac{h^2}{8\pi^2 m_j k_B} (3\pi^2)^{2/3} n_j^{2/3} \quad (1.2)$$

To classify a classical and quantum plasma, let us introduce a dimensionless parameter χ_j , given as

$$\chi_j = \frac{T_{Fj}}{T} = \frac{1}{2} (3\pi^2)^{2/3} (n_j \lambda_{Bj}^3)^{2/3} \quad (1.3)$$

When the plasma temperature T becomes smaller than the Fermi temperature T_{Fj} or simply when $\chi_j \geq 1$, the quantum effects would be dominant [36]. On the other hand, when $T \gg T_{Fj}$ or $\chi_j \leq 1$, the plasma would be in the classical domain and in this case it would be governed by the Maxwell-Boltzmann type of distribution,

$$f_{MB}(\varepsilon) = A \exp [-(\varepsilon - \mu) / k_B T] \quad (1.4)$$

where A is normalization constant. For $\chi_j \geq 1$ it would follow Fermi-Dirac distribution,

$$f_{FD}(\varepsilon) \propto \frac{1}{(\exp [(\varepsilon - \mu) / k_B T] + 1)} \quad (1.5)$$

where μ is the chemical potential and ε is energy variable.

For quantum plasmas, there is another dimensionless useful parameter Γ_Q , which is known as the quantum coupling parameter. It is defined by the ratio of Coulomb type of interaction energy $E_{int}(= e^2 n_j^{1/3})$ and the Fermi energy $E_{Fj}(= k_B T_{Fj})$, i.e.,

$$\Gamma_Q = \frac{E_{int}}{E_{Fj}} = \frac{2}{(3\pi^2)^{2/3}} \frac{e^2 m_j}{\hbar^2 n_j^{1/3}} \sim \left(\frac{\hbar \omega_{pj}}{2 k_B T_{Fj}} \right)^2 \quad (1.6)$$

where $\hbar = h/2\pi$, ω_{pj} is the plasma frequency for j th-species and $\hbar \omega_{pj}$ represents the plasma energy due to the local oscillations of shielded plasma particles [8, 36]. It is

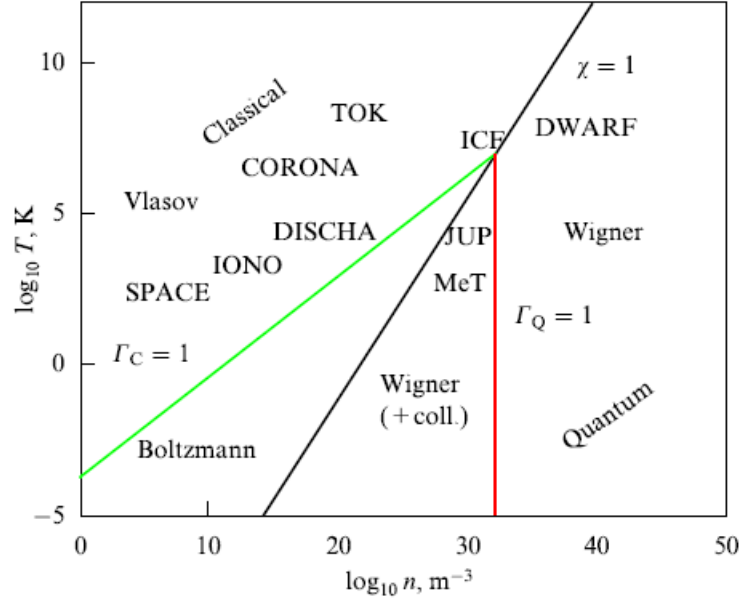


Figure 1-1: Phase diagram of plasma in thermodynamic equilibrium in space and laboratory plasmas.

very interesting to notice here that one can retrieve the classical results by replacing T_{Fj} with T and λ_{Fj} with λ_D . One can also define a parametric regime for which the quantum coupling parameter $\Gamma_Q > 1$ and it is known as *quantum collisional* or strongly coupled plasma. On the other hand, when $\Gamma_Q < 1$, the plasma is termed as weakly coupled or *quantum collisionless* plasma. It is obvious that *dense plasmas* show more collective behavior as compared to low density plasmas. Fig. (1-1), shows a plot of plasma temperature viz. number density for various plasma systems, namely the ionospheric plasma (IONO), space plasma (SPACE), solar corona (CORONA), electric discharge (DISCHA), tokamak plasma (TOK), inertial confinement fusion (ICF), metal clusters (MET), Jupiter's core (JUP) and white dwarf star (DWARF) [8].

The pioneering work of Bohm & Pines and Pines [13, 14] has opened up the doors for several researchers to study various aspects of dense electron-ion (e-i), electron-positron (e-p-i) and dusty quantum plasmas. For instance, by employing statistical approach,

various thermodynamical properties of highly degenerate electron-ion plasmas has been investigated for a broad range of number densities and temperatures both analytically [37] as well as numerically [38]. Ultra-high density and strongly coupled plasmas has been discussed in some detail in Ref. [39]. The QHD model has also been employed to study the propagation of linear and nonlinear waves in inhomogeneous quantum plasmas. For instance, new electron drift wave in dense quantum magnetoplasma has been derived by Shukla and Stenflo [40] and found that the electron Bohm potential term significantly modify the electron drift mode. El-Taibany and Wadati [11] studied the dynamics of nonlinear quantum dust-acoustic waves in a nonuniform quantum dusty plasma and found that the formation of solitons manifest a dependence on a critical value of plasma parameters unlike a homogeneous plasma. Haque and Mahmood [41] studied the linear and nonlinear drift-waves in inhomogeneous quantum plasmas with neutrals in the background. The authors of Ref. [41] found that the quantum corrections appreciably modify the drift-solitons and shocks in quantum magnetoplasmas.

Quite recently, Haque and Saleem [42] proposed that monopolar and dipolar quantum vortices could appear in a uniform dense e-i-plasmas. *We have extended the said work by considering a nonuniform, dissipative quantum electron-ion plasma with sheared ion flow parallel to the ambient magnetic field by employing the quantum hydrodynamic (QHD) model. Linear as well as nonlinear properties of quantum ion-acoustic waves are investigated [43]. We found that parallel ion shear flow can drive the quantum ion-acoustic wave unstable. Stationary solutions of the nonlinear equations that govern the quantum ion acoustic waves are also obtained. It is found that electrostatic monopolar, dipolar, and vortex street type solutions can appear in such a plasma. It is observed that the inclusion of the quantum statistical and Bohm potential terms significantly modify the scalelengths of these structures. The relevance of present investigation in the dense astrophysical plasma is also pointed out where the quantum effects might play very important role.*

The electron-positron plasmas have been observed to behave differently in sharp contrast to the typical electron-ion (e-i) plasmas [11, 24]. One of the important feature of

electron-positron (e-p) plasma in comparison with electron-ion plasma is the same mass but equal and opposite charge of electron-positron plasma. Electron-positron plasmas have been observed in active galactic nuclei [44], in pulsars magnetosphere [45], in the polar regions of neutron stars [46], as well as in the intense laser fields [47]. Electron positron plasma is also believed to exist in the early universe [48] as well as at the centre of our own galaxy [49]. Electron-positron-ion plasmas have also been a subject of investigation in quantum plasmas. For instance, Ali *et al.* [50], investigated linear and nonlinear ion-acoustic waves in an unmagnetized electron-positron-ion (e-p-i) quantum plasma. The authors derived the Korteweg-de-Vries (KdV) equation for quantum e-p-i plasma and an energy equation for arbitrary amplitude ion-acoustic waves and discussed the relevance of their results. Mushtaq and Khan [51] investigated the characteristics and stability of quantum ion-acoustic solitary waves in an e-p-i plasma with transverse perturbations and found that the quantum corrections significantly modify the linear and nonlinear propagation characteristics of ion-acoustic waves. Masood *et al.* [52], explored the quantum ion-acoustic wave propagation in a magnetized e-p-i plasma and found that the soliton structure of the ion-acoustic wave depends upon quantum statistical pressure, concentration of positrons, strength of magnetic field, and the propagation angle.

We have investigated linear and nonlinear properties of quantum ion-acoustic waves in a nonuniform, dissipative quantum plasma (composed of electrons, positrons, and ions) with sheared ion flow parallel to the ambient magnetic field, using hydrodynamic model for quantum plasma [53]. We found that ion acoustic waves becomes unstable for quantum plasma in the presence of parallel sheared ion flows for $|S_i| k_y > k_z$. Stationary solutions of the nonlinear equations that govern the quantum ion-acoustic waves are also obtained. It is found that electrostatic monopolar, dipolar, and vortex street type solutions can appear in such a plasma. It is observed that the inclusion of positron, quantum statistical, and Bohm potential terms significantly modify the scalelengths of these nonlinear structures.

A considerable interest among the plasma physicists arises in dusty plasma due to

the ubiquitous nature. A dusty plasma is loosely defined as a normal electron-ion plasma with an additional constituent of micron or submicron sized dust grains. We shall discuss in some detail dusty plasma and its characteristics in Chapter 5. Dusty plasma is quite different from multi species plasma because of the presence of extremely massive and highly charged dust grains, several new ultra-low frequency collective modes on completely different scale length may appear. In dusty plasmas, it is well known that the two normal modes of unmagnetized, weakly coupled plasmas are the dust-acoustic (DA) and dust-ion-acoustic (DIA) waves, respectively. These modes were theoretically predicted by Rao, Shukla and Yu [44], as well as by Shukla and Silin [45]. In the DA wave, the restoring force comes from the inertialess electrons and ions in the comparison with extremely massive dust grains while the dust mass gives the inertia. The frequency range of this wave is much lower and the phase velocity much smaller than the ion acoustic velocity. On the other hand, the phase velocity of the DIA wave is greater than both dust and ion thermal velocities. The inertia is provided by dust and ions while the restoring force comes from the electron pressure. Another way to view this mode is to treat dust as immobile. Both these modes have been detected in several dusty plasma experiments [46, 47, 48, 49]. Low-frequency dust ion-acoustic perturbations can propagate in cosmic plasma environments as well as in dusty plasma of Earth's mesosphere. They also contribute towards the low-frequency noise in the F-ring of Saturn [45]. It also occurs in the candle flame, zodiacal light, in the lightening of thunderstorms, in the eruption of volcanoes. It has also several applications in industry such as in microelectronics [54] and carbon nanotubes [55]. Dust particles has also been observed in fusion plasmas [56] due to sputtering of wall material of tokamak device which is made of beryllium and carbon tiles. Ikezi [57] predicted theoretically the Coulomb crystallization of dust charge grains in (1986) which was later experimentally verified with the observation of dust plasma crystal (DPC) formation [58]. The phase transition in dust plasma crystals has been observed in several experiments [59]. It is generally believed that a major boost to the field of dusty plasma came after the discovery of DAW and DPC formation. Since the

density of dust plasma crystals is very high, so one would expect quantum effects play very crucial role.

Haas [24] presented QHD model for dense quantum plasma and discussed quantum ideal magnetostatic equilibria. Shukla and Stenflo [40] reported two new drift-modes in nonuniform ultracold magnetoplasmas. When dusty plasma cooled down to extremely low-temperatures, the de-Broglie wavelength of the charged particles become comparable to the dimensions of the system, then the ultra-cold dusty plasma behaves like a Fermi gas and consequently the quantum effects are expected to play central role. Shukla and Ali [6] derived a linear dispersion relation for the quantum dust-acoustic waves by considering ultra-cold quantum dusty plasma using QHD model. Later Ali and Shukla [60] investigated QDA solitary waves through Korteweg-de Vries (KdV) equation using QHD model. On the other hand, Taibany and Wadati [11] studied the nonlinear quantum dust-acoustic wave in a nonuniform dusty plasma in the ultracold plasma limit. By employing reductive perturbation method, they found the possibility of solitons formation for inhomogeneous quantum dusty plasma case. As discussed earlier that Haque and Saleem [42] found ion-acoustic vortex formation in a uniform dense quantum plasma. Whereas, *we have investigated [61] the coupled quantum drift-dust acoustic vortex formation in the presence of background density inhomogeneity as well as the sheared plasma dust flow parallel to the ambient magnetic field. We have also investigated [62] coupled Shukla-Varma (SV) and convective cell mode in classical and quantum inhomogeneous dusty magnetoplasmas. It is shown that the inclusion of electron thermal effects significantly modifies the original coupled SV and convective cell mode. The limiting cases are also discussed. It is shown that in the absence of electron pressure, the coupled SV and convective cell mode reduces to the original expression derived by Shukla and Varma [63, 64] in classical plasmas.*

It is well known that a nonlinear dispersive medium admits shock-like solutions. This happens due to the balance between the non-linearity (causing wave steepening) and dissipation (e.g., caused by viscosity, collisions, wave particle interaction, etc.). However,

when a medium has both dispersive and dissipative properties, then the propagation of small amplitude perturbations can be adequately described by Korteweg-de Vries-Burgers (KdVB) equation. The Burger term in the nonlinear wave equation arises when one takes into account the kinematic viscosity among the plasma constituents [65]. When the wave braking due to non-linearity is balanced by the collective effect of dispersion and dissipation, a monotonic or oscillatory dispersive shock wave is generated in a plasma [66].

We study the one-dimensional propagation of dust-ion-acoustic (DIA) shock waves in a quantum plasma in both planar and nonplanar geometries. When we put the dissipative coefficient equal to zero then we obtain standard equation for the quantum dust-ion-acoustic soliton in planar and nonplanar cases. The said equation has been numerically solved so as to study DIA soliton formation for spherical geometry case for various time scales. We found that the height of the soliton decreases with the increase of time. Furthermore, when the amplitude of the soliton decreases its width increases. In this model, we consider immobile dust (either negative or positive), dynamical ions and inertialess electrons. The dissipation is introduced by taking into account the kinematic viscosity among the plasma constituents. We use the QHD model and for small amplitude approximation, and derive KdVB equation for DIA shock wave in a quantum plasma in the nonplanar geometry. The effects of quantum corrections on the stability of KdVB equation are also investigated for the first time in this work [67].

Dense quantum plasma physics is very rich and promising field of plasma physics. The research work is motivated by its number of applications in plasma assisted carbon nanostructures, nanotechnologies as well as in the x-ray sources. It is essential to understand the fundamentals of various collective processes in quantum plasmas. How various plasma phenomena evolve in high-density, low-temperature regime is an active area of research. During the past few years, lot of research work has been done in this important field, especially in the nonlinear effects of dense quantum plasma system by using QHD model. A detailed analysis would give us a guideline for deep understanding

the origin of various nonlinear structure formation and collective motions in high-density, and low-temperature quantum plasmas.

1.2 Layout of the Thesis

The organization of the thesis is as follows: In chapter 1, historical developments and various characteristics of dense quantum plasmas alongwith their applications are briefly described.

The second chapter deals with the quantum hydrodynamic equations. Specifically, we discuss in some detail simple derivation of quantum hydrodynamic (QHD) equations, which are extensively used to describe quantum plasmas, by using Schrödinger-Poisson and Wigner-Poisson model equations. Since, mostly plasma behave as a fluid, and in the presence of electric and magnetic fields, this charged fluid would experience various types of drift motions, a brief derivation of drift-approximation is thus presented in section 2.3.

Chapter 3 is devoted to study of linear and nonlinear properties of quantum ion-acoustic vortices in an inhomogeneous dissipative quantum magnetoplasma with sheared ion flows. Basic set of nonlinear equations for quantum electron-ion plasma are presented in subsection 3.2. New dispersion relation and various interesting limiting cases are presented in Sec. 3.2.1. In subsection 3.2.2, nonlinear analysis is presented and various types of vortex structures are shown to exist under certain approximations. Numerical results are presented and a comprehensive summary of new findings is given in summary section 3.3.

Chapter 4, deals with electron-positron-ion (e-p-i) plasmas. In the introduction section 4.1, we give a brief historical review of some important work in the field of classical and quantum e-p-i plasmas. Then in Sec. 4.2, we present governing model equations for quantum e-p-i plasma. Linear dispersion relation has been derived and discussed in subsection 4.2.1, and stationary nonlinear solutions are presented in subsection 4.2.2. Finally, in Sec. 4.3, we summarize the work.

In chapter 5, we consider dense dusty plasma. After a brief introduction and historical background to dusty plasma, some novel linear modes are reviewed, namely the dust-acoustic (DA) and dust-ion-acoustic (DIA) modes in subsections 5.1.1 and 5.1.2, respectively. Mathematical modeling of the governing nonlinear equations, to describe quantum dusty plasma, is presented in Sec. 5.2. The linear and nonlinear analysis is presented in Subsections 5.2.1 and 5.2.2, respectively. We finally, summarize the results in subsection 5.2.3. Then in Sec. 5.3, Shukla-Varma and convective cell modes are revisited for classical (subsection 5.3.2) and for quantum (subsection 5.3.3) dusty plasmas. The results are then summarized in subsection 5.3.4.

Chapter 6 is devoted to the study of solitary and shock waves in a multicomponent dusty plasma for planar and nonplanar geometries. In section 6.1, a brief history of solitary wave and KdV equation as well as shock waves as solutions of the Burger equation (or simply KdVB equation) are presented. We have reviewed classical dust-acoustic solitary waves in Sec. 6.2 for planar geometry and in Sec. 6.2 for nonplanar geometry. Whereas, in sections 6.4 and 6.5, we present model equations for quantum dust-ion-acoustic solitary and shock waves for planar geometry. Then in Sec. 6.6, we present KdV equation for nonplanar geometry and in Sec. 6.7, the KdVB equation for nonplanar case is presented for quantum dusty plasmas. Numerical results of KdV and KdVB equations are presented in Sec. 6.8. Stability conditions of dust-ion-acoustic shock waves are discussed in Sec. 6.9. Finally, in Sec. 6.10, we summarize the work.

Chapter 2

Model Equations for Quantum Plasmas

2.1 Schrödinger-Poisson Model

In this chapter, we shall very briefly review the Schrödinger-Poisson and Wigner-Poisson models for electrostatic, unmagnetized, collisionless quantum plasmas [36]. We may start with an ensemble of degenerate Fermions in dense plasmas. The Schrödinger equation for N -particles wave functions ψ_i which obeys N independent Schrödinger and Poisson's equations can be written as

$$i\hbar \frac{\partial \psi_i}{\partial t} = -\frac{\hbar^2}{2m} \frac{\partial^2 \psi_i}{\partial x^2} - (e\phi) \psi_i \quad (2.1)$$

$$\frac{\partial^2 \phi}{\partial x^2} = 4\pi e \left[\sum_{i=1}^N p_i |\psi_i|^2 - n_0 \right] \quad (2.2)$$

$$n_i(x, t) = \sum_{i=1}^N p_i |\psi_i|^2 \quad (2.3)$$

where $\hbar \equiv h/2\pi$, the subscript $i = 1, \dots, N$ and n_0 represents the number density of fixed ions and p_i represents the occupation probability of quantum mixture of states ψ_i .

By introducing the wave function

$$\psi_i = \sqrt{n_i(x, t)} e^{i \frac{\varphi_i(x, t)}{\hbar}} \quad (2.4)$$

where $n_i = |\psi_i|^2$, $m_i u_i = \partial_x \varphi_i$ and u_i represents the fluid velocity. Using the above equation, we get

$$i\hbar \partial_t \psi_i = -\sqrt{n_i(x, t)} e^{i \frac{\varphi_i(x, t)}{\hbar}} \partial_t \varphi_i + i\hbar e^{i \frac{\varphi_i(x, t)}{\hbar}} \partial_t \sqrt{n_i(x, t)} \quad (2.5)$$

Differentiating twice with respect to x , we get

$$\begin{aligned} \partial_x^2 \psi_i &= \frac{i}{\hbar} \sqrt{n_i} e^{i \frac{\varphi_i(x, t)}{\hbar}} (\partial_x^2 \varphi_i) + \left(\frac{i}{\hbar} \right)^2 \sqrt{n_i} (\partial_x \varphi_i) e^{i \frac{\varphi_i(x, t)}{\hbar}} (\partial_x \varphi_i) \\ &+ \frac{i}{\hbar} e^{i \frac{\varphi_i(x, t)}{\hbar}} (\partial_x \varphi_i) (\partial_x \sqrt{n_i}) + (\partial_x^2 \sqrt{n_i}) e^{i \frac{\varphi_i(x, t)}{\hbar}} + \frac{i}{\hbar} (\partial_x \sqrt{n_i}) e^{i \frac{\varphi_i(x, t)}{\hbar}} (\partial_x \varphi_i) \end{aligned} \quad (2.6)$$

Substituting Eqs. (2.5) and (2.6) in (2.1), we obtain the following result

$$\begin{aligned} &-\sqrt{n_i} e^{i \frac{\varphi_i(x, t)}{\hbar}} \partial_t \varphi_i + i\hbar e^{i \frac{\varphi_i(x, t)}{\hbar}} \partial_t \sqrt{n_i} = -\frac{\hbar^2}{2m} \left[\frac{i}{\hbar} \sqrt{n_i} e^{i \frac{\varphi_i(x, t)}{\hbar}} (\partial_x^2 \varphi_i) \right. \\ &+ \left(\frac{i}{\hbar} \right)^2 \sqrt{n_i} (\partial_x \varphi_i) e^{i \frac{\varphi_i(x, t)}{\hbar}} (\partial_x \varphi_i) + \frac{i}{\hbar} e^{i \frac{\varphi_i(x, t)}{\hbar}} (\partial_x \varphi_i) (\partial_x \sqrt{n_i}) \\ &\left. + e^{i \frac{\varphi_i(x, t)}{\hbar}} (\partial_x^2 \sqrt{n_i}) + \frac{i}{\hbar} (\partial_x \sqrt{n_i}) e^{i \frac{\varphi_i(x, t)}{\hbar}} (\partial_x \varphi_i) \right] - (e\phi) \psi_i \end{aligned} \quad (2.7)$$

Collecting the imaginary parts of Eq. (2.7) and using the definition of fluid velocity, we get

$$\frac{\partial n_i}{\partial t} + \frac{n_i}{2m} \partial_x^2 \varphi_i + \frac{1}{m} \partial_x \varphi_i \partial_x n_i = 0$$

or

$$\frac{\partial n_i}{\partial t} + \frac{\partial}{\partial x} (n_i v) = 0 \quad (2.8)$$

which is the desired continuity equation. Similarly, collecting the real parts of Eq. (2.7),

we obtain the following result

$$\frac{\partial \varphi_i}{\partial t} + \frac{1}{2m} (\partial_x \varphi_i)^2 = e\phi + \frac{\hbar^2}{2m\sqrt{n_i}} \partial_x^2 \sqrt{n_i}$$

Differentiating the above equation with respect to x and after simplification, we get

$$(\partial_t + v_i \partial_x) v_i = \frac{e}{m} \partial_x \phi + \frac{\hbar^2}{2m} \frac{\partial}{\partial x} \left(\frac{\partial_x^2 \sqrt{n_i}}{\sqrt{n_i}} \right) \quad (2.9)$$

where

$$v_i \frac{\partial v_i}{\partial x} = \frac{1}{m} \frac{\partial \varphi_i}{\partial x} \frac{\partial}{\partial x} \left(\frac{1}{m} \frac{\partial \varphi_i}{\partial x} \right)$$

Equation (2.9) represents an equation of motion for quantum fluid. The second term on the right hand side of Eq. (2.9) is the quantum Bohm potential term.

2.2 Wigner-Poisson Model

The quantum analogue of the Vlasov-Poisson model is the Wigner-Poisson model. For N identical fermions, the Schrödinger equation for N particles wave function can be expressed by the Slater determinant, which can be expressed as

$$\psi(q_1, q_2, \dots, q_N; t) = \frac{1}{\sqrt{N!}} \begin{vmatrix} \psi_1(q_1, t) & \psi_2(q_1, t) & \cdot & \cdot & \cdot & \psi_N(q_1, t) \\ \psi_1(q_2, t) & \psi_2(q_2, t) & \cdot & \cdot & \cdot & \psi_N(q_2, t) \\ \cdot & \cdot & \cdot & \cdot & \cdot & \cdot \\ \cdot & \cdot & \cdot & \cdot & \cdot & \cdot \\ \cdot & \cdot & \cdot & \cdot & \cdot & \cdot \\ \psi_1(q_N, t) & \psi_2(q_N, t) & \cdot & \cdot & \cdot & \psi_N(q_N, t) \end{vmatrix} \quad (2.10)$$

which shows that the total wave function vanishes if two rows are identical. This is in accordance with the Pauli exclusion principle which states that no two identical Fermions can occupy the same energy state. In the ultra-cold plasma limit, all the lower energy

states are fully occupied by electrons up a maximum energy state which is known as Fermi energy level. The Wigner distribution function satisfy the following equation in one-dimension,

$$\begin{aligned} \frac{\partial f_e}{\partial t} + v \frac{\partial f_e}{\partial x} = & -\frac{iem_e^3}{(2\pi)^3 \hbar^4} \int \int \exp \left[im_e (v - v') \frac{\lambda}{\hbar} \right] \\ & \times \left[\phi \left(x + \frac{\lambda'}{2} t \right) - \phi \left(x - \frac{\lambda'}{2} t \right) \right] f_e(x, v', t) d\lambda dv' \end{aligned} \quad (2.11)$$

where $\phi(x)$ is the effective potential due to N -electrons with a background of fixed ions.

The Poisson's equation can be written as

$$\frac{\partial^2 \phi}{\partial x^2} = 4\pi e \left(\int f_e dv - n_0 \right) \quad (2.12)$$

Taking various moments of Eq. (2.11) and retaining the terms of the order of \hbar^2 , we readily obtain the following set of dense quantum electron fluid equations which are also termed as quantum Madelung fluid equations in the literature,

$$\begin{aligned} \frac{\partial n_e}{\partial t} + \frac{\partial (n_e v_e)}{\partial x} &= 0, \\ m_e \left(\frac{\partial}{\partial t} + v_e \frac{\partial}{\partial x} \right) v_e &= e \frac{\partial \phi}{\partial x} - \frac{1}{n_e} \frac{\partial p_{Fe}}{\partial x} + \frac{\hbar^2}{2m_e} \frac{\partial}{\partial x} \left(\frac{\partial^2 (n_e^{1/2}) / \partial x^2}{\sqrt{n_e}} \right) \end{aligned}$$

where the first equation is the well known electron continuity equation and the second one is the electron momentum equation with the quantum statistical pressure term (p_{Fe} , which is known as Fermi pressure) and the last term is known as quantum force term. In three dimensional space, the above two equations can be re-written as

$$\frac{\partial n_e}{\partial t} + \nabla \cdot (n_e \mathbf{v}_e) = 0, \quad (2.13)$$

$$m_e \left(\frac{\partial}{\partial t} + \mathbf{v}_e \cdot \nabla \right) \mathbf{v}_e = e \nabla \phi - \frac{1}{n_e} \nabla p_{Fe} + \frac{\hbar^2}{2m_e} \nabla \left(\frac{\nabla^2 \sqrt{n_e}}{\sqrt{n_e}} \right) \quad (2.14)$$

Here the Fermi pressure term for degenerate electrons obeying Fermi-Dirac distribution can be expressed as [68],

$$p_{Fe} = \frac{m_e n_0 v_{Fe}^2}{3} \left(\frac{n_e}{n_0} \right)^{(D+2)/D} \quad (2.15)$$

where D represents the number of degrees of freedom and v_{Fe} is known as the Fermi velocity which can be related to the Fermi temperature (T_{Fe}) through the relation $\frac{1}{2} m_j v_{Fj}^2 = k_B T_{Fj}$. Here k_B represents the Boltzmann constant and n_0 is equilibrium number density of ions and electrons in electron-ion plasma.

The quantum force term can be expressed as a gradient of Bohm potential (ϕ_B) in the following manner

$$\mathbf{F}_q = \nabla \left(\frac{\hbar^2}{2m_e} \frac{\nabla^2 \sqrt{n_e}}{\sqrt{n_e}} \right) = -\nabla \phi_B \quad (2.16)$$

The quantum force term arises due the quantum mechanical tunneling of electrons through the Bohm potential and it vanishes for classical plasma systems (for which $\hbar \rightarrow 0$). The Wigner-Poisson's equations are extensively used to study various types of linear and nonlinear waves in dense quantum plasmas.

2.3 Drift-Approximation

In the next chapters, we shall use drift-approximation to study drift waves in quantum plasma. We shall present a brief derivation of drift-approximation and the underlying physics in this section. Since plasma behave as a fluid which is composed of many individual particles, one would expect the fluid to have drift motion in a direction which is perpendicular to the extended magnetic field. The drift-motion perpendicular to the external magnetic field is due to magnetization of the plasma particles. To derive drift-

approximation, we start with the following fluid equation of motion,

$$m_j \left(\frac{\partial}{\partial t} + \mathbf{v}_j \cdot \nabla \right) \mathbf{v}_j = q_j (\mathbf{E} + \mathbf{v}_j \times \mathbf{B}) - \frac{1}{n_j} \nabla p_{Fj} + \frac{\hbar^2}{2m_j} \nabla \left(\frac{\nabla^2 \sqrt{n_j}}{\sqrt{n_j}} \right) \quad (2.17)$$

where $|q_j|$ is the magnitude of charge, m_j is the mass of the j th species i.e., $j = e$ for electrons and i for ions, n_j is the number density and $\mathbf{B} = B_0 \hat{z}$, \hat{z} is a unit vector along the z -axis. Assuming electrostatic perturbations (i.e., $\mathbf{E} = -\nabla\phi$, where ϕ is the electrostatic wave potential) and taking cross product of above equation with \hat{z} , we get

$$\begin{aligned} (\partial_t + \mathbf{v}_j \cdot \nabla) \hat{z} \times \mathbf{v}_j &= \frac{q_j}{m_j} (-\hat{z} \times \nabla\phi + B_0 [\mathbf{v}_j (\hat{z} \cdot \hat{z}) - \hat{z} (\hat{z} \cdot \mathbf{v}_j)]) \\ &\quad - \frac{1}{m_j n_j} \hat{z} \times \nabla p_{Fj} + \frac{\hbar^2}{2m_j^2} \hat{z} \times \nabla \left(\frac{\nabla^2 \sqrt{n_j}}{\sqrt{n_j}} \right) \end{aligned} \quad (2.18)$$

For low-frequency perturbations for which we may assume $\omega \ll \omega_{cj}$, where ω is the perturbation frequency, $\omega_{cj} = |q_j| B_0 / m_j c$ is known as the gyrofrequency of j th species and c is the speed of light. Using algebraic iterative procedure, the above equation can be written as,

$$\begin{aligned} \mathbf{v}_{\perp j} &= \frac{1}{B_0} (\hat{z} \times \nabla\phi) + \frac{1}{B_0} \frac{m_j}{q_j} \frac{d}{dt} (\hat{z} \times \mathbf{v}_j) + \frac{1}{q_j B_0 n_j} \hat{z} \times \nabla p_{Fj} \\ &\quad - \frac{\hbar^2}{2m_j q_j B_0} \hat{z} \times \nabla \left(\frac{\nabla^2 \sqrt{n_j}}{\sqrt{n_j}} \right), \end{aligned} \quad (2.19)$$

where $d/dt = \partial_t + \mathbf{v}_j \cdot \nabla$, the first term on the right hand side of Eq. (2.19) is the usual $\mathbf{E} \times \mathbf{B}$ drift, the second term is the polarization drift and the last two terms are known as the diamagnetic drift terms which arises due the pressure gradients. As we have discussed earlier, that in dense quantum plasma system, we have the Fermi pressure and the Bohm term. Since the $\mathbf{E} \times \mathbf{B}$ drift is dominating, we can define various terms and can write

the total perpendicular component of fluid velocity as,

$$\mathbf{v}_{\perp j} = \mathbf{v}_E + \mathbf{v}_{pj} + \mathbf{v}_{Dj},$$

where,

$$\begin{aligned}\mathbf{v}_E &= \frac{1}{B_0} (\hat{z} \times \nabla \phi), \\ \mathbf{v}_{pj} &= -\frac{1}{B_0 \omega_{ci}} \left[\frac{\partial}{\partial t} + (\mathbf{v} \cdot \nabla) \right] \nabla \phi, \\ \mathbf{v}_{Dj} &= \frac{1}{q_j n_j B_0} \hat{z} \times \nabla p_{Fj} - \frac{\hbar^2}{2m_j q_j B_0} \hat{z} \times \nabla \left(\frac{\nabla^2 \sqrt{n_j}}{\sqrt{n_j}} \right).\end{aligned}$$

where \mathbf{v}_{Dj} is the diamagnetic drift velocity in a quantum plasma.

Chapter 3

Quantum Ion-Acoustic Vortices in a Nonuniform Electron-Ion Plasma

In this chapter, we shall discuss some linear and nonlinear properties of quantum ion-acoustic waves in a nonuniform, dissipative magnetized plasma with sheared ion flows. By employing the QHD model, we found that parallel ion sheared flow can drive the quantum ion-acoustic wave unstable. Stationary solutions of the nonlinear equations that govern the quantum ion acoustic waves are also obtained. It is found that electrostatic monopolar, dipolar, and vortex street type solutions can appear in such a plasma. It is observed that the inclusion of the quantum statistical and Bohm potential terms significantly modify the scalelengths of these structures. The present work may have relevance in the dense astrophysical environments where quantum effects are expected to play a significant role.

3.1 Introduction

It is well known that the plasma occurs in a turbulent state whenever it is driven away from its thermodynamic equilibrium due to free energy sources. For instance due to laser light interaction, radio frequency heating and beam particle interaction etc. In the presence of free energy sources, the plasma distribution may deviate from its thermodynamic

equilibrium distribution known as Maxwell Boltzmann type distribution. The turbulence provides a mechanism to a relaxed state via self-organization through superimposition of waves, vortex formation as well as zonal flows [69]. Where the *self-organization means a process through which the internal organization of a system increases without guided or managed by external sources. A vortex is defined as a spinning turbulent flow or simply a spiral whirling motion having closed streamlines.* A vortex motion of a fluid arises due to $\nabla \times \mathbf{v}$, where \mathbf{v} represents the fluid velocity. Whenever, there is vorticity in a fluid, the fluid becomes more and more curled and eventually starts rotating in the form of various types of vortices. The vortex motion in magnetized plasmas is governed by nonlinear equations such as Navier-Stokes equation, Charney equation as well as Hasegawa-Mima equation [70, 71] etc. The solution of these nonlinear equations admits various types of vortices in wide variety of plasma systems such as in upper atmosphere, in heliosphere, in magnetosphere as well as in laboratory produced plasmas. The Navier-Stokes and Hasegawa-Mima equations are nonlinear partial differential equations containing nonlinearity in the form of two-dimensional vector product which can be expressed in terms of a Poisson bracket which can be written as $J[f, g] = \hat{z} \times \nabla f \cdot \nabla g$. It is well established that the two-dimensional nonlinear differential equations possessing Poisson bracket or Jacobian nonlinearity admits vortex structures. Charney [70] explained the formation of large scale atmospheric vortex with the help of Rossby waves. On the other hand, Hasegawa and Mima [71] showed a close similarity of drift waves and Rossby waves. The fluid starts rotating due to Coriolis force or due to Lorentz force in a magnetized plasma. In order to understand the vortex formation in a magnetized plasma, we may consider a collisionless plasma in the presence of a uniform magnetic field pointing in the z-direction. Due to charge bunching an internal electric field may exist. Due to the presence of electric and magnetic field, the plasma column starts rotating due to $\mathbf{E} \times \mathbf{B}$ drift. Most commonly seen vortices in a magnetized plasma are monopolar and dipolar vortices. A monopolar vortex is single circularly symmetric vortex possessing a nonzero angular momentum and it causes an excess of local charge density. Whereas, the dipole vortex essentially rep-

resents two closely packed monopole vortices with opposite polarity and rotation. The dipolar vortex has nonzero linear momentum, while its angular momentum is zero. There are several types of vortex structures have been observed in neutral fluids as well as in plasma systems. The study of vortex motion is important to explain the formation of self-organized structures as well as energy transport in magnetized plasmas. Due to vortex formation, the fluid starts rotating and significantly effect the transport mechanism. It also plays important role in strong turbulent state of several physical systems such as in magnetized plasmas, rotating fluids as well as in oceanography etc.

As discussed earlier, there is a lot of interest during the past few years, in the field of quantum plasmas due to various potential applications namely in microelectronic devices [1], in dense astrophysical plasmas [2, 3] (like in neutron stars and in white dwarfs etc.), in high-power laser-produced plasma experiments [4] as well as in dusty plasmas [5, 6, 7]. The classical plasmas deals with low-density and high-temperature plasmas, in which, the quantum effects are ignorable. Whereas, in high density and low-temperature plasmas, the quantum effects are expected to play important role.

To deal with quantum plasmas, two well known mathematical formulations are: the Wigner-Poisson and the Schrödinger-Poisson models. The quantum hydrodynamic (QHD) model which has been extensively used based on Schrödinger-Poisson formulation, so as to investigate various the linear as well as nonlinear processes in dense plasmas [8, 9, 10]. The main advantage of using QHD model is numerical efficient, and the direct use of various macroscopic variables of interest and ease with the use of appropriate boundary conditions. However, the QHD model cannot explain the so called Landau damping or simply the wave particle interaction, since it has been derived by taking appropriate moments of the Wigner distribution function [11].

The QHD model has also been used to study linear and nonlinear properties of inhomogeneous quantum plasmas. For instance, El-Taibany and Wadati [11] studied the nonlinear dynamics of quantum dust-acoustic waves in a nonuniform quantum dusty plasma and found that the formation of solitons manifest a dependence on a critical

value of plasma parameters unlike a homogeneous plasma. Shukla and Stenflo [40] found new drift-modes in nonuniform quantum magnetoplasmas and observed that the electron Bohm potential term significantly modify the electron drift wave frequency. Haque and Mahmood [41] studied the linear and nonlinear drift-waves in inhomogeneous quantum plasmas with neutrals in the background and found that the quantum effects significantly modify the drift-solitons and shock structures in quantum magnetoplasmas. Quite recently, Haque and Saleem [42] proposed that monopolar and dipolar quantum ion-acoustic vortices could appear in a uniform dense plasmas.

In this chapter, we shall extend the said work and investigate the coupled quantum drift-ion acoustic vortices in the presence of background density inhomogeneity as well as the sheared plasma ion flow [43] parallel to the ambient magnetic field. In the next section, we shall derive nonlinear set of equations for the coupled drift ion-acoustic waves for quantum plasma. In subsection 3.2.2, we shall present stationary solutions in the form of various types of nonlinear structures namely the monopolar, dipolar, and vortex street type solutions. These profiles are also presented both analytically as well as numerically. In Section 3.3, we summarize the main findings.

3.2 Nonlinear Equations

We consider here, a nonuniform electron and ion plasma, embedded in a uniform external magnetic field $\mathbf{B} = B_0 \hat{z}$, where B_0 is the strength of magnetic field and \hat{z} is a unit vector pointing in the z -direction. We assume that there exists an equilibrium plasma flow $v_{i0}(x) \hat{z}$, with velocity and electron (ion) equilibrium density gradients in the x -direction. We assume that some external sources maintain the equilibrium density and velocity gradients. We also assume that the range of phase velocity as follows: $v_{Fi} \ll \omega/k \ll v_{Fe}$ (where v_{Fj} the Fermi velocity of the j -th species). By employing the quantum hydrodynamic (QHD) model, the set of equations which governs the dynamics of electron and ion fluids are written in the following way:

The equation of motion of electron fluid for dense quantum plasma can be written as

$$m_e n_e (\partial_t + \mathbf{v}_e \cdot \nabla) \mathbf{v}_e = e n_e \left(\nabla \phi - \frac{1}{c} \mathbf{v}_e \times \mathbf{B}_0 \right) - \nabla p_e + \frac{\hbar^2}{2m_e} \nabla \left(\frac{\nabla^2 \sqrt{n_e}}{\sqrt{n_e}} \right) \quad (3.1)$$

where ϕ is the electrostatic potential, $n_e(m_e)$ is the number density (mass) of electron, and e is the magnitude of charge of electron. Assuming one-dimensional Fermi gas, the electrons obey the following equation of state [68],

$$p_e = \frac{2}{3} \frac{m_e v_{Fe}^2}{2n_{e0}^2} n_e^3 \quad (3.2)$$

where v_{Fe} is the Fermi velocity of electrons which can be related with the Fermi electron temperature T_{Fe} , by $\frac{1}{2} m_e v_{Fe}^2 = k_B T_{Fe}$, where k_B is the usual Boltzmann constant.

The z-component of equation of motion (3.1) for inertialess electrons yield the following result,

$$e \partial_z \phi - \frac{1}{n_e} \partial_z p_e + \frac{\hbar^2}{2m_e} \partial_z \left(\frac{\nabla^2 \sqrt{n_e}}{\sqrt{n_e}} \right) = 0 \quad (3.3)$$

Considering electrons inertialess for low-frequency waves such that $\partial_t \ll \omega_{ce}$ (where ω_{ce} is the electron cyclotron frequency) with $\rho_e k_\perp \rightarrow 0$. Letting $n_e = n_{e0}(x) + n_{e1}$ in Eq. (3.3) and using Eq. (3.2), where $n_{e0}(n_{e1})$ is the equilibrium and perturbed number density of electrons such that $n_{e1} \ll n_{e0}$, we get

$$e \partial_z \phi - \frac{1}{n_e} \partial_z \left[\frac{2}{3} \frac{k_B T_{Fe}}{n_{e0}^2} (n_{e0} + n_{e1})^3 \right] + \frac{\hbar^2}{2m_e} \partial_z \left(\frac{\nabla^2 \sqrt{(n_{e0} + n_{e1})}}{\sqrt{(n_{e0} + n_{e1})}} \right) = 0$$

By employing Taylor's series expansion for the Fermi pressure and Bohm potential terms under the assumption that the quantum corrections to be small [42], we obtained the perturbed number density of electrons,

$$\frac{n_{e1}}{n_{e0}} \simeq \frac{e}{2k_B T_{Fe}} \phi + \frac{\hbar^2}{16m_e k_B^2 T_{Fe}^2} \nabla^2 (e\phi) \quad (3.4)$$

Assuming ions to be cold, the equation of motion for collisional ions can be written as

$$m_i n_i (\partial_t + \mathbf{v}_i \cdot \nabla) \mathbf{v}_i = -en_i \left(\nabla \phi - \frac{1}{c} \mathbf{v}_i \times \mathbf{B}_0 \right) - m_i n_i \nu_{in} \mathbf{v}_i$$

which can also be re-written as

$$m_i n_i (d_t + \nu_{in} + \mathbf{v}_i \cdot \nabla) \mathbf{v}_i = -en_i \left(\nabla \phi - \frac{1}{c} \mathbf{v}_i \times \mathbf{B}_0 \right) \quad (3.5)$$

where the differential operator has been defined as $d_t = \partial_t + v_{i0} \partial_z$ and ν_{in} represents the collision frequency between the ion and neutral particles.

The ion fluid velocity component perpendicular to the external magnetic field using Eq. (3.5) can be written as

$$\mathbf{v}_{i\perp} = \frac{c}{B_0} \hat{z} \times \nabla_{\perp} \phi - \frac{c}{B_0 \omega_{ci}} \left(d_t + \nu_{in} + \frac{c}{B_0} \hat{z} \times \nabla_{\perp} \phi + v_{iz} \partial_z \right) \nabla_{\perp} \phi \quad (3.6)$$

Here we have used low-frequency approximation which is valid for $|\partial_t| \ll \omega_{ci}$, such that $\omega_{ci} (\equiv eB_0/m_i c)$ is the frequency of gyration of the ions around the applied magnetic field. It is worth-mentioning here that the first term on the right-hand side of equation (3.6) is the usual $\mathbf{E} \times \mathbf{B}_0$ drift velocity and the other term is the ion polarization drift velocity. The Poisson's equation, in this case can be written as

$$\nabla^2 \phi = -4\pi e (n_i - n_e) \quad (3.7)$$

Using Eq. (3.4), we can write Eq. (3.7) as

$$\frac{n_{i1}}{n_{i0}} = \Phi - (\lambda_{Fe}^2 - H^2) \nabla^2(\Phi) \quad (3.8)$$

Here we have defined a normalized electrostatic potential $\Phi = e\phi / (2k_B T_{Fe})$, and electron Fermi wavelength $\lambda_{Fe} = \sqrt{k_B T_{Fe} / 2\pi n_0 e^2}$ with $n_{i0} = n_{e0} = n_0$, and $H = \sqrt{\hbar^2 / 8m_e k_B T_{Fe}}$

represents the electron Bohm potential term. The continuity equation for the ion fluid is

$$\frac{\partial n_i}{\partial t} + \nabla \cdot (n_i \mathbf{v}_i) = 0 \quad (3.9)$$

From equations (3.6), (3.8) and ((3.9), we obtain the following result

$$\begin{aligned} D_\phi [\Phi - (\lambda_{Fe}^2 - H^2) \nabla^2 \Phi - \rho_i^2 \nabla_\perp^2 \Phi] - \nu_{in} [\Phi - (\lambda_{Fe}^2 - H^2) \nabla^2 \Phi] \\ - \frac{c_s^2}{\omega_{ci}} \partial_x n_{i0} \Phi \partial_y \Phi + \frac{c_s^2}{\omega_{ci} n_{i0}} \hat{z} \times \nabla_\perp \Phi \cdot \nabla n_{i0} + \partial_z v_{iz} = 0 \end{aligned} \quad (3.10)$$

where $D_\phi = d_t + \nu_{in} + (c_s^2/\omega_{ci}) \hat{z} \times \nabla \Phi \cdot \nabla_\perp + v_{iz} \partial_z$, $c_s = \sqrt{2k_B T_{Fe}/m_i}$ represents the quantum ion acoustic speed, and the ion Larmor radius is defined as $\rho_i (= c_s/\omega_{ci})$.

The z-component of ion fluid equation (3.5) gives

$$D_\phi v_{iz} = -c_s^2 \partial_z \Phi - \frac{c_s^2}{\omega_{ci}} (\hat{z} \times \nabla_\perp \Phi \cdot \nabla) v_{i0}$$

which on simplification gives

$$D_\phi v_{iz} = -c_s^2 [\partial_z - S_i \partial_y] \Phi \quad (3.11)$$

Here the ion sheared flow parameter is defined as $S_i = -(\partial_x v_{i0})/\omega_{ci}$.

3.2.1 Linear dispersion relation

In this section, we shall derive a local dispersion relation from Eqs. (3.10) and (3.11), by dropping out the nonlinear terms, and by assuming $\exp[i(k_y y + k_z z - \omega t)]$ type perturbations, we finally obtain the following result

$$\left(\omega' + i\nu_{in} \right)^2 k_\perp^2 \rho_i^2 + \left(\omega' + i\nu_{in} \right) \left[\omega (1 + (\lambda_{Fe}^2 - H^2) k^2 - \omega^*) - k_z^2 c_s^2 \left(1 - \frac{k_y}{k_z} S_i \right) \right] = 0 \quad (3.12)$$

where the ion drift-frequency is defined by $\omega^* = -(c_s^2/\omega_{ci}) d_x(\ln n_{i0})$ and the Doppler shift frequency $\omega' = (\omega - k_z v_{i0})$. For collisionless and uniform density plasma, Eq. (3.12) reduces to

$$\omega' = k_z c_s \left(\frac{1 - k_y S_i / k_z}{(1 + (\lambda_{Fe}^2 - H^2)k^2 + k_\perp^2 \rho_i^2)} \right)^{1/2} \quad (3.13)$$

The above expression shows that quantum ion acoustic waves can be destabilized for $k_y S_i > k_z$.

On the other hand, if we keep the ion collision frequency term, equation (3.12) shows an oscillatory ion-drift waves instability for $\omega' \ll i\nu_{in}$. By writing down $\omega = \omega^* + i\gamma$, we get

$$\gamma = -\frac{\nu_{in}^2 k_\perp^2 \rho_i^2}{1 + (\lambda_{Fe}^2 - H^2)k^2} - \frac{k_z^2 c_s^2 \left(1 - \frac{k_y}{k_z} S_i\right)}{1 + (\lambda_{Fe}^2 - H^2)k^2} \quad (3.14)$$

Eq. (3.14) shows that the quantum corrections modify the scalelengths of the system. Note that in the absence of parallel shear velocity, the wave is damped, however, the ion drift dissipative instability gives growth for $|S_i| k_y > k_z$. Therefore, it follows from Eq. (3.14) that ion drift waves can be driven by the combined effects of ion sheared flow and the ion neutral drag provided $|S_i| k_y > k_z$.

3.2.2 Nonlinear analysis

In the previous section, we showed that ion sheared flow and collisions can drive electrostatic drift-waves and ion acoustic waves unstable for dense quantum plasma. Due to nonlinear interaction of finite amplitude drift and ion acoustic waves, various types of coherent nonlinear structures can be formed. For localized vortex type solution, we may define a reduced coordinate $\xi = y + \alpha z - ut$. Here, u represents translational speed of the vortex and α is some constant. For simplicity, we assume a collisionless plasma and retain the leading order nonlinearities in our calculations such that we have assumed

$|\mathbf{v}_E \cdot \nabla| \gg |v_{iz} \partial_z|$. Equation (3.11) takes the following form:

$$D_\phi v_{iz} = -c_s^2 [\alpha \partial_\xi - S_i \partial_\xi] \Phi$$

where the differential operator $D_\phi = \partial_\xi - (c_s^2/U\omega_{ci}) (\partial_x \Phi \partial_\xi - \partial_\xi \Phi \partial_x)$ and $U = u - \alpha v_{i0}$.

The solution of above equation is

$$v_{iz} = \frac{c_s^2}{U} (\alpha - S_i) \Phi \quad (3.15)$$

Substituting the value of v_{iz} by using Eq. (3.15) in Eq. (3.10), we readily obtain

$$U \partial_\xi \Phi + \frac{c_s^2}{\omega_{ci}} (\partial_x \ln n_{i0}) \Phi \partial_\xi \Phi - U^* \partial_\xi \Phi - \frac{\alpha c_s^2}{U} (\alpha - S_i) \partial_\xi \Phi + \frac{c_s^2}{\omega_{ci}} J[\Phi, a_1 \nabla_\perp^2 \Phi] - U \partial_\xi \nabla_\perp^2 \Phi = 0$$

which on simplification gives

$$\left(1 - \frac{U^*}{U} - \left(\frac{U_{sh}}{U}\right)^2\right) \partial_\xi \Phi + \frac{c_s^2}{U\omega_{ci}} J[\Phi, a_s \nabla_\perp^2 \Phi] + \frac{c_s^2}{U\omega_{ci}} (\partial_x \ln n_{i0}) \Phi \partial_\xi \Phi - \partial_\xi \nabla_\perp^2 \Phi = 0 \quad (3.16)$$

where $U^* = -(c_s^2/\omega_{ci}) d_x (\ln n_{i0})$, $U_{sh} = \sqrt{(\alpha c_s^2/U)(\alpha - S_i)}$. Here U_{sh} represents the shear in the parallel velocity, and $a_s = (\lambda_{Fe}^2 - H_e^2 + \rho_i^2)$. In the absence of scalar nonlinearity (that involves $\Phi \partial_\xi \Phi$) and for $\left(1 - \frac{U^*}{U} - \left(\frac{U_{sh}}{U}\right)^2\right) = 0$, we obtain the following equation

$$\partial_\xi \nabla_\perp^2 \Phi - \frac{c_s^2}{\sqrt{a_s} U \omega_{ci}} J[\Phi, \nabla_\perp^2 \Phi] = 0 \quad (3.17)$$

where $\nabla_\perp^2 = \partial_x^2 + \partial_\xi^2$. Here ∇_\perp^2 operator is normalized with a_s^2 . The solution of equation (3.17) is given as

$$\nabla_\perp^2 \Phi = \frac{4\Phi_0}{a_0^2} \exp \left[-\frac{2}{\Phi_0} \left(\Phi - \frac{U\omega_{ci}}{c_s^2} x \right) \right] \quad (3.18)$$

where Φ_0 and a_0 are some constants. The solution of Eq. (3.18) would be

$$\Phi = \frac{\sqrt{a_s} U \omega_{ci}}{c_s^2} x + \Phi_0 \ln \left[2 \cosh x + 2 \left(1 - \frac{1}{a_0^2} \right) \cos \xi \right] \quad (3.19)$$

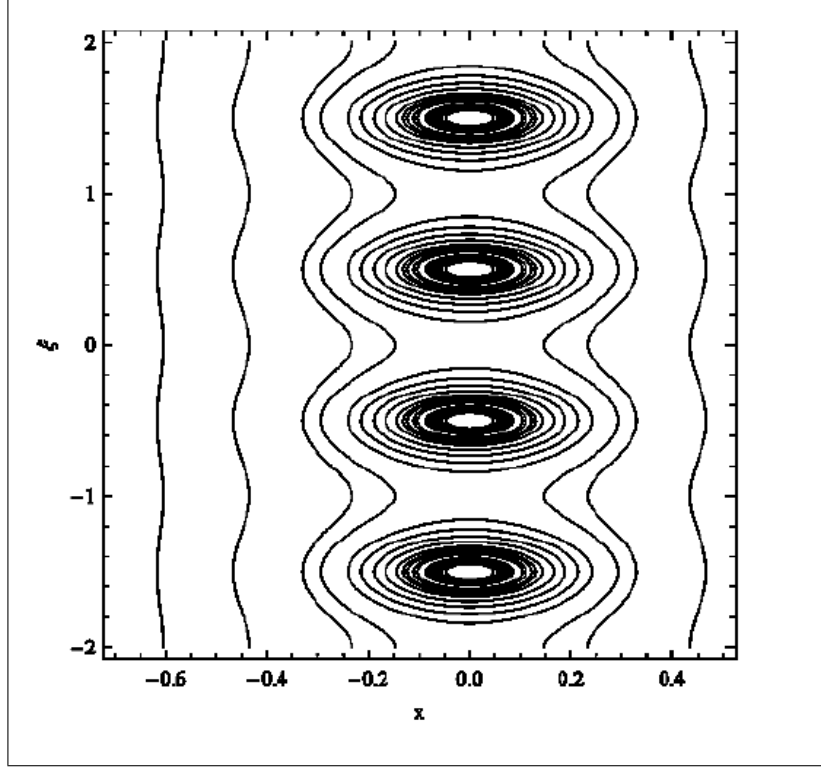


Figure 3-1: A vortex chain type solution obtained by solving equation (3.19) for a uniform density and dense astrophysical plasma case.

Equation (3.19) gives Kelvin-Stuart "cats eyes" type solution which represents chains of vortices for $a_0^2 > 1$ [72, 73]. Here $U = [U^* \pm \sqrt{(U^*)^2 + 4(U_{sh})^2}]/2$ represents the speed of vortex chain. Fig. (3-1) shows a vortex chain type profile in (x, ξ) plane and by using parameters of dense astrophysical plasmas for constant density plasma case for which [42, 43]: $n_0 \sim 10^{27} \text{ cm}^{-3}$, $B_0 = 2 \times 10^9 \text{ Gauss}$, $M = U/c_s = 0.8$, $R_0/\rho_i = 1$, $\alpha = 0.2$ and $S_i = 0.1$. The Fermi temperature of electron is $T_{Fe} = 4.32 \times 10^7 \text{ }^\circ\text{K}$ and $H_e = 3.7 \times 10^{-5}$. We found a periodic vortex street type of profile with periodicity in ξ variable. A three-dimensional view of vortex streets type profile is shown in Fig. (3-2).

If we ignore the scalar nonlinearity in Eq. (3.16), we obtain

$$\partial_\xi \nabla_\perp^2 \Phi - \frac{c_s^2}{U\omega_{ci}} J[\Phi, a_s \nabla_\perp^2 \Phi] - \left(1 - \frac{U^*}{U} - \left(\frac{U_{sh}}{U}\right)^2\right) \partial_\xi \Phi = 0 \quad (3.20)$$

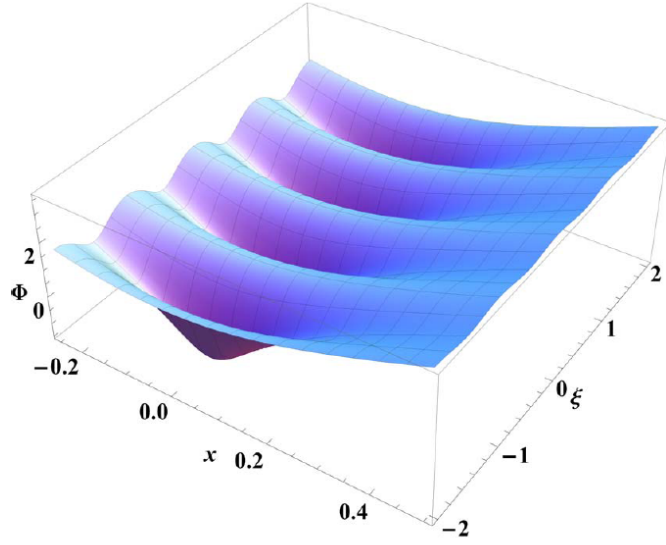


Figure 3-2: 3-D vortex profile obtained by solving equation (3.19) by using the parameters as used in Fig. (3-1).

where $\psi_1 = \left(1 - \frac{U^*}{U} - \left(\frac{U_{sh}}{U}\right)^2\right)$. The general solution of above equation (3.20) would be

$$\nabla_{\perp}^2 \Phi - \psi_1 \Phi = f\left(\Phi - \frac{U\omega_{ci}}{c_s^2}x\right) \quad (3.21)$$

The function $f\left(\Phi - \frac{U\omega_{ci}}{c_s^2}x\right) = W\left(\Phi - \frac{U\omega_{ci}}{c_s^2}x\right)$ satisfied a linear relation[68], such that W is constant. The Eq. (3.21) thus gives us

$$\nabla_{\perp}^2 \Phi - \psi_1 \Phi = W\left(\Phi - \frac{U\omega_{ci}}{c_s^2}x\right) \quad (3.22)$$

Using polar coordinates, the outer ($r < R_0$) and inner ($r > R_0$) solution of above equation (3.22) for a vortex of radius R_0 would be

$$\Phi_{out}(r, \theta) = C_1 K_1(\psi_1 r) \cos \theta \quad (3.23)$$

and

$$\Phi_{in}(r, \theta) = \left[C_2 J_1(\psi_2 r) + \left(\frac{\psi_1^2 + \psi_2^2}{\psi_2^2} \right) \frac{U \omega_{ci}}{c_s^2} r \right] \cos \theta \quad (3.24)$$

where $\psi_2^2 = -(\psi_1^2 + W)$, $W = -(\psi_1^2 + \psi_2^2)$, and $J_1(K_1)$ are ordinary (modified) Bessel function. Here C_1 and C_2 are some constants which can be determined by using appropriate boundary conditions i.e., the continuity of Φ , $\partial_r \Phi$, and $\nabla_\perp^2 \Phi$ at the circle $r = R_0$ such that

$$C_1 = \frac{U \omega_{ci}}{c_s^2} \frac{R_0}{K_1(\psi_1 R_0)}, \quad C_2 = \frac{U \omega_{ci}}{c_s^2} \left(-\frac{\psi_1^2}{\psi_2^2} \right) \frac{R_0}{J_1(\psi_2 R_0)} \quad (3.25)$$

and ψ_2 from the following expression

$$\frac{K_2(\psi_1 R_0)}{K_1(\psi_1 R_0)} = -\frac{\psi_1}{\psi_2} \frac{J_2(\psi_2 R_0)}{J_1(\psi_2 R_0)} \quad (3.26)$$

Equation (3.26) admits a typical dipolar vortex solution [74, 75]. In Fig. (3-3), we have displayed a contour plot of the solutions given by the Eqs. (3.23) and (3.24) by choosing $n_0 = 10^{27} \text{ cm}^{-3}$, $\alpha = 0.1$,

$B_0 = 2 \times 10^{12} \text{ Gauss}$, $S_i = 6.0$ and $U/c_s = 0.8$. One finds $\rho_i = 4.36 \times 10^{-9} \text{ cm}$, $T_{Fe} = 4.32 \times 10^7 \text{ }^\circ\text{K}$ with $H = 3.7 \times 10^{-2}$. If we choose the magnetic field $B_0 = 2 \times 10^9 \text{ Gauss}$ and $n_0 = 10^{27} \text{ cm}^{-3}$, then the Larmor radius $\rho_i = 4.36 \times 10^{-6} \text{ cm}$ with small value of quantum parameter $H = 3.7 \times 10^{-5}$. It is evident that both the vortex street and dipolar vortices are formed on a very short scalelength, typically of the order of ion Larmor radius ρ_i (i.e., of the order of 10^{-6} cm).

Finally, in the case when the scalar nonlinearity is stronger than the vector nonlinearity, Eq. (3.16) reduces to

$$\partial_\xi \nabla_\perp^2 \Phi - \frac{c_s^2}{U \omega_{ci}} (\partial_x \ln n_{i0}) \Phi \partial_\xi \Phi - \left(1 - \frac{U^*}{U} - \left(\frac{U_{sh}}{U} \right)^2 \right) \partial_\xi \Phi = 0 \quad (3.27)$$

which admits monopolar type vortex solutions [75].

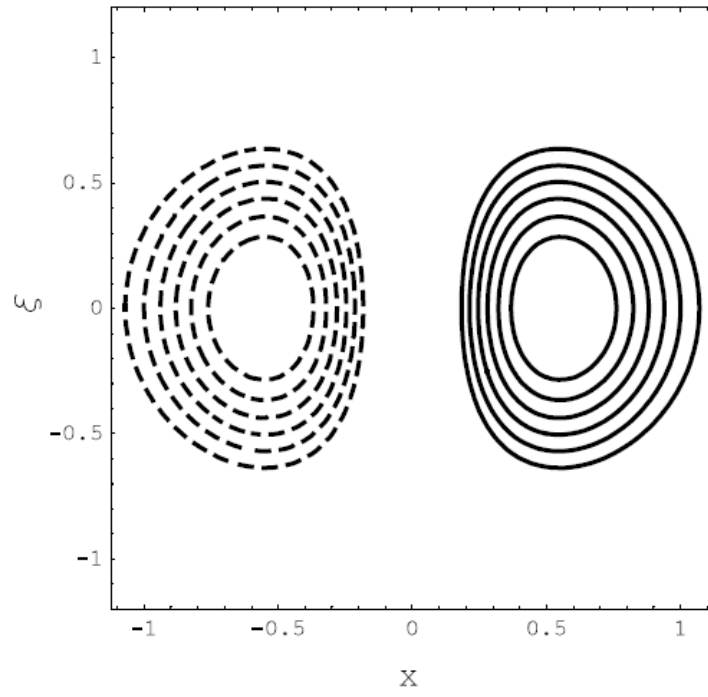


Figure 3-3: Two dimensional contour plot of Φ by solving equations (3.23) and (3.24) for some typical plasma parameters as given in the text.

3.3 Summary

In this chapter, linear as well as nonlinear propagation of electrostatic ion-acoustic waves and drift-dissipative quantum magnetoplasma has been investigated in the presence of sheared ion flows parallel to the ambient magnetic field [43]. It is shown that the ion sheared flow can drive the quantum ion-acoustic waves unstable. It is found that the linear ion drift waves are driven by the combined effects of parallel ion sheared flows and the ion neutral drag provided $|S_i| k_y > k_z$. The effects of the quantum corrections on the linear drift waves are also highlighted. On the other hand, upon the interaction of finite amplitude quantum drift waves and ion acoustic waves, various types of coherent nonlinear vortex (such as monopolar, dipolar and vortex street) are formed in a collisionless plasma. We found that in the presence of quantum statistical as well as Bohm potential terms, the scalelength of nonlinear structures are significantly gets modified. These results are very useful to understand the physics of nonlinear structure formation in dense astrophysical plasmas.

Chapter 4

Quantum Ion-Acoustic Vortices in Electron-Positron-Ion Plasmas

In this chapter, we have presented nonlinear dynamics of low-frequency electrostatic quantum ion-acoustic waves in a nonuniform, dissipative electron-positron-ion plasma with sheared ion flows. In this model, the ions are treated classical, whereas, the electrons and positrons dynamics is governed by the QHD model. The parallel sheared ion flow derives the quantum ion-acoustic waves unstable for $|S_i|k_y > k_z$. Whereas, stationary solution of the mode coupling equations in the form of various types of vortex structures in such a plasma. We found that the quantum effects in e-p-i plasma significantly modify the scalelengths of nonlinear structures. The present investigation might have very useful applications in dense astrophysical environments [53].

4.1 Introduction

Electron-positron (e-p) is believed to exist in the pulsars, in the inner region of the accretion disks around the central black holes [76, 77] as well as in the intergalactic jets, in the early universe (at the center of our galaxy), Van Allen belts, solar flares [78, 79, 80]. the e-p pair plasma can also be produced due to the interaction of intense

laser-light with solid target surface [81]. Pair plasma can also be produced in a laboratory by the accumulation of positrons from a radio-active source in normal electron-ion plasma [82] using an electrostatic trap. Although, the electron-positron pair exists in several astrophysical plasmas such as active galactic nuclei, pulsars magnetosphere as well as in early universe with a background of small percentage of ions. Due to finite life time of positrons, both the astrophysical and laboratory plasma becomes a mixture of electrons, ions and positrons. Such admixture or three component electron-positron-ion (e-p-i) plasma has been created on laboratory scale and investigated in literature [85]. When intense short laser pulses pass through an electron-ion plasma, due to pair production results in e-p-i plasma [84]. Due to large mass difference of ions and electrons, even a small percentage of ions can excite several low-frequency modes which do not exist in a normal electron-positron plasma. Therefore, it is very important to study epi-plasma so as to understand the behavior of laboratory as well as astrophysical plasmas. Lakhina and Buti [85] have investigated the e-p-i plasma for pulsars magnetosphere case. It is well known that nonlinear behavior of electron-ion plasma becomes quite different in the presence of positrons [86]. For instance, Hasegawa *et al.* [87] have investigated the positron acceleration to relativistic energies by shock waves in epi-plasma.

The electron-positron plasma behaves very differently in comparison with normal electron-ion plasma [86, 88]. One of the important features of electron-positron (e-p) plasma in comparison with electron-ion plasma is the same mass but equal and opposite charge of electron-positron plasma. The presence of electron-positron plasma in active galactic nuclei [89], pulsars magnetosphere [76], in the polar regions of neutron stars [90], as well as in the intense laser field [91], is well known. It also exists in the early universe [92] as well as at the centre of our own galaxy [93]. Electron-positron-ion plasma has been a subject of investigation in quantum plasma. For instance, Ali *et al.* [50], has investigated ion-acoustic waves in an unmagnetized e-p-i-quantum plasma in the absence of external magnetic field. In the said reference, nonlinear Korteweg de Vries type equation was derived for quantum e-p-i plasma and discuss the relevance of their new findings. Mushtaq

and Khan [51] have investigated some linear and nonlinear characteristics of ion-acoustic waves, in quantum e-p-i plasma with transverse perturbations. Masood *et al.* [52], investigated the soliton formation in quantum e-p-i plasma and found that it depends upon Fermi pressure, positron concentration, the magnitude of applied magnetic field, as well as the propagation angle.

Recently, Haque and Saleem [42] showed the existence of monopolar and dipolar vortices in homogeneous electron-ion quantum magnetoplasma. This work was further extended by Masood *et al.* [43] for nonuniform, quantum collisional magnetoplasma in the presence of ion shear flows. Linear as well as nonlinear properties of ion-acoustic waves were investigated. For negative ion shear flow, they found that drift waves drive the system unstable. They have also showed that the presence of dust introduced a new large scalelength of the system. It is found that the vortex structure scalelength become of the order of dust Larmor radius which is of the order of 10^{-5} cm instead of 10^{-10} cm for magnetic field strength of the order of 10^9 Gauss for fixed dust charge state $z_d = 100$ [61]. In this chapter, we shall investigate the coupled quantum drift-ion acoustic vortex formation in a nonuniform magnetized e-p-i plasma in the presence of parallel ion sheared flows [53]. In the next section, we shall derive nonlinear set of equations to describe quantum drift ion-acoustic waves in electron-positron-ion magnetoplasma and a linear dispersion relation in Sec. 4.2.1. In Sec. 4.2.2, various types of nonlinear vortex structures shall be presented which are stationary solutions of the nonlinear mode coupling equations. Specifically, monopolar, dipolar, and vortex street type solutions will be presented both analytically as well as numerically. Finally, we recapitulate the main findings of the paper in the summary section.

4.2 Governing Nonlinear Equations

Let us consider nonlinear propagation of low-frequency electrostatic waves in a nonuniform electron-positron-ion (e-p-i) plasma in a constant magnetic field $B_0 \hat{z}$, where B_0 is

the magnitude of applied magnetic field and \hat{z} is a unit vector pointing in the z-direction [53]. Whereas, the ion sheared flow is maintained by some external sources. We assume that the equilibrium ion velocity ($\partial v_{i0}/\partial x$), and density gradient ($\partial n_{i0}/\partial x$) are in the x-direction. The phase velocity of the wave is assumed to be $v_{Fi} \ll \omega/k \ll v_{Fe}; v_{Fp}$ (where v_{Fj} is the Fermi velocity of the j th-species). The fluid equation for the j th-species can be written as:

The quantum hydrodynamic model equations for electron and positron can be written as

$$m_e n_j (\partial_t + \mathbf{v}_j \cdot \nabla) \mathbf{v}_j = \mp e n_j \left(\mathbf{E} + \frac{1}{c} \mathbf{v}_j \times \mathbf{B}_0 \right) - \nabla p_j + \frac{\hbar^2 n_j}{2m_e} \nabla \left(\frac{\nabla^2 \sqrt{n_j}}{\sqrt{n_j}} \right) \quad (4.1)$$

Here, the electrostatic field can be related with the electric potential ϕ through the relation $\mathbf{E} = -\nabla \phi$. Where n_j represents the number density of the j th-species such that $j = e$ for electrons and p for positrons, m_e is the mass of electron and e is the charge of electrons. Here $-(+)$ sign is used for the electron(positron). Here both the electrons and positrons are assumed to satisfy one dimensional (1-D) Fermi gas equation of state[68], such that

$$p_j = \frac{1}{3} \frac{m_e v_{Fj}^2}{n_{j0}^2} n_j^3 \quad (4.2)$$

In this case, one can easily relate the Fermi velocity of electron (positron) with the Fermi temperature T_{Fj} , through the relation $\frac{1}{2} m_e v_{Fj}^2 = k_B T_{Fj}$. Here k_B represents the usual Boltzmann constant.

In this case, the z-component of Eq. (4.1) by considering massless electrons/positrons gives

$$\pm e \partial_z \phi - \frac{1}{n_e} \partial_z p_j + \frac{\hbar^2}{2m_e} \partial_z \left(\frac{\nabla^2 \sqrt{n_j}}{\sqrt{n_j}} \right) = 0 \quad (4.3)$$

Here we have ignored the inertia of electrons and positrons for low frequency waves such that $|\partial_t| \ll \omega_{cj}$ and in the limit $\rho_j k_\perp \rightarrow 0$ (such that $j = e, p$). Assuming quantum

correction to be very small, we have expanded the Fermi pressure and the Bohm potential terms by using Taylor series[53], and finally obtained the following result

$$\frac{n_{e1}}{n_{j0}} = \frac{e}{2k_B T_{Fe}} \phi + \frac{\hbar^2}{16m_e k_B^2 T_{Fe}^2} \nabla^2(e\phi) \quad (4.4)$$

Similarly, by adopting the same procedure, one can easily wrote down the following expression for the positrons,

$$\frac{n_{p1}}{n_{p0}} = -\frac{1}{\sigma_p} \Phi - \frac{\hbar^2}{16\sigma_p^2 m_e k_B^2 T_{Fe}^2} \nabla^2(e\phi) \quad (4.5)$$

where $\sigma_p = T_{Fp}/T_{Fe}$ and $\Phi = e\phi/(2k_B T_{Fe})$ is the normalized electrostatic potential.

Assuming ions are cold, the equation of motion for the ions can be written as

$$m_i n_i (\partial_t + \mathbf{v}_i \cdot \nabla) \mathbf{v}_i = en_i \left(\mathbf{E} + \frac{1}{c} \mathbf{v}_i \times \mathbf{B}_0 \right) - m_i n_i \nu_{in} \mathbf{v}_i$$

or simply

$$m_i n_i (d_t + \nu_{in}) \mathbf{v}_i = en_i \left(\mathbf{E} + \frac{1}{c} \mathbf{v}_i \times \mathbf{B}_0 \right) \quad (4.6)$$

here the differential operator d_t is defined as $d_t = \partial_t + \mathbf{v}_{i\perp} \cdot \nabla_{\perp} + (v_{i0} + v_{iz}) \partial_z$.

Again taking the cross product of above equation with \mathbf{B}_0 , we finally obtained the perpendicular component of ion velocity expression in the following form:

$$\mathbf{v}_{i\perp} \simeq \frac{c}{B_0} \hat{z} \times \nabla_{\perp} \phi - \frac{c}{B_0 \omega_{ci}} \left(\partial_t + \nu_{in} + \frac{c}{B_0} \hat{z} \times \nabla_{\perp} \phi + (v_{i0} + v_{iz}) \partial_z \right) \nabla_{\perp} \phi \quad (4.7)$$

where the first term on the right hand side $(c/B_0) \hat{z} \times \nabla_{\perp} \phi$ is the $\mathbf{E} \times \mathbf{B}$ drift. Here, we have used the drift approximation which is valid for low-frequency waves such that $|\partial_t| \ll \omega_{ci}$ (where the ion gyrofrequency is $\omega_{ci} \equiv eB_0/m_i c$).

Poisson's equation for e-p-i plasma can be written as

$$\nabla^2 \phi = -4\pi e (n_i + n_p - n_e) \quad (4.8)$$

Using Eqs. (4.4) and (4.5), we can write Eq. (4.8) as

$$\frac{n_{i1}}{n_{i0}} = \chi \left[\Phi - \frac{(\lambda_{Fe}^2 - \chi_1 H^2)}{\chi} \nabla^2 \Phi \right] \quad (4.9)$$

Here, the Fermi wavelength of electrons can be written as: $\lambda_{Fe} = \sqrt{k_B T_{Fe} / 2\pi n_{e0} e^2}$ and the plasma density in equilibrium is defined by $n_{i0} + n_{p0} = n_{e0}$, with electron Bohm potential $H = \sqrt{\hbar^2 / 8m_e k_B T_{Fe}}$ (here $H_e = H_p = H$). $p = n_{i0} / n_{e0}$, $\chi = 1/p + (1-p)/p\sigma_p$ and $\chi_1 = 1/p + (1-p)/p\sigma_p^2$.

The continuity equation for the ion fluid is given by

$$\frac{\partial n_i}{\partial t} + \nabla \cdot (n_i \mathbf{v}_i) = 0 \quad (4.10)$$

Using Eqs. (4.7) and (4.9) in Eq. (4.10), we obtain

$$D_\phi [\Phi - (\lambda_{Fe}^2 - H^2) \nabla^2 \Phi - \rho_i^2 \nabla_\perp^2 \Phi] - \nu_{in} [\Phi - (\lambda_{Fe}^2 - H^2) \nabla^2 \Phi] - \frac{c_{si}^2}{\omega_{ci}} (\partial_x n_{i0}) \Phi \partial_y \Phi + \frac{c_{si}^2}{\omega_{ci}} \hat{z} \times \nabla_\perp \Phi \cdot \nabla \ln n_{i0} + \partial_z v_{iz} = 0 \quad (4.11)$$

where $D_\phi = d_t + \nu_{in} + (c_{si}^2 / \omega_{ci}) \hat{z} \times \nabla \Phi \cdot \nabla_\perp + v_{iz} \partial_z$. Here the quantum ion-acoustic speed is defined as $c_{si} = \sqrt{2k_B T_{Fe} / m_i}$ and the ion Larmor radius by ρ_i .

The parallel component of ion momentum equation (4.6) yields

$$D_\phi v_{iz} = -c_{si}^2 \partial_z \Phi - \frac{c_{si}^2}{\omega_{ci}} (\hat{z} \times \nabla_\perp \Phi \cdot \nabla) v_{i0}$$

which on simplification gives

$$D_\phi v_{iz} = -c_{si}^2 [\partial_z - S_i \partial_y] \Phi \quad (4.12)$$

where $S_i = -(\partial_x v_{i0}) / \omega_{ci}$ is the ion shear flow term.

4.2.1 Linear analysis

In the linear limit, we assume that ϕ and v_{iz} are proportional to $\exp[i(k_y y + k_z z - \omega t)]$, where ω and k are the frequency and wavevector, respectively. To derive a local dispersion relation from Eqs. (4.11) and (4.12), we neglect the nonlinear terms and after Fourier transformation, we get

$$\left(\omega' + i\nu_{in}\right)^2 k_{\perp}^2 \rho_i^2 + \left(\omega' + i\nu_{in}\right) \left[\omega(\chi + (\lambda_{Fe}^2 - H^2)k^2 + \omega^*) - k_z^2 c_{si}^2 \left(1 - \frac{k_y}{k_z} S_i\right)\right] = 0 \quad (4.13)$$

where $\omega' = \omega - kv_{i0}$ is the Doppler shifted frequency and $\omega^* = -(c_{si}^2/\omega_{ci}) d_x(\ln n_{i0})$ is the drift-frequency. This is the coupled drift-dissipative and ion-acoustic mode in the presence of sheared ion-flow (S_i -term) in electron-positron-ion magnetoplasma. For collisionless plasma and uniform density plasma, Eq. (4.13) becomes

$$\omega' = k_z c_{si} \left(\frac{1 - k_y S_i / k_z}{\chi + (\lambda_{Fe}^2 - H^2)k^2 + k_{\perp}^2 \rho_i^2} \right)^{1/2} \quad (4.14)$$

For $k_y S_i > k_z$, the modified ion-acoustic waves for dense plasma becomes unstable. The above expression (4.14) also shows that the presence of positron concentration modify the dispersion relation.

For collisional plasma case, equation (4.13) yields an oscillatory instability for $|\omega'| < \nu_{in}$. If we let $\omega = \omega^* + i\gamma$, we get [53]

$$\gamma = -\frac{\nu_{in} k_{\perp}^2 \rho_i^2}{\chi + (\lambda_{Fe}^2 - H^2)k^2} - \frac{k_z^2 c_{si}^2 (1 - k_y S_i / k_z)}{\nu_{in} [\chi + (\lambda_{Fe}^2 - H^2)k^2]} \quad (4.15)$$

The above expression (4.15) shows that scalelengths of the system gets modified for quantum plasmas. On the other hand, the wave gets damped for $S_i = 0$ case. The ion drift waves become unstable for $|S_i| k_y > k_z$ case. It is evident from the above expression (4.15), that ion sheared flow and ion-neutral collisions derive the ion-drift waves unstable for $|S_i| k_y > k_z$. The growth/damping rate of ion-drift waves gets modified in the presence of positron concentration for epi-plasma case.

4.2.2 Nonlinear solutions

In the previous section, we have found that the velocity gradient and collisions can destabilize the e-p-i plasma. As we did in the previous chapter, in order to find the localized vortex type solutions, we transform the modeled equations by defining a co-moving frame with the vortex $\xi = y + \alpha z - ut$, where u is some constant speed of that frame, by ignoring the dissipative term, Eq. (4.12) in the said new frame is satisfied by the following relation [53],

$$D_\phi v_{iz} = -c_{si}^2 (\alpha - S_i) \partial_\xi \Phi$$

where $D_\phi = \partial_\xi - (c_{si}^2/U\omega_{ci}) (\partial_x \Phi \partial_\xi - \partial_\xi \Phi \partial_x)$ is a differential operator and $U = u - \alpha v_{i0}$, such that $u \neq \alpha v_{i0}$. The possible solution of above equation gives

$$v_{iz} = \frac{c_{si}^2}{U} (\alpha - S_i) \Phi \quad (4.16)$$

Using Eq. (4.16) in Eq. (4.11), we obtain

$$\begin{aligned} & \sqrt{a_s} \partial_\xi \Phi + \frac{c_{si}^2 \sqrt{a_s}}{\omega_{ci} U \chi n_{i0}} (\partial_x \chi n_{i0}) \Phi \partial_\xi \Phi - \sqrt{a_s} \frac{U^*}{U} \partial_\xi \Phi - \frac{\alpha c_{si}^2 \sqrt{a_s}}{\chi U^2} (\alpha - S_i) \partial_\xi \Phi \\ & + \frac{c_{si}^2 \sqrt{a_s}}{\omega_{ci} U} J[\Phi, a_s \nabla_\perp^2 \Phi] - \sqrt{a_s} \partial_\xi \nabla_\perp^2 \Phi = 0 \end{aligned}$$

or

$$\left(1 - \frac{U^*}{U} - \left(\frac{U_{sh}}{U}\right)^2\right) \partial_\xi \Phi + J[\Phi, a_s \nabla_\perp^2 \Phi] + \frac{1}{\chi} (\partial_x \ln n_{i0}) \Phi \partial_\xi \Phi - \partial_\xi \nabla_\perp^2 \Phi = 0 \quad (4.17)$$

The coordinates ξ and x are normalized by $\sqrt{a_s}$ and $c_{si}^2/U\omega_{ci}$ respectively. $U^* = -(1/\chi) d_x (\ln n_{i0})$ is the normalized drift velocity, $U_{sh} = \sqrt{\alpha(\alpha - S_i)/\chi c_{si}}$, $a_s = (\lambda_{Fe}^2 - H^2 + \rho_i^2)/\chi$, $\nabla_\perp^2 = \partial^2/\partial x^2 + \partial^2/\partial \xi^2$ and the Jacobian is defined as $J[f, g] \equiv \partial_x f \partial_\xi g - \partial_\xi f \partial_x g$. If we ignore the scalar nonlinearity (that involves $\Phi \partial_\xi \Phi$) and set $(1 - U^*/U -$

$(U_{sh}/U)^2 = 0$, then we obtain the following expression

$$\partial_\xi \nabla_\perp^2 \Phi - J[\Phi, \nabla_\perp^2 \Phi] = 0 \quad (4.18)$$

where $\nabla_\perp^2 = \partial_x^2 + \partial_\xi^2$. It may be noted here that ∇_\perp^2 operator has been normalized with a_s^2 . The solution of above equation (4.18) is given by

$$\nabla_\perp^2 \Phi = \frac{4\Phi_{00}}{r_0^2} \exp \left[-\frac{2}{\Phi_{00}} (\Phi - x) \right] \quad (4.19)$$

Here Φ_{00} and r_0 represent some constants. The solution of above equation can be written as

$$\Phi = x + \Phi_{00} \ln \left[2 \cosh x + 2 \left(1 - \frac{1}{r_0^2} \right) \cos \xi \right] \quad (4.20)$$

For $r_0^2 > 1$ Eq. (4.20) yields the standard Kelvin-Stuart "cats eyes" type solution which represents a typical vortex chains type solution [72, 73]. In this case the speed of vortex chain would be $U_p = [U^* \pm \sqrt{(U^*)^2 + 4(U_{sh})^2}]/2$. By choosing some typical parameters of dense astrophysical e-p-i plasmas, and plotted Φ in (x, ξ) plane and obtained Fig. (4-1) exhibiting vortex chain type profile [52, 53]: $n_{e0} = 1 \times 10^{28} \text{ cm}^{-3}$, $n_{p0} = 0.8 \times 10^{28} \text{ cm}^{-3}$, $n_{i0} = 2 \times 10^{27} \text{ cm}^{-3}$, and the magnetic field $B_0 = 5 \times 10^9 \text{ Gauss}$, Mach number $M = U_p/c_{si} = 0.8$, $\alpha = 0.2$ and ion sheared flow parameter $S = 0.1$. Here the electron and positron Fermi temperatures are given by $T_{Fe} = 1.96 \times 10^8 K$ and $T_{Fp} = 1.69 \times 10^8 K$ with $H = 1.99 \times 10^{-2}$, $\lambda_{Fe} = 1.37 \times 10^{-9} \text{ cm}$, $U^* = 1.79 \times 10^8 \text{ cm/sec}$, $U_{sh} = 8.49 \times 10^6 \text{ cm/sec}$, $c_{si} = 1.8 \times 10^8 \text{ cm/sec}$ and $\rho_i = 3.76 \times 10^{-6} \text{ cm}$. It shows a periodic vortex street with the periodicity in ξ . Fig. (4-2) shows how the vortex streets manifest themselves in a 3-D plot which is an other way to visualize vortex structure.

If we drop the scalar nonlinearity in Eq. (4.17), we get

$$\partial_\xi \nabla_\perp^2 \Phi - J[\Phi, a_s \nabla_\perp^2 \Phi] - \left(1 - \frac{U^*}{U} - \left(\frac{U_{sh}}{U} \right)^2 \right) \partial_\xi \Phi = 0 \quad (4.21)$$

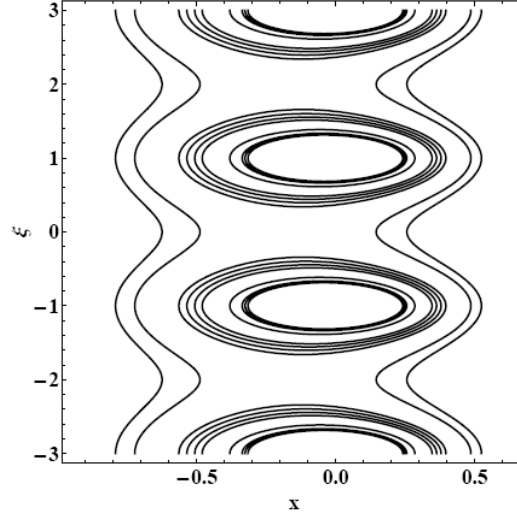


Figure 4-1: Plot of vortex chains profile obtained from Eq. (4.20) for some dense astrophysical parameters in e-p-i plasmas.

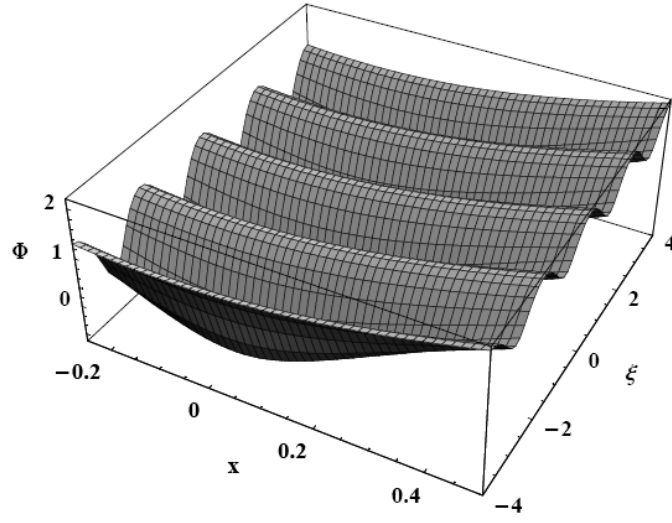


Figure 4-2: 3-D vortex profile obtained by solving equation (4.20) for the parameters used in Fig. (4-1).

where $\psi_1 = \left(1 - \frac{U^*}{U} - \left(\frac{U_{sh}}{U}\right)^2\right)$. The general solution of above equation can be written as

$$\nabla_{\perp}^2 \Phi - \psi_1 \Phi = f(\Phi - x) \quad (4.22)$$

The function $f(\Phi - x) = W(\Phi - x)$ is assumed to behave linearly [74], where W is a constant. The Eq. (4.22) thus gives us

$$\nabla_{\perp}^2 \Phi - \psi_1 \Phi = W(\Phi - x) \quad (4.23)$$

Using polar coordinates, one can transform in (r, θ) coordinates and write the outer ($r < R_0$) and inner ($r > R_0$) solutions in the following way (where R_0 is the size of vortex):

$$\Phi_{out}(r, \theta) = C_1 K_1(\psi_1 r) \cos \theta \quad (4.24)$$

and

$$\Phi_{in}(r, \theta) = \left[C_2 J_1(\psi_2 r) + \left(\frac{\psi_1^2 + \psi_2^2}{\psi_2^2} \right) r \right] \cos \theta \quad (4.25)$$

where $\psi_2^2 = -(\psi_1^2 + W)$, $W = -(\psi_1^2 + \psi_2^2)$, and $K_1(J_1)$ are the usual modified(ordinary) Bessel functions of order one. Here C_1 and C_2 constants can be calculated by using the continuity of Φ , $\partial_r \Phi$, and $\nabla_{\perp}^2 \Phi$ at the boundary of the vortex $r = R_0$ such that

$$C_1 = \frac{R_0}{K_1(\psi_1 R_0)}, \quad C_2 = \left(-\frac{\psi_1^2}{\psi_2^2} \right) \frac{R_0}{J_1(\psi_2 R_0)} \quad (4.26)$$

and ψ_2 from the following nonlinear solution

$$\frac{K_2(\psi_1 R_0)}{K_1(\psi_1 R_0)} = -\frac{\psi_1 J_2(\psi_2 R_0)}{\psi_2 J_1(\psi_2 R_0)} \quad (4.27)$$

Eqs. (4.24) and (4.25) represents a dipolar vortex type solution [75]. We have plotted the solutions (4.24) and (4.25) in Fig. (4-3) by taking the same parameter as described earlier. It can be seen that like the vortex street solutions, the nonlinear dipolar structures are

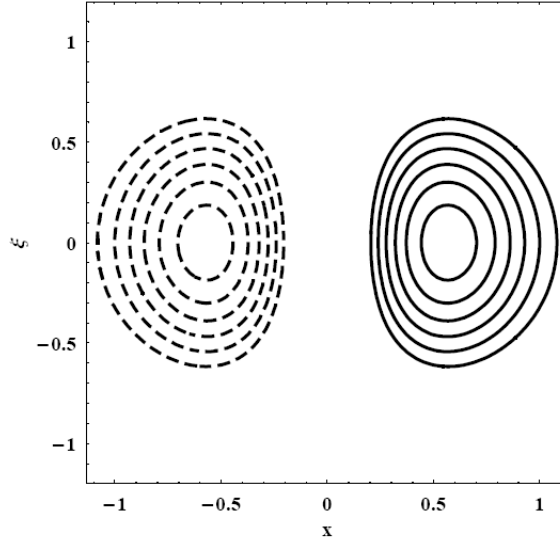


Figure 4-3: Two dimensional view of Φ obtained by solving equations (4.24) and (4.25) for the same plasma parameters as taken in Fig. (4-1).

also formed on a very short scalelength i.e., of the order of ion Larmor radius ρ_i (i.e., of the order of 10^{-6} cm).

Finally, in the case when the scalar nonlinearity is stronger than the vector nonlinearity, Eq. (4.17) reduces to

$$\partial_\xi \nabla_\perp^2 \Phi - \frac{1}{\chi n_{i0}} (\partial_x n_{i0}) \Phi \partial_\xi \Phi - \left(1 - \frac{U^*}{U} - \left(\frac{U_{sh}}{U} \right)^2 \right) \partial_\xi \Phi = 0 \quad (4.28)$$

which admits monopolar vortex like solutions [75].

4.3 Summary

In this chapter, linear and nonlinear propagation of ion-acoustic and drift dissipative mode in e-p-i quantum magnetoplasma has been investigated [53] in the presence of ion sheared flow. We found that the sheared ion flow can drive the quantum ion-acoustic wave

unstable. It is found that the linear ion drift waves are driven by the combined effects of parallel ion sheared flows and the ion neutral drag provided $|S_i| k_y > k_z$. The effects of the quantum corrections and the positron concentration on the linear ion-drift waves are also highlighted. Stationary solutions of the nonlinear equations that govern the dynamics of quantum ion-acoustic waves are also obtained. It is found that electrostatic monopolar, dipolar, and vortex street type solutions can appear in such a plasma. It is observed that the inclusion of the quantum statistical and Bohm potential terms as well as the positron concentration significantly modify the scalelengths of these structures. The present investigation may have relevance in the dense astrophysical plasmas where the quantum effects are pronounced.

Chapter 5

Dust-Acoustic Vortices and Shukla-Varma Mode in Quantum Plasma

In this chapter, we first present a brief introduction to dusty plasma and its applications. Some novel fundamental modes in a collisionless, uniform dusty plasma are also reviewed. We have investigated linear and nonlinear properties of dust-acoustic waves in a nonuniform, dense dissipative quantum plasma (composed of electrons, ions, and extremely massive negatively charged dust particles) in the presence of parallel dust sheared flow, by employing quantum hydrodynamic model (QHD). It is shown that parallel dust-shear flow drive the quantum dust-acoustic mode unstable. Stationary solutions of the nonlinear mode coupling equations that govern the dynamics of quantum dust-acoustic waves are also presented. It is shown that various types of electrostatic vortex structures can be formed. The coupled Shukla-Varma (SV) and convective cell mode is rederived in classical and quantum dusty magnetoplasma case. We found that the said mode is significantly modified for quantum dusty plasma case. Interesting limiting cases are also discussed. The relevance of our new findings with regard to the dense astrophysical environments is also pointed out.

5.1 Introduction to Dusty Plasma

A dusty plasma is normal electron-ion plasma with micron or sub-micron size dust grains. The dust-grains are either negatively or positively charged depending on their surrounding plasma environment. "*An admixture of such charged dust grains, electrons, ions and neutral particles form a dusty plasma*".

Dusty plasmas are low-temperature fully or partially ionized electrically conducting gases. In the absence of external forces, the dusty plasma satisfies the charge neutrality condition in equilibrium i.e., $q_i n_{i0} = e n_{e0} - q_d n_{d0}$, where q_j is the charge and n_{j0} represents number density of the j th species ($j = i$ for ions, e for electrons and d for the dust grains). The typical sizes of dust-particles ranges from 10 nm to μm and typical charge on the dust-grains $q_d \sim (10^3 - 10^6) e$, where e represents the charge of electron. Figure (5-1) is a typical example of Carbon grains grown in an experiment performed by Praburam and Goree [94] at temperatures of the order of 300-600 °K. The shape dust grains resembles with cauliflowers. It is well known that most of space plasmas such as interstellar molecular clouds, asteroid zones, planetary rings, nebulae, cometary tail and earth's environment, the presence of dust is well established [95, 96, 97, 98]. Typically, the dust grains in interstellar and circumstellar clouds are in the form of ice or silicates and metallic type such as graphite, magnetite or in the form of amorphous carbon type. Whereas, in the interplanetary medium, the existence of dust particles is also well known from the zodiacal light. The zodiacal light is due the presence of dust particles in the solar system. The dust particles are also produced to mutual collisions of asteroids in the asteroid belt. The interplanetary dust which is usually rich in carbon id often very fragile and fluffy. It is well established that most of the rings of outer giant planets are composed of various types of dust grains. It plays very fundamental role in the formation of planetary rings (such as Jupiter, Saturn, Uranus and Neptune), comet tails and nebulas. In our earth's atmosphere, the dust is produced due to man made pollution such as due to rocket and space shuttle exhausts. Recently, with the help of direct rocket probe measurements, the presence of both negatively and positively charged dust grains

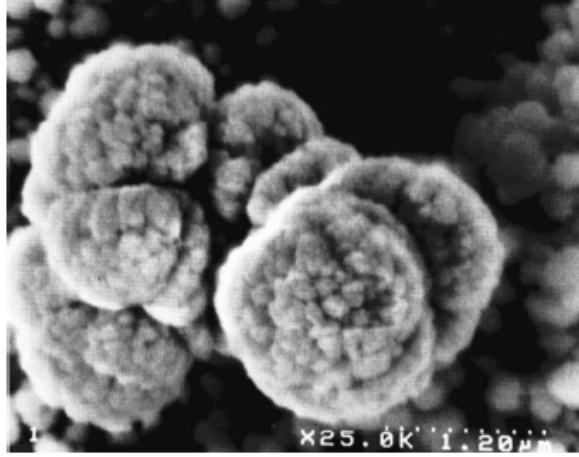


Figure 5-1: Carbon grains grown in a plasma having size of the order of 10nm to $1\mu\text{m}$ [94].

in the polar mesopause has been reported [99], where the polar mesosphere is located at altitudes from 80 to 93 km. There are several industrial applications of dusty plasma, such as in microelectronics, carbon nanotubes, the growth of Carbon to form a pure diamond structure [100] and in thermonuclear fusion plasmas [56]. In fusion devices, the dust particles are produced due to the sputtering of tokamak wall material which is composed of beryllium and carbon tiles. The presence of small fraction of dust play significant role to understand the transport process in tokamak plasma [101]. The dusty plasma support several new types of modes and instabilities in a uniform/nonuniform magnetized plasma.

One of the most fundamental mode in dusty plasma is the excitation of dust-acoustic wave (DAW) which was discovered by Shukla in (1989). Later Rao *et al.* [44], presented theory of linear and nonlinear dust-acoustic-waves (DAWs) by taking into account the dust-particle dynamics and Boltzmann distributed electrons and ions. The theoretical prediction of Rao *et al.* [44], was confirmed experimentally by Barkan *et al.* [46]. Later, dust-ion-acoustic-wave (DIAW) was theoretically predicted by Shukla and Silin [45] in

(1992) by considering electrons inertialess and follow Boltzmann type of distribution, whereas the ions were treated inertial and stationary extremely massive dust grains. The restoring force in dust-ion-acoustic-wave comes from the electron pressure, whereas, the ion mass provides the inertia. The effect of dust comes through the charge neutrality condition in equilibrium. For $|\omega| \gg \nu_{in}$ and $k^2 \lambda_{De}^2 \ll 1$, the DIAW satisfies a linear dispersion relation of type $\omega = k \sqrt{n_{i0}/n_{e0}} C_{sd}$, where ω is the perturbation wave frequency, k is the magnitude of the wavevector, ν_{in} is the effective ion collision frequency with dust or with neutrals and $C_{sd} = \sqrt{k_B T_e / m_i}$ is the dust ion-acoustic speed. Later, Barkan *et al.* [102], performed an experiment on dusty plasma and measured the phase speed of the wave which was found to be in good agreement with the theoretical predictions of Shukla and Silin [45]. The Coulomb crystal formation via the charged dust grains interaction was theoretically predicted by Ikezi [57] by considering Yukawa type repulsive force, when the Coulomb coupling parameter exceeds 170. Chu and I [58] experimentally verified the theoretical prediction of dust plasma crystal (DPC) which is in the form of regular ordered structure i.e., body centered and face centered cubic dust crystal structures. There exist dust lattice waves (DLW) in strongly coupled dusty plasma [103]. It is well established that dusty plasma supports various types of nonlinear structures such as dust-acoustic [104] and dust ion-acoustic [105] shock waves. As we have discussed earlier that in Ref. [40], Haque and Saleem found the possibility of various types of vortex structure formation in a nonuniform, dense quantum, highly magnetized electron-ion plasma. In this chapter, we shall study the quantum drift-dust acoustic vortices in inhomogeneous dusty plasma with dust sheared flow. In this case, various types of vortex are shown to exist. It is also found that in the presence dust, with quantum statistical and Bohm potential terms, the scale length of nonlinear vortical structures are significantly modified. These results are useful to explain nonlinear vortex structure formation in dense astrophysical environments [62].

5.1.1 A simple derivation of dust-acoustic mode

As discussed in the introduction section, that the novel dust-acoustic waves was predicted by Rao, Shukla and Yu [44], by taking into account the dust dynamics and assuming both the electrons and ions follow Boltzmann type of distribution, such that the perturbed number density of electrons and ions can be written as

$$n_{e1} \simeq n_{e0} \frac{e\phi}{k_B T_e} \quad (5.1)$$

and

$$n_{i1} \simeq -n_{i0} \frac{e\phi}{k_B T_i} \quad (5.2)$$

Whereas, the perturbed number density of dust can be calculated by using the dust-continuity and dust equation of motion, such that

$$\frac{\partial n_{d1}}{\partial t} + n_{d0} \nabla \cdot \mathbf{V}_d = 0 \quad (5.3)$$

and

$$m_d \frac{\partial \mathbf{V}_d}{\partial t} = Ze \nabla \phi \quad (5.4)$$

where m_d is the mass of dust, $-Ze$ is some constant charge on the dust grain surface, n_{d1} and \mathbf{V}_d are the perturbed number density of the dust and the dust fluid velocity, respectively, and ϕ is the electrostatic wave potential. To close the system of equations, we may use the Poisson's equation

$$\nabla^2 \phi = -4\pi e (n_{i1} - n_{e1} - Zn_{d1}) \quad (5.5)$$

To derive a local dispersion relation, we assume that all the perturbed quantities are varying as $\exp[-i(\omega t - \mathbf{k} \cdot \mathbf{r})]$, where ω and k are the angular frequency of the wave and

the wavevector, respectively, Eqs. (5.1) to (5.5) yield the following result

$$\omega^2 = \beta_0^2 k^2 C_{sd}^2 \left[1 + \frac{k^2 \lambda_{De}^2}{(1 + \eta \delta)} \right]^{-1} \quad (5.6)$$

which is the desired dispersion relation for the dust-acoustic waves. Here, $\delta = n_{i0}/n_{e0}$, $\lambda_{De} = \sqrt{k_B T_e / 4\pi n_{e0} e^2}$, $\beta_0^2 = Z(\delta - 1) / (1 + \eta \delta)$, $\eta = T_e / T_i$, and $C_{sd} = \sqrt{k_B T_e / m_d}$ is the dust-acoustic speed. Here, we have also used the charge neutrality condition in equilibrium i.e., $n_{i0} = n_{e0} + Z n_{d0}$. It may be noted here that for the dust acoustic waves, the electron and ion pressure provides the restoring force, whereas, the inertia comes from the dust mass. Since the mass of dust is extremely large as compared to the electron and ion mass, therefore, the dust-acoustic wave frequency would be very small as compared to the dust plasma frequency.

5.1.2 Dust ion-acoustic mode

In the previous subsection, we have derived a linear dispersion relation for dust-acoustic waves by assuming that both the electrons and ions are inertialess and thus follow Boltzmann type of distribution in the dust-acoustic wave potential ϕ . Shukla and Silin [45] predicted the dust-ion-acoustic waves in dusty plasma. They have assumed that the phase velocity of the said wave is much smaller than the electron thermal speed and larger than the ion and dust thermal speeds, such that the electrons are assumed to be inertialess and follow Boltzmann distribution. Whereas, ions are dynamic and the perturbed number density of the ions and ion fluid velocity can be obtained from the following ion continuity equation, such that

$$\frac{\partial n_{i1}}{\partial t} + n_{i0} \nabla \cdot \mathbf{V}_i = 0 \quad (5.7)$$

and the ion equation of motion

$$m_i \frac{\partial \mathbf{V}_i}{\partial t} = -e \nabla \phi - 3 \frac{k_B T_i}{n_{i0}} \nabla n_{i1} \quad (5.8)$$

where the ion fluid velocity is \mathbf{V}_i . Taking partial time derivative of Eq. (5.7) and using Eqs. (5.8) and (5.5), after Fourier transforming, we obtain the following dispersion relation

$$1 + \frac{1}{k^2 \lambda_{De}^2} - \frac{\omega_{pi}^2 + \omega_{pe}^2}{\omega^2} = 0 \quad (5.9)$$

In the derivation of Eq. (5.8), we taken stationary dust such that $n_{d1} = 0$ and also assumed $\omega/k \gg V_{ti}; V_{td}$, where V_{ti} (V_{td}) is the thermal velocity of the ions (dust). Since the dust mass is very large as compared to the ion mass, therefore, the ion plasma frequency would be larger than the dust plasma frequency. Consequently, Eq. (5.9) can be rewritten as

$$\omega^2 = \frac{k^2 C_s^2}{(1 + k^2 \lambda_{De}^2)} \quad (5.10)$$

where $C_s = \sqrt{(n_{i0}/n_{e0})} c_s$, and $c_s = \sqrt{k_B T_e / m_i}$ is the usual ion-acoustic speed. For perturbation wavelength larger than the electron Debye length, Eq. (5.10) yield the following dispersion relation of dust-ion-acoustic waves

$$\omega = k \sqrt{\left(\frac{n_{i0}}{n_{e0}} \right) \frac{k_B T_e}{m_i}} \quad (5.11)$$

Since in duty plasma, with negatively charged dust grains, the ion number density is much larger than the electron number density, therefore, the phase velocity of dust-ion-acoustic wave would be always larger than the ion acoustic speed. Like the dust-acoustic waves, the dust-ion-acoustic waves has also been detected experimentally [46, 48] with a typical frequency of kHz range.

So far, we have discussed a simple derivation of dust-acoustic and dust-ion-acoustic waves in a classical plasma. In the next section, we shall present linear and nonlinear study of dust-acoustic mode in dense quantum plasma using QHD model.

5.2 Nonlinear Model for Quantum Dust-Acoustic Waves

We consider a dusty plasma which consists of electrons, ions and negatively charged dust grains. We assume that the dust charge state z_d is fixed and the plasma is inhomogeneous and the applied magnetic field is uniform such that $\mathbf{B} = B_0 \hat{z}$, where B_0 is the strength of external magnetic field and \hat{z} is a unit vector along the z -axis. We also assume that in equilibrium, there is a streaming flow of the dust given by $v_{d0}(x) \hat{z}$, having velocity gradient as well as dust density gradient ($\partial n_{d0}/\partial x$) along the x -axis. We further assume that both the streaming flow of the dust as well as density gradients are maintained by some external sources. For low-frequency quantum dust-acoustic type modes, we assume that the phase velocity of the wave is $v_{Fd} \ll \omega/k \ll v_{Fi}; v_{Fe}$ (where v_{Fj} is the Fermi velocity of the j th-species, such that $j = e, i$, and d for electron, ion and dust, respectively). Using the quantum hydrodynamic (QHD) model, and following the same procedure as described in Sec. 3.2, the parallel component of inertialess electron equation of motion with quantum corrections, yield the following result

$$\frac{n_{e1}}{n_{e0}} = \frac{e}{2k_B T_{Fe}} \phi + \frac{\hbar^2}{16m_e k_B^2 T_{Fe}^2} \nabla^2(e\phi) \quad (5.12)$$

For inertialess ions, the parallel component of equation of motion yield the following result

$$\frac{n_{i1}}{n_{i0}} = -\frac{1}{\sigma_i} \frac{e}{2k_B T_{Fe}} \phi \quad (5.13)$$

where $\sigma_i = T_{Fi}/T_{Fe}$. It may be noted here that we have ignored the Bohm potential term for the ions, since the mass of ion would appear in the denominator and would make this term very small in the comparison with the electron term. Furthermore, we are treating the dust as a classical fluid.

The equation of motion for a collisional cold dust can be written as

$$m_d n_d (d_t + \nu_{dn} + \mathbf{v}_d \cdot \nabla) \mathbf{v}_d = -e z_d n_d \left(\mathbf{E} + \frac{1}{c} \mathbf{v}_d \times \mathbf{B}_0 \right) \quad (5.14)$$

where $d_t = \partial_t + v_{d0}\partial_z$ and $\mathbf{E} = -\nabla\phi$ for electrostatic case.

Under the drift-approximation, which is valid for low-frequency waves such that $|\partial_t| \ll \omega_{cd}$ ($\omega_{cd} \equiv (ez_d B_0/m_d c)$ is the dust gyrofrequency), the perpendicular component of dust fluid velocity can be expressed as

$$v_{d\perp} = \frac{c}{B_0} \hat{z} \times \nabla_{\perp} \phi + \frac{c}{B_0 \omega_{cd}} \left(d_t + \nu_{dn} + \frac{c}{B_0} \hat{z} \times \nabla_{\perp} \phi + v_{dz} \partial_z \right) \nabla_{\perp} \phi \quad (5.15)$$

where $(c/B_0) \hat{z} \times \nabla_{\perp} \phi$ term represents the usual electric field drift and the second term is the polarization drift.

For dusty plasma, the Poisson's equation can be written as

$$\nabla^2 \phi = -4\pi e(n_i - n_e - z_d n_d) \quad (5.16)$$

Using Eqs. (5.12) and (5.13), the above equation yields,

$$\frac{n_{d1}}{n_{d0}} = \chi \left[-\Phi + \left(\frac{\lambda_{Fd}^2 - \chi_1 H^2}{\chi} \right) \nabla^2 \Phi \right] \quad (5.17)$$

where the electrostatic potential ϕ has been normalized and defined as $\Phi = e\phi/(2k_B T_{Fe})$, $\chi = (1/\sigma_i + p)/(1-p)$, $\chi_1 = p/(1-p)$, and $p = n_{e0}/n_{i0}$. Here, $\lambda_{Fd} = \sqrt{k_B T_{Fe}/2\pi z_d n_{d0} e^2}$ is the Fermi wavelength in dusty plasma, and $n_{i0} = n_{e0} + z_d n_{d0}$ is the charge neutrality condition in equilibrium, and $H = \sqrt{\hbar^2/8m_e k_B T_{Fe}}$ is the electron Bohm potential.

The continuity equation for the dust can be written as

$$\frac{\partial n_d}{\partial t} + \nabla \cdot (n_d \mathbf{v}_d) = 0 \quad (5.18)$$

From Eqs. (5.15), (5.17) and (5.18), we get

$$\begin{aligned} & D_{\phi} \left[-\Phi + \left(\frac{\lambda_{Fd}^2 + \rho_d^2 - \chi_1 H^2}{\chi} \right) \nabla^2 \Phi \right] - \nu_{dn} \left[-\Phi + \left(\frac{\lambda_{Fd}^2 - \chi_1 H^2}{\chi} \right) \nabla^2 \Phi \right] \\ & + \frac{c_{sd}^2}{\omega_{cd}} (\partial_x \ln(\chi n_{d0})) \Phi \partial_y \Phi + \frac{c_{sd}^2}{\omega_{cd} \chi} \hat{z} \times \nabla_{\perp} \Phi \cdot \nabla \ln n_{d0} + \frac{1}{\chi} \partial_z v_{dz} = 0 \end{aligned} \quad (5.19)$$

where $D_\phi = d_t + \nu_{dn} + (c_{sd}^2/\omega_{cd}) \hat{z} \times \nabla \Phi \cdot \nabla_\perp + v_{dz} \partial_z$, $c_{sd} = \sqrt{2k_B T_{Fe}/m_d}$ is the quantum dust-acoustic speed, ω_{cd} is the dust gyro-frequency, and ρ_d is the Larmor radius of the dust.

The equation of motion of dust along the z-axis can be written as

$$D_\phi v_{dz} = -c_s^2 \partial_z \Phi - \frac{c_s^2}{\omega_{ci}} (\hat{z} \times \nabla_\perp \Phi \cdot \nabla) v_{d0}$$

or

$$D_\phi v_{dz} = c_{sd}^2 [\partial_z + S_d \partial_y] \Phi \quad (5.20)$$

where $S_d = (\partial_x v_{d0})/\omega_{cd}$ is the shear in the parallel velocity component.

5.2.1 Dispersion relation

To derive linear dispersion relation from Eqs. (5.19) and (5.20), we neglect the nonlinear terms and assume that all the perturbed quantities are proportional to $\exp[i(k_y \hat{y} + k_z \hat{z} - \omega t)]$, we get

$$\left(\omega' + i\nu_{dn}\right)^2 k_\perp^2 \rho_i^2 + \left(\omega' + i\nu_{dn}\right) [\omega(1 + (\lambda_{Fd}^2 - H^2)k^2 - \omega^*) - k_z^2 c_{sd}^2 \left(1 - \frac{k_y}{k_z} S_d\right)] = 0 \quad (5.21)$$

where ω' is the Doppler shifted frequency and $\omega^* = -(c_s^2/\omega_{cd}) d_x (\ln n_{i0})$ is the drift-frequency. For collisionless plasma, the above dispersion relation yields

$$\omega' = k_z c_{sd} \left(\frac{1 - k_y S_d / k_z}{1 + (\lambda_{Fd}^2 - H^2)k^2 + k_\perp^2 \rho_d^2} \right)^{1/2} \quad (5.22)$$

It is evident from the above expression that the quantum dust acoustic mode becomes unstable for $k_y S_d > k_z$.

Equation (5.21) predicts an oscillatory drift-dust wave instability for $\omega' \ll \nu_{dn}$. By

letting $\omega = \omega^* + i\gamma$, we get

$$\gamma = -\frac{\nu_{dn}^2 k_{\perp}^2 \rho_d^2}{1 + (\lambda_{Fd}^2 - H^2)k^2} - \frac{k_z^2 c_{sd}^2 \left(1 - \frac{k_y}{k_z} S_d\right)}{1 + (\lambda_{Fd}^2 - H^2)k^2} \quad (5.23)$$

Eq. (5.23) shows that the quantum corrections modify the scalelengths of the system. Note that in the absence of parallel dust shear velocity, the wave is damped, however, the dust-drift-dissipative instability gives growth provided that $|S_d| k_y > k_z$. Therefore, it follows from Eq. (5.23) that dust-drift waves can be driven by the combined effects of dust-sheared flow and the dust-neutral drag provided $|S_d| k_y > k_z$.

5.2.2 Nonlinear analysis

To illustrate how vortex structures can be formed in a dense quantum dusty plasma, we consider a collisionless highly magnetized plasma. To find localized vortex type solution, we may define new coordinate ξ such that $\xi = y + \alpha z - ut$, where u is the vortex speed and α is some constant. Notice that we are assuming $|\mathbf{v}_E \cdot \nabla| \gg |v_{dz} \partial_z|$, where $\mathbf{v}_E = (c/B_0) \hat{z} \times \nabla_{\perp} \phi$. Equation (5.21) in the transformed frame can be expressed in the following manner

$$D_{\phi} v_{dz} = -c_{sd}^2 [\alpha \partial_{\xi} + S_d \partial_{\xi}] \Phi$$

where $D_{\phi} = \partial_{\xi} - (c_{sd}^2 / U \omega_{cd}) (\partial_x \Phi \partial_{\xi} - \partial_{\xi} \Phi \partial_x)$ is a differential operator and $U = u - \alpha v_{d0}$. The possible solution of above equation gives

$$v_{dz} = -\frac{c_{sd}^2}{U} (\alpha + S_d) \Phi \quad (5.24)$$

Using Eqs. (5.19) and (5.24), we get

$$\begin{aligned} & \sqrt{a_s} \partial_{\xi} \Phi + \frac{c_{sd}^2 \sqrt{a_s}}{\omega_{cd} U \chi n_{d0}} (\partial_x \chi n_{d0}) \Phi \partial_{\xi} \Phi - \frac{c_{sd}^2 \sqrt{a_s}}{\omega_{cd} U \chi n_{d0}} \frac{dn_{d0}}{dx} \partial_{\xi} \Phi \\ & - \frac{\alpha c_{sd}^2 \sqrt{a_s}}{\chi U^2} (\alpha + S_d) \partial_{\xi} \Phi + \frac{c_{sd}^2 \sqrt{a_s}}{\omega_{cd} U} J[\Phi, a_s \nabla_{\perp}^2 \Phi] - \sqrt{a_s} \partial_{\xi} a_s \nabla_{\perp}^2 \Phi = 0 \end{aligned}$$

or

$$(1 - U^* - U_{sh}^2) \partial_\xi \Phi + J[\Phi, \nabla_\perp^2 \Phi] + \frac{1}{\chi n_{d0}} (\partial_x \chi n_{d0}) \Phi \partial_\xi \Phi - \partial_\xi \nabla_\perp^2 \Phi = 0 \quad (5.25)$$

The coordinates ξ and x are normalized by $\sqrt{a_s}$ and $c_{sd}^2/U\omega_{cd}$ respectively. $U^* = -d_x (\ln n_{d0}) / \chi$ is the normalized drift velocity and $U_{sh} = (\alpha c_{sd}^2 / \chi U^2) (\alpha + S_d)$. Here U_{sh} is related to the dust shear flow, and $a_s = (\lambda_{Fe}^2 - H^2 + \rho_d^2) / \chi$. If we ignore the scalar nonlinearity (i.e., $\Phi \partial_\xi \Phi$) and set $(1 - U^* - U_{sh}^2) = 0$, then we obtain the following equation

$$\partial_\xi \nabla_\perp^2 \Phi - J[\Phi, \nabla_\perp^2 \Phi] = 0 \quad (5.26)$$

where $\nabla_\perp^2 = \partial_x^2 + \partial_\xi^2$. Here again, we have normalized ∇_\perp^2 operator with a_s^2 . Eq. (5.26) is satisfied by

$$\nabla_\perp^2 \Phi = \frac{4\Phi_0}{a_0^2} \exp \left[-\frac{2}{\Phi_0} \left(\Phi - \frac{\sqrt{a_s} U \omega_{ci}}{c_s^2} x \right) \right]$$

Here Φ_0 and a_0 are some constants. Above equation is satisfied by the following solution

$$\Phi = \frac{\sqrt{a_s} U \omega_{ci}}{c_s^2} x + \Phi_{d0} \ln \left[2 \cosh x + 2 \left(1 - \frac{1}{R_0^2} \right) \cos \xi \right] \quad (5.27)$$

For $R_0^2 > 1$ the vortex profile given by Eq. (5.27) resembles the Kelvin-Stuart "cats eyes" that are chains of vortices [73], where R_0 represents the vortex size. The vortex chain speed is $U_d = [U^* \pm \sqrt{(U^*)^2 + 4(U_{sh})^2}] / 2$. We have plotted Eq. (5.27) (x, ξ) plane by choosing some typical dense astrophysical plasma parameters for homogeneous plasma case [42]: $n_0 \sim 10^{27} \text{ cm}^{-3}$ and the magnetic field $B_0 = 2 \times 10^9 \text{ Gauss}$, $M = U_d / c_{sd} = 0.8$, $R_0 / \rho_d = 1$, $\alpha = 0.2$ and dust sheared flow parameter $S_d = 0.1$. The electron Fermi temperature is $T_{Fe} = 4.32 \times 10^7 \text{ }^\circ\text{K}$ and $H = 3.7 \times 10^{-2}$. It shows a periodic vortex street with the periodicity in ξ .

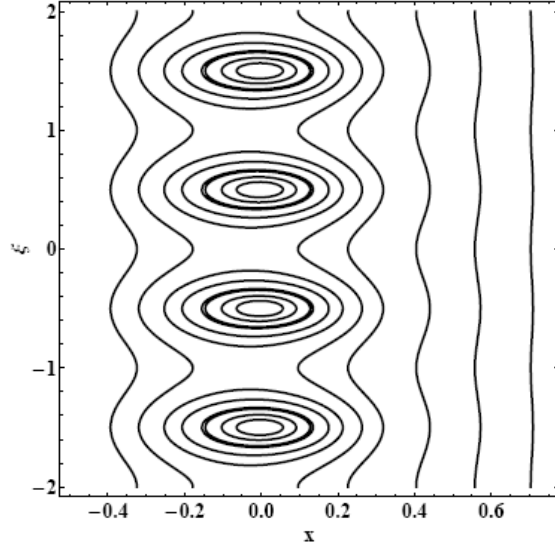


Figure 5-2: A vortex chain profile is plotted by solving equation (5.27) for dense astrophysical plasma parameters.

If we ignore the scalar and vector nonlinearities in Eq. (5.25), we obtain

$$\partial_\xi \nabla_\perp^2 \Phi - \left(1 - \frac{U^*}{U} - \left(\frac{U_{sh}}{U} \right)^2 \right) \partial_\xi \Phi = 0 \quad (5.28)$$

where $\psi_1 = \left(1 - \frac{U^*}{U} - \left(\frac{U_{sh}}{U} \right)^2 \right)$. The above equation is satisfied with the following expression

$$\nabla_\perp^2 \Phi - \psi_1 \Phi = f \left(\Phi - \frac{U \omega_{ci}}{c_{sd}^2} x \right) \quad (5.29)$$

The function $f \left(\Phi - \frac{U \omega_{ci}}{c_{sd}^2} x \right) = W \left(\Phi - \frac{U \omega_{ci}}{c_{sd}^2} x \right)$ is assumed to follow linearly the Larchiev Reznik technique, where W is a constant. The Eq. (5.29) thus gives us

$$\nabla_\perp^2 \Phi - \psi_1 \Phi = W \left(\Phi - \frac{U \omega_{ci}}{c_{sd}^2} x \right) \quad (5.30)$$

This equation was transformed in plane polar coordinates for the outer ($r < R_0$) as well as for the inner ($r > R_0$) regions by defining a circle of radius R_0 . The general solutions for the said two regions are written in the following way

$$\Phi_{out}(r, \theta) = C_1 K_1(\psi_1 r) \cos \theta \quad (5.31)$$

and

$$\Phi_{in}(r, \theta) = \left[C_2 J_1(\psi_2 r) + \left(\frac{\psi_1^2 + \psi_2^2}{\psi_2^2} \right) \frac{U \omega_{ci}}{c_s^2} r \right] \cos \theta \quad (5.32)$$

where $\psi_2^2 = -(\psi_1^2 + W)$, $W = -(\psi_1^2 + \psi_2^2)$. Here again $K_1(J_1)$ represents the modified(ordinary) Bessel functions of the first kind. The two constants C_1 and C_2 are calculated by using the continuity of Φ , $\partial_r \Phi$, and $\nabla_\perp^2 \Phi$ at $r = R_0$,

$$C_1 = \frac{U \omega_{ci}}{c_{sd}^2} \frac{R_0}{K_1(\psi_1 R_0)}, \quad C_2 = \frac{U \omega_{ci}}{c_{sd}^2} \left(-\frac{\psi_1^2}{\psi_2^2} \right) \frac{R_0}{J_1(\psi_2 R_0)} \quad (5.33)$$

and ψ_2 from the following nonlinear solution

$$\frac{K_2(\psi_1 R_0)}{K_1(\psi_1 R_0)} = -\frac{\psi_1 J_2(\psi_2 R_0)}{\psi_2 J_1(\psi_2 R_0)} \quad (5.34)$$

In Fig. (5-3), we have plotted the solutions (5.31) and (5.32) in the form of a dipolar vortex [75] for various plasma parameters: $n_{i0} = 1.43 \times 10^{26} \text{cm}^{-3}$, $n_{d0} = 0.43 \times 10^{22} \text{cm}^{-3}$, $z_d = 10^3$, $B_0 = 10^{13} \text{ Gauss}$, $\alpha = 0.2$, and $U_p/c_{sd} = 0.8$. We find that $\rho_{sd} = 4.518 \times 10^{-10} \text{ cm}$, $T_{Fe} = 1.133 \times 10^7 \text{ }^\circ\text{K}$ and the normalized quantum parameter $H = 3.123 \times 10^{-10}$ and shear flow parameter $S_d = 0.1$. It can be seen that like the vortex street solutions, the nonlinear dipolar structures are also formed on a very short scalelength i.e., of the order of dust Larmor radius ρ_{sd} .

Finally, in the case when the scalar nonlinearity is stronger than the vector nonlin-

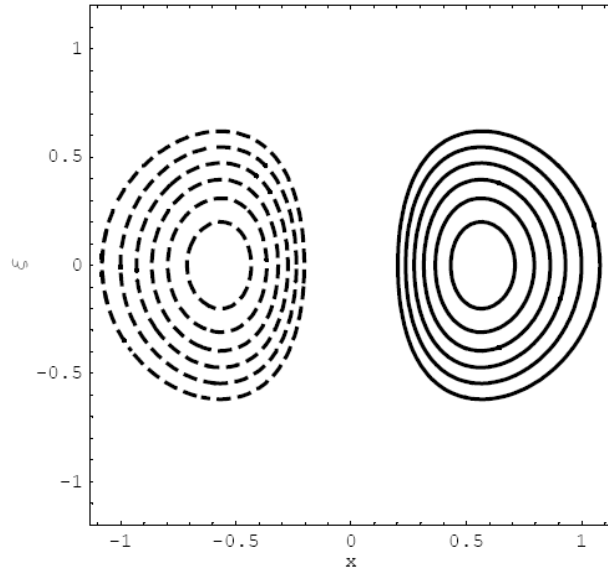


Figure 5-3: Two dimensional contour plot of Φ obtained by solving equations (5.31) and (5.32) for the same parameters as given in the text.

earity, Eq. (5.25) reduces to

$$\partial_\xi \nabla_\perp^2 \Phi - \frac{1}{\chi^{n_{d0}}} (\partial_x \chi^{n_{d0}}) \Phi \partial_\xi \Phi - \left(1 - \frac{U^*}{U} - \left(\frac{U_{sh}}{U} \right)^2 \right) \partial_\xi \Phi = 0 \quad (5.35)$$

which admits monopolar vortex like solutions [61, 75].

5.2.3 Summary

In this chapter, we have investigated [61] the linear and nonlinear propagation characteristics of quantum dust-acoustic waves (QDAW) in an inhomogeneous and dissipative dense magnetoplasma with sheared dust flows parallel to the ambient magnetic field. It is found that the linear drift dissipative waves can drive the system unstable provided the gradient of the shear flow is negative. The effects of the quantum corrections on the linear drift waves are also highlighted. It is observed that the inclusion of dust enhances the scale length of the system over which the wave propagates. Stationary solutions of the nonlinear equations that governs the dynamics of quantum dust-acoustic waves are also obtained. It is found that electrostatic monopolar, dipolar and vortex street type solutions can appear in such a plasma. It is observed that the quantum statistical and Bohm potential terms significantly modify the scale lengths of these structures. The present investigation may be beneficial to understand the dense astrophysical plasmas where the quantum effects are expected to play a vital role. Finally, we would like to mention that although a lot of work has been done on electromagnetic vortices in the classical domain. However, the area is still unexplored in quantum plasmas. The future investigations should incorporate the electromagnetic effects in nonuniform plasmas.

5.3 Shukla-Varma and Convective Cell Mode in Quantum Dusty Plasma

The coupled Shukla-Varma (SV) and convective cell mode is revisited in classical and quantum dusty magnetoplasmas. It is shown that the inclusion of electron thermal effects modifies the original coupled SV and convective cell modes. It is also discussed how the quantum effects can be incorporated in the coupled SV and convective cell modes.

5.3.1 Introduction

During the last two decades, there has been a considerable interest in the plasma physicists community to understand new features of dusty plasmas [97, 98, 99]. Dusty plasma is ubiquitous in nature and its constituents are electrons, ions and micron or submicron sized highly charged dust grains. The dust particles can be negatively or positively charged depending upon the background plasma conditions. Since the presence of additional dust component enhances the complexity of the plasma, therefore, very often in the literature it is also referred as complex plasma. The applications of dusty plasma ranges from astrophysical to laboratory plasmas [44, 75]. Since the typical mass of dust grains is of the order of $(10^6 - 10^8) m_p$, where m_p is the mass of proton, consequently, it introduces new scale lengths which are not so common in traditional electron-ion plasma.

As discussed in Sec. (5.1), that there are two well known two normal modes in a weakly coupled dusty plasma, namely the dust-acoustic (DA) and dust-ion-acoustic (DIA) modes, in unmagnetized plasma. These two novel modes were predicted by Rao, Shukla and Yu [44], and Shukla and Silin [45] theoretically. In the normal dust-acoustic mode, the inertialess Boltzmann distributed electrons and ions provide the restoring force, whereas, massive dust provides the inertia. In the case of dust-ion-acoustic mode, the phase velocity of DIA mode is assumed to be larger than the thermal velocity of dust and ion. In this case, the inertia come from the massive dust and ions and the electron pressure provide restoring force. In the dust ion acoustic mode, the dust is taken to be

immobile. Both the dust-acoustic and dust-ion-acoustic modes have been experimentally detected [46, 47, 48]. For instance, in the cosmic plasma and in the earth’s mesosphere, ultra-low-frequency dust ion acoustic wave propagate. In the Saturn’s F-region, very low-frequency DIAW’s noise can also be produced [45].

Dust-contaminated magnetoplasmas are generally believed to be inhomogeneous and capable to excite several new types of drift-waves. As discussed earlier, quantum plasma has gained interest during the last few years due to its applications in a wide variety of physical situations in complex plasmas [61]: such as in dense astrophysical environments [3], in microelectronic devices [1], in laser-plasma experiments [5], in quantum optics [35, 108], etc. At very low-temperatures of plasma, the de-Broglie wavelength of the plasma particles becomes comparable to the interparticle spacing or simply when the plasma temperature becomes comparable or less than the Fermi temperature, the plasma behaves like a highly degenerate Fermi gas and quantum mechanical effects start playing role.

For quantum plasmas, the Schrödinger-Poisson, Wigner-Poisson, and Dirac-Maxwell models are most widely used models to study quantum plasmas. The said quantum models are very similar to fluid and kinetic models of the classical plasmas. To model quantum plasmas, the quantum hydrodynamic (QHD) model is widely used. The QHD model is different from the classical model due to an additional term which is known as the “Bohm potential” term. In accordance with the Bohr correspondence principle, all the classical results should be recovered in the limit $\hbar \rightarrow 0$.

In the next section, we shall rederive the coupled Shukla-Varma (SV) and convective cell mode in a classical and quantum dusty plasma with electron thermal effects. Some interesting limiting cases are also discussed. We have also shown how the Shukla-Varma and convective cell mode is modified in quantum plasma. effects can be incorporated in the coupled Shukla-Varma and convective cell mode.

5.3.2 Shukla-Varma and convective cell mode: classical case

To derive coupled Shukla-Varma and convective cell mode in the presence of electron pressure. Let us consider an inhomogeneous dusty magnetoplasma with fixed dust. We assume that in equilibrium the density gradients of electrons, ions and dust are in the x direction. To obtain a linear dispersion relation for the low-frequency (by comparison with the ion gyrofrequency, $\omega_{ci} (\equiv eB_0/m_i c)$), long-wavelength (by comparison with the ion-gyroradius, r_L) electrostatic SV and convective cell mode, we assume that the external magnetic field is uniform and pointing along the z -axis and the wave is propagating in the x - y plane. The charge neutrality condition for equilibrium can be written as

$$n_{i0} = n_{e0} + z_d n_{d0}, \quad (5.36)$$

where n_{j0} is the equilibrium number density of the j th-species ($j = i$ for ions, e for electrons, and d for the dust species) and z_d is fixed charged state of negatively charged dust. The equation of motion for the ions is,

$$m_i n_i (\partial_t + \mathbf{v}_i \cdot \nabla) \mathbf{v}_i = en_i \left(\mathbf{E} + \frac{1}{c} \mathbf{v}_i \times \mathbf{B}_0 \right), \quad (5.37)$$

where \mathbf{v}_i is the ion fluid velocity, m_i is the mass of ion, n_i is the number density of ion and e is the magnitude of the electron charge. For electrostatic perturbations, we have $\mathbf{E} = -\nabla\phi$, where ϕ is the electrostatic potential and \mathbf{B}_0 is the ambient magnetic field. The perpendicular component of ion fluid velocity under drift-approximation from Eq. (5.37) can be written as

$$\mathbf{v}_{i\perp} = \frac{c}{B_0} \hat{\mathbf{z}} \times \nabla_{\perp} \phi - \frac{c}{B_0 \omega_{ci}} \left(\partial_t + \frac{c}{B_0} \hat{\mathbf{z}} \times \nabla_{\perp} \phi \cdot \nabla + v_{iz} \partial_z \right) \nabla_{\perp} \phi, \quad (5.38)$$

Here on the right hand side, the first term is $\mathbf{E} \times \mathbf{B}$ drift and the second one is the polarization drift. The parallel equation of motion of ions is

$$\frac{\partial v_{iz}}{\partial t} = -\frac{e}{m_i} \frac{\partial \phi}{\partial z}. \quad (5.39)$$

The equation of motion for the hot electrons is given by

$$m_e n_e (\partial_t + \mathbf{v}_e \cdot \nabla) \mathbf{v}_e = -en_e \left(\mathbf{E} + \frac{1}{c} \mathbf{v}_e \times \mathbf{B}_0 \right) - k_B T_e \nabla n_e, \quad (5.40)$$

where m_e is the mass of electron, n_e is the electron number density, and \mathbf{v}_e is the electron fluid velocity. The perpendicular component of electron velocity from Eq. (5.40) yields

$$\mathbf{v}_{e\perp} \approx \frac{c}{B_0} \hat{z} \times \nabla_{\perp} \phi, \quad (5.41)$$

where the electron polarization drift and diamagnetic drift have been ignored in the above expression, for simplicity. The z-component of electron fluid velocity is given by

$$\frac{\partial \mathbf{v}_{ez}}{\partial t} = \frac{e}{m_e} \frac{\partial \phi}{\partial z} - \frac{k_B T_e}{m_e n_e} \frac{\partial n_e}{\partial z}. \quad (5.42)$$

The continuity equation of electron is given by

$$\frac{\partial n_e}{\partial t} + \nabla \cdot (n_e \mathbf{v}_e) = 0, \quad (5.43)$$

Using Eq. (5.41) the above equation (5.43) becomes

$$\frac{\partial n_{e1}}{\partial t} + \frac{c}{B_0} \hat{z} \times \nabla \phi \cdot \nabla n_{e0} + n_{e0} \frac{\partial v_{ez}}{\partial z} = 0. \quad (5.44)$$

The ion continuity equation using drift-approximation for the ions given by Eq. (5.38), we get

$$\frac{\partial n_{i1}}{\partial t} + \frac{c}{B_0} \hat{z} \times \nabla \phi \cdot \nabla n_{i0} - \frac{c}{B_0 \omega_{ci}} \left(\partial_t + \frac{c}{B_0} \hat{z} \times \nabla \phi \cdot \nabla + v_{iz} \partial_z \right) \nabla_{\perp}^2 \phi + n_{i0} \frac{\partial v_{iz}}{\partial z} = 0. \quad (5.45)$$

Subtracting Eqs. (5.45) from (5.44), after using the quasi-neutrality condition ($n_{i1} \approx n_{e1}$), and ignoring the parallel ion dynamics, we have

$$\frac{\partial \nabla_{\perp}^2 \phi}{\partial t} + \frac{\omega_{ci}^2}{\omega_{pi}^2} \frac{4\pi c}{B_0} \hat{z} \times \nabla (q_d n_{d0}) \cdot \nabla \phi + \frac{p B_0 \omega_{ci}}{c} \frac{\partial v_{ez}}{\partial z} = 0, \quad (5.46)$$

where $\omega_{pi} = \sqrt{4\pi n_{0i} e^2 / m_i}$ is the ion plasma frequency, $q_d = e z_d$, and $p = n_{e0} / n_{i0}$. Eqs. (5.42), (5.44), and (5.46) are the desired set of equations to study the convective cells and dust drift-ion acoustic waves in dust-contaminated magnetoplasma. The traditional coupled SV and convective cell mode was derived under cold plasma limit $|\partial_t| \gg V_{Te} |\partial_z|$ [63, 64]. Here, we have rederived the SV and convective cell mode by retaining the electron thermal effect. Fourier transforming Eqs. (5.42), (5.44) and (5.46), we obtain the following dispersion relation

$$\omega^3 - \omega_{SV} \omega^2 - (\omega_{cc}^2 + v_{Te}^2 k_z^2) \omega + \left(\omega_{SV} k_z^2 v_{Te}^2 - \frac{\omega_{cc}^2 k_y \kappa_{ne0}}{\omega_{ce}} v_{Te}^2 \right) = 0, \quad (5.47)$$

where $\omega_{SV} = \omega_{ci}^2 4\pi c \partial_x (q_d n_{d0}) / (\omega_{pi}^2 k_y B_0)$, $\omega_{cc} = k_z \sqrt{p \omega_{ci} \omega_{ce}} / k_y$, $\omega_{ce} = |e B_0 / m_e c|$ and $\kappa_{ne0} = \partial_x \ln n_{e0}$. Eq. (5.47) is the modified Shukla-Varma and convective cell mode in the presence of electron thermal effects. It is worth-mentioned here that when the phase velocity of the mode becomes very close to the electron thermal velocity, the Landau damping effect can not be ignored and hence the kinetic effects should be incorporated in the present study. However, the original coupled Shukla-Varma and convective cell mode [63, 64] is completely recovered by taking the limit $|\partial_t| \gg V_{Te} |\partial_z|$. However, if we set the last term in Eq. (5.47) equal to zero, then we get the following result

$$\omega^2 - \frac{\omega_{ci}^2}{\omega_{pi}^2} \frac{4\pi c}{k_y B_0} \partial_x (q_d n_{d0}) \omega - (\omega_{cc}^2 + v_{Te}^2 k_z^2) = 0. \quad (5.48)$$

5.3.3 Shukla-Varma and convective cell modes: for quantum plasmas

In the last sub-section, we have derived the coupled SV and convective cell mode in a classical plasma. However, when the density of plasma becomes very high, the quantum effects seems to become important. In this section, we shall rederive the coupled Shukla-Varma and the convective cell mode for quantum plasma by using QHD model for the electrons for which the electron pressure term can be written as [68]

$$p_e = \frac{\hbar^2}{5m_e} (3\pi^2)^{\frac{2}{3}} n_e^{\frac{5}{3}}, \quad (5.49)$$

The z -component equation of motion for the electrons can be written as

$$\frac{\partial \mathbf{v}_{ez}}{\partial t} = \frac{e}{m_e} \frac{\partial \phi}{\partial z} - \frac{1}{m_e n_e} \frac{\partial p_e}{\partial z} + \frac{\hbar^2}{2m_e^2} \frac{\partial}{\partial z} \left(\frac{\nabla^2 \sqrt{n_e}}{\sqrt{n_e}} \right). \quad (5.50)$$

Here, we have assumed that the applied magnetic field is pointing in the z -direction. Using sinusoidal approximation for the perturbed quantities, Eqs. (5.44), (5.50), and (5.46), yield the following result

$$\begin{aligned} & \omega^4 - \omega_{sv} \omega^3 - \left[\omega_{cc}^2 + \frac{1}{3} k_z^2 v_{Fe}^2 \left(1 - \frac{3}{4} \frac{H_e^2 k^2}{v_{Fe}^2} \right) \right] \omega^2 \\ & + \frac{1}{3} \left[\omega_{sv} \left(1 - \frac{3}{4} \frac{H_e^2 k^2}{v_{Fe}^2} \right) k_z^2 v_{Fe}^2 - \frac{\omega_{cc}^2 k_y \kappa_{ne0}}{\omega_{ce}} v_{Fe}^2 \right] \omega - \frac{1}{4} \omega_{cc}^2 k_z^2 \frac{H_e^2 k^2}{4} = 0, \end{aligned} \quad (5.51)$$

which is the desired dispersion relation for coupled Shukla-Varma and convective cell mode for quantum plasmas with electron pressure term. Here, $k = \sqrt{k_y^2 + k_z^2}$, $v_{Fe} = \sqrt{2k_B T_{Fe}/m_e}$ and $H_e = \hbar/m_e$. Notice that when the phase velocity of the wave becomes close to Fermi velocity of electron, the kinetic Landau damping effect can not ignored.

Generally, the quantum statistical term is very large as compared to the quantum Bohm potential term, Eq. (5.51) becomes

$$\omega^3 - \omega_{SV}\omega^2 - \left(\omega_{cc}^2 + \frac{1}{3}k_z^2v_{Fe}^2\right)\omega + \frac{1}{3}\left(\omega_{SV}k_z^2v_{Fe}^2 - \frac{\omega_{cc}^2k_y\kappa_{ne0}}{\omega_{ce}}v_{Fe}^2\right) = 0 \quad (5.52)$$

It may be noted here also that if we ignore the electron pressure in Eq. (5.52), then it reduces to the classical SV and convective cell mode [64].

In order to depict the existence of a new coupled Shukla-Varma and convective cell mode for quantum dusty plasma, we choose some typical parameters of dense quantum dusty plasma and plot the new dispersion relation (5.51) for $n_{i0} = 1.43 \times 10^{26} \text{ cm}^{-3}$, $n_{d0} = 0.43 \times 10^{26} \text{ cm}^{-3}$, $Z_d = 10^3$, the external magnetic field $B_0 = 10^{13} \text{ Gauss}$ for which the electron Fermi temperature is $T_{Fe} = 1.133 \times 10^7 \text{ K}$. Figure 5-4 shows the existence of a new mode. The mode is unstable for small k_y decays for large k_y values.

5.3.4 Summary

To summarize, we have extended the classical Shukla-Varma mode in classical and quantum magnetoplasmas with electron thermal effects. The electron thermal effects seem to significantly modify the coupled SV and convective cell mode. Some interesting limiting cases are very briefly mentioned. We have shown both analytically as well as numerically that how the quantum effects can significantly modify the coupled SV and convective cell mode. On the other hand, when we ignore the electron thermal effect, the coupled SV and convective cell mode reduces to the original expression derived by Shukla and Varma in classical plasmas.

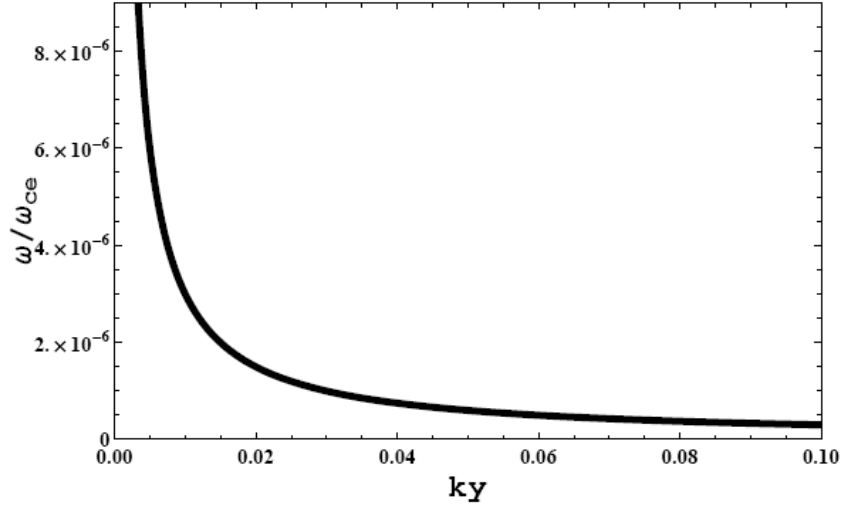


Figure 5-4: Variation of the normalized growth rate as a function of k_y of coupled SV and convective cell mode for $n_{i0} = 1.43 \times 10^{26} \text{ cm}^{-3}$, $n_{d0} = 0.43 \times 10^{26} \text{ cm}^{-3}$, $Z_d = 10^3$, the external magnetic field $B_0 = 10^{13} \text{ Gauss}$ $k_{ne} = 10^4 \text{ cm}^{-1}$ and $k_d = 10 k_{ne}$ with $k_z = 0.1 k_{ne}$, where $k_{ne}(k_d)$ represents the electron (dust) scale-length.

Chapter 6

Quantum DIA Shock and Solitons in Planar and Nonplanar Cases

The dust ion-acoustic solitons and shock waves are investigated in quantum plasma in the presence of external magnetic field. The dusty plasma consists of electrons, ions, and very massive dust particles by using the standard QHD model. We derive the Korteweg-de Vries-Burger (KdVB) equation by using small amplitude perturbation expansion method. The dissipation effects are introduced by considering the kinematic viscosity term. We found that the amplitude of quantum DIA shock wave is maximum for spherical, intermediate for cylindrical, and minimum for planar geometry cases. We have also investigated how the kinematic viscosity and dust concentration as well as Bohm potential effects the formation of DIA shock. The temporal evolution of dust ion acoustic KdV type solitons and Burger shocks by ignoring the dissipative and dispersive coefficients. We have also investigated the effect of quantum Bohm potential on dust ion acoustic shock wave. This work might be useful to understand quantum dusty plasma which has applications in microelectronic devices as well as in astrophysical plasmas.

6.1 Introduction

So far, we have discussed various types of waves for dense quantum plasmas by assuming that the amplitude of the wave is small. However, when the amplitude of the waves becomes large, nonlinear effects cannot be ignored. It is known that the nonlinear effects might come from the nonlinear Lorentz force, wave particle interaction or the trapping of plasma particles. The nonlinear effects may lead to the formation of various types of coherent nonlinear structure formation such as vortices, solitons and shocks. During the past few decades, a lot of interest and progress has been made to understand nonlinear physics. In Chapters 3-5, we mainly dealt with various types of vortex structure formation in quantum plasmas such as electron-ion, electron-ion-positron and dusty plasmas. In this chapter, we shall discuss in some detail another type of nonlinear structure formation which is known as soliton. Soliton is basically localized nonlinear wave and posses a remarkable property that it propagate without dissipation and retain its shape upon collision with another soliton. Historically, the solitary wave was first observed by Russell [109] on Edinburgh canal in (1834) and then he performed several laboratory experiments and derived an empirical formula which relates the speed (C_g) of the solitary structure with the wave amplitude (a), the unperturbed depth of water (h) such that $C_g = \sqrt{g(a + h)}$, where g is the acceleration due to gravity. This wave is also known as gravity wave, which is basically a solitary wave. Then afterwards, in 1895, two Germans, Korteweg and de Vries [110] proposed a nonlinear partial differential equation to model the shallow water waves which was witnessed by Russel. This famous equation is know as Korteweg-de Vries or KdV equation in literature. The solution of nonlinear KdV equation would relate the change of amplitude of the wave as it travels in space and time is known as solitary wave or the KdV solitons. One of the important features of KdV equation is that the speed of solitary wave structure is related with the amplitude of the wave. Zabuskey and Kruskal [111] found that the solitons behave more like particles since they retain their identity upon collision with another soliton. They obtain the above mentioned results by numerically solving the KdV equation. Thus the solution of

KdV equation represents solitons which propagates without changing shape and this is due to a neat balance of dispersion and nonlinearity. Since the solitary wave spreads out due to the dispersion and the wave amplitude decreases, whereas, the wave gets steep and narrower due to the nonlinear effects. When these two effects balance one and other a solitary wave is formed which propagates by retaining its shape. There is another type of stationary waveform which results from the balance of nonlinearity and dissipative effects which is known as Shock wave and is the solution of Burger equation. The shock waves are described by the KdV Burger or KdVB equation. To the best of our knowledge Sagdeev [112] was the first who has discovered the solitary plasma waves in ion-acoustic and magnetosonic modes. As discussed in Chapter 5 that in most of space and laboratory plasma, the presence of dust particles excite several new modes and instabilities as well as nonlinear structures which are not prevalent in the normal electron-ion plasma. In this chapter, we shall discuss in some detail the soliton and shock wave formation in dust-contaminated plasma in classical and dense quantum plasmas, specifically, we shall discuss the quantum dust ion acoustic shock and soliton formation.

6.2 Dust-Acoustic Solitary Waves

As discussed earlier in the Introduction, that solitons are generally formed when there is balance of dispersion and nonlinearity for a given nonlinear and dispersive system. Generally, due to nonlinearity, the wave gets steepened and the dissipation effects come from the collisions, and viscous effects etc. On the other hand, it is also well known that in the presence of dissipation and nonlinearity, small amplitude perturbations would be described by the KdVB type equation. The kinematic viscosity is the source of Burger term in nonlinear KdVB equation [65]. It has been seen that oscillatory dispersive shock wave is produced whenever the nonlinearity is balanced by the dissipation [66].

In this section, we shall discuss the one-dimensional dust-acoustic solitary waves. In this model, the electrons and ions are taken to be Boltzmann type whereas the dust

dynamics is governed by nonlinear set of dust continuity, dust equation of motion and Poisson's equation, as described by Rao *et al.*[40],

$$\frac{\partial n_d}{\partial t} + \frac{\partial}{\partial z} (n_d u_d) = 0, \quad (6.1)$$

$$\frac{\partial u_d}{\partial t} + u_d \frac{\partial u_d}{\partial z} - \frac{\partial \varphi}{\partial z} = 0, \quad (6.2)$$

$$\frac{\partial^2 \varphi}{\partial z^2} = (n_d + \mu_e n_e - \mu_i n_i), \quad (6.3)$$

where the fluid velocity of the dust is normalized with $C_d = \sqrt{z_d k_B T_i / m_d}$, φ is normalized with $k_B T_i / e$ and n_j is normalized with n_{j0} such that $j = e, i, d$. Here $\mu_i = n_{i0} / z_{d0} n_{d0} = \delta / (\delta - 1)$, $\mu_e = n_{e0} / z_{d0} n_{d0} = 1 / (\delta - 1)$, $\delta = n_{i0} / n_{e0}$, and $\sigma_i = T_i / T_e$. The Boltzmann distributed electrons and ions in the normalized form can be written as,

$$n_e = \exp[\sigma_i \varphi], \quad (6.4)$$

$$n_i = \exp[-\varphi], \quad (6.5)$$

By employing reductive perturbation method [113], Eqs. (6.1)-(6.5) were solved by using the stretched coordinated: $\zeta = \epsilon^{1/2} (z - v_0 \tau)$, where ϵ is smallness parameter, $\tau = \epsilon^{3/2} t$, and v_0 is the normalized soliton speed. Next we expand n_d , u_d and the normalized electrostatic wave potential φ in power series of ϵ in the following form:

$$u_d = \epsilon u_d^{(1)} + \epsilon^2 u_d^{(2)} + \dots \quad (6.6)$$

$$n_d = 1 + \epsilon n_d^{(1)} + \epsilon^2 n_d^{(2)} + \dots \quad (6.7)$$

$$\varphi = 1 + \epsilon\varphi^{(1)} + \epsilon^2\varphi^{(2)} + \dots \quad (6.8)$$

To the lowest order in ϵ , Eqs. (6.1)-(6.8) give:

$$n_d^{(1)} = -\varphi^{(1)}/v_0^2; \quad u_d^{(1)} = -\varphi^{(1)}/v_0; \quad \text{and} \quad v_0 = (\mu_i + \sigma_i\mu_e)^{-1/2}. \quad (6.9)$$

To the next higher order in ϵ , we have

$$\frac{\partial n_d^{(1)}}{\partial \tau} - v_0 \frac{\partial n_d^{(2)}}{\partial \zeta} + \frac{\partial u_d^{(2)}}{\partial \zeta} + \frac{\partial (n_d^{(1)} u_d^{(1)})}{\partial \zeta} = 0, \quad (6.10)$$

$$\frac{\partial u_d^{(1)}}{\partial \tau} - v_0 \frac{\partial u_d^{(2)}}{\partial \zeta} - \frac{\partial \varphi^{(2)}}{\partial \zeta} + u_d^{(1)} \frac{\partial u_d^{(1)}}{\partial \zeta} = 0, \quad (6.11)$$

$$\frac{\partial^2 \varphi^{(1)}}{\partial \zeta^2} - \frac{1}{v_0^2} \varphi^{(2)} - n_d^{(2)} + \frac{1}{2} (\mu_i - \sigma_i^2 \mu_e) [\varphi^{(1)}]^2 = 0, \quad (6.12)$$

From Eqs. (6.10)-(6.12), we obtain the following KdV equation [65]:

$$\frac{\partial \varphi^{(1)}}{\partial \tau} + a_0 \varphi^{(1)} \frac{\partial \varphi^{(1)}}{\partial \zeta} + b_0 \frac{\partial \varphi^{(1)}}{\partial \zeta} = 0, \quad (6.13)$$

where $a_0 = v_0^3(\mu_i - \sigma_i^2 \mu_e - 3/v_0^4)/2$ and $b_0 = v_0^3/2$. The analytical solution of above KdV can be obtained by defining a new transformation such that $\xi = \zeta - u_0\tau$ and $\tau = \tau$, where u_0 is some constant speed which is normalized with C_d . Using the boundary conditions i.e., $\varphi \rightarrow 0$, $d^2\varphi^{(1)}/d\xi^2 \rightarrow 0$, $d\varphi^{(1)}/d\xi \rightarrow 0$ at $\xi \rightarrow \pm\infty$, the stationary solution of KdV equation (6.13) would be

$$\varphi^{(1)} = \frac{3u_0}{a_s} \sec h^2 \left[(\xi - u_0\tau) / \sqrt{4b_s/u_0} \right] \quad (6.14)$$

It is evident from the above solution that for small amplitude solitary waves, the wave potential would be negative or positive, depending upon the signature of a_s . If we write $a_s = -v_0^3 [\delta^2 + (3\delta + \sigma_i)\sigma_i + \delta(1 + \sigma_i^2)/2]$ which is always negative for all values

of δ and σ_i . The amplitude of dust-acoustic solitary wave increases with a decrease of width. Arbitrary amplitude dust-acoustic solitary waves has also been investigated by Shukla and Mamun [64] using Sagdeev potential approach using appropriate boundary conditions, which is out of the scope of present literature review. For quantum plasmas, it is very difficult to use Sagdeev potential approach to find the solution of KdV in cylindrical or spherical geometry. We shall therefore use the reductive perturbation method to develop KdV and KdVB type equations for the study of dust-ion-acoustic solitons and shock waves.

6.3 Dust Acoustic Solitary Waves in Cylindrical and Spherical Geometry

In the last section, we have discussed dust-acoustic-solitary waves in one-dimensional geometry. Since in most of the laboratory and space plasmas, one encounter with cylindrical or spherical dust-acoustic solitary wave structures. In this section, we shall discuss the propagation of radially imploding dust-acoustic-solitary wave in cylindrical or spherical geometry. The nonlinear dynamics of ultra-low frequency dust-acoustic solitary waves in spherical and spherical geometry can be expressed as

$$\frac{\partial n_d}{\partial t} + \frac{1}{r^\nu} \frac{\partial}{\partial r} (r^\nu n_d u_d) = 0, \quad (6.15)$$

$$\frac{\partial u_d}{\partial t} + u_d \frac{\partial u_d}{\partial z} - \frac{\partial \varphi}{\partial r} = 0, \quad (6.16)$$

$$\frac{1}{r^\nu} \frac{\partial}{\partial r} \left(r^\nu \frac{\partial \varphi}{\partial r} \right) = (n_d + \mu_e \exp[\sigma_i \varphi] - \mu_i \exp[-\varphi]), \quad (6.17)$$

where $\nu = 1(2)$ for cylindrical(spherical) geometry and r is the radial distance which has been normalized with effective Debye length λ_{Dm} . To obtain a generic equation which describe the in going solution based on Eqs. (6.15) to (6.17), we may use the stretched coordinates $\zeta = -\epsilon^{1/2}(r + v_0 t)$ and $\tau = \epsilon^{3/2}t$ and using the same perturbation expansion

procedure discussed in the previous section (6.2), we get

$$\frac{\partial \varphi^{(1)}}{\partial \tau} + \frac{\nu}{2\tau} \varphi^{(1)} + a_s \varphi^{(1)} \frac{\partial \varphi^{(1)}}{\partial \zeta} + b_s \frac{\partial \varphi^{(1)}}{\partial \zeta} = 0, \quad (6.18)$$

The above equation is the modified KdV equation with the same coefficients defined in the previous section. The second term is a new term and it arises due to cylindrical/spherical geometry. Using the standard two-level finite difference method [114], one can solve the modified KdV equation for dust-acoustic-solitary wave in cylindrical and spherical geometry by choosing appropriate parameters of classical dusty plasmas and the results are given in Ref. [115]. As discussed earlier, since our primary objective here is to develop modified KdV type equation for quantum dust-ion-acoustic solitary waves. In the next section, we shall present our new findings.

For this purpose, we consider the propagation of small amplitude quantum dust ion acoustic wave in planar as well as in nonplanar cases [67]. Since we are studying DIA shock waves, we shall consider immobile dust, dynamic ions and Boltzmann distributed electrons. To introduce dissipation, we retain the kinematic viscosity term in our model. We use the standard quantum hydrodynamic model equations and derive KdV and KdVB type equations by using small amplitude approximation so as to investigate the propagation of DIA solitons and shock waves in quantum plasma. In Sec. 6.4, we present a generic model equations for 1-D KdVB equation for QDIA shock for plane geometry case. In the next section 6.5, we derive 1-D KdVB type equation for QDIA shock wave for nonplanar geometry case. Then the results are presented and discussed in Sec. 6.8. We have also presented the stability analysis of KdVB for the first time in our investigation.

6.4 Model Equations for Planar Geometry Case

In this model [67], we assume that the dense electrons obey Fermi degenerate gas obeying the following one-dimensional gas law, such that

$$p_e = \frac{1}{3} \frac{m_e v_{Fe}^2}{n_{e0}^2} n_e^3 \quad (6.19)$$

where $v_{Fe} = \sqrt{2k_B T_{Fe}/m_e}$ is the Fermi velocity of electrons, k_B is the Boltzmann constant, and T_{Fe} is the electron Fermi temperature. Here, $n_e(n_{e0})$ is the electron number density (equilibrium number density of electrons). The charge neutrality condition in equilibrium can be written as

$$n_{i0} = n_{e0} + z_d n_{d0}$$

We assume that the phase velocity of the wave is: $v_{Fi}; v_{Fd} \ll \omega/k \ll v_{Fe}$, where v_{Fj} is the Fermi velocity of the j th-species (such that $j = e, i, d$). We assume that the dust is stationary, ions are dynamic and the electrons are inertialess and Boltzmann distributed. For dust-ion-acoustic (DIA) waves in plane geometry case, can be written as:

The ion continuity equation is

$$\frac{\partial n_i}{\partial t} + \frac{\partial}{\partial x} (n_i u_i) = 0 \quad (6.20)$$

The normalized ion equation of motion can be written as

$$\frac{\partial u_i}{\partial t} + u_i \frac{\partial u_i}{\partial x} = -\frac{\partial \phi}{\partial x} + \eta_i \frac{\partial^2 u_i}{\partial x^2} \quad (6.21)$$

The equation of motion for inertialess electrons can be written as

$$0 = \frac{\partial \phi}{\partial x} - n_e \frac{\partial n_e}{\partial x} + \frac{H_e^2}{2} \frac{\partial}{\partial x} \left[\frac{\frac{\partial^2}{\partial x^2} \sqrt{n_e}}{\sqrt{n_e}} \right] \quad (6.22)$$

The Poisson's equation is given by

$$\frac{\partial^2 \phi}{\partial x^2} = (pn_e + (1-p)n_d - n_i) \quad (6.23)$$

where ϕ is the normalized electrostatic wave potential with $2k_B T_{Fe}/e$, the ion fluid velocity is normalized with quantum ion acoustic speed $c_s = (2k_B T_{Fe}/m_i)^{1/2}$, and the number density, n_j with equilibrium number density n_{j0} . The space coordinates x is normalized with quantum Debye length $\lambda_D = \sqrt{2\varepsilon_o K_B T_{Fe}/n_{i0}e^2}$ and the time coordinate t is normalized with ion plasma period $\omega_{pi}^{-1} = \sqrt{(\varepsilon_o m_i/n_{i0}e^2)}$. Here, $p = n_{e0}/n_{i0}$, and $\eta_i = \mu_i \omega_{pi}/c_{si}^2$, where the ion kinematic viscosity is represented by μ_i and $H_e = \sqrt{\hbar^2 \omega_{pi}^2 / m_e m_i c_{si}^4}$. We have assumed that the dust is positively charged having fixed charge state z_d .

Equations (6.19)-(6.23) are the modeled equations to study three component electron-ion-dust quantum plasma. The Fermi pressure and quantum Bohm potential represents the quantum correction terms in equation (6.22). We use the quantum statistics by employing 1-D equation of state [see e.g., equation (6.19)]. Solving equation (6.22) and by using the boundary conditions: At $x \rightarrow \pm\infty$, $n_e = 1$ and $\varphi = 0$, we get

$$\phi = -\frac{1}{2} + \frac{1}{2}n_e^2 - \frac{H_e^2}{2} \left(\frac{1}{\sqrt{n_e}} \frac{\partial^2 \sqrt{n_e}}{\partial x^2} \right) \quad (6.24)$$

Notice that we have ignored the quantum Fermi pressure and Bohm potential terms while writing down Eq. (6.21) for the ions, since the mass of electrons is very small as compared to the ions. It is also worth mentioning here that one can not write electrons as inertialess, since the mass of electrons appears in the Bohm potential term which is normally taken in the classical plasma case (such as in the derivation of classical Boltzmann type relation). Finally, we have ignored the electron kinematic viscosity μ_e term, since it is of the order m_e/m_i .

6.5 KdV Equation for Plane Geometry Case

In the absence of kinematic viscosity (i.e. putting $\eta = 0$ in Eq. (6.21)), we apply the reductive perturbation technique to Eqs. (6.20), (6.21), (6.23), and (6.24) to obtain KdVB equation in 1-D to study quantum dust-ion-acoustic wave propagation [67]. We have expanded various plasma parameters in terms of smallness parameter ϵ , such that

$$\begin{aligned} n_\alpha &= 1 + \epsilon n_{\alpha 1} + \epsilon^2 n_{\alpha 2} + \dots \\ v_i &= \epsilon v_{i1} + \epsilon^2 v_{i2} + \dots \\ \varphi &= \epsilon \varphi_1 + \epsilon^2 \varphi_2 + \dots \end{aligned} \tag{6.25}$$

Notice that various plasma parameters are functions of x and t , and the expansion parameter ϵ is very small ($0 < \epsilon \leq 1$). Here the strength of the nonlinearity is represented by ϵ , and stretched variables are defined by $\xi = \epsilon^{1/2}(x - \lambda t)$ and $\tau = \epsilon^{3/2}t$. Inserting the above expansions and stretching, Eqs. (6.20), (6.21), (6.23) and (6.24), to the first power in ϵ give

$$\begin{aligned} n_{i1} &= \frac{1}{\lambda} u_{i1} \\ u_{i1} &= \frac{1}{\lambda} \phi_1 \\ n_{e1} &= \phi_1 \\ p n_{e1} &= n_{i1} \end{aligned} \tag{6.26}$$

Solving for λ , we get

$$\lambda = \sqrt{p}$$

whereas the higher powers of ϵ yield the following set of equations

$$\begin{aligned}
-\lambda \frac{\partial n_{i2}}{\partial \xi} + \frac{\partial u_{i2}}{\partial \xi} &= -\frac{\partial n_{i1}}{\partial \tau} - \frac{\partial}{\partial \xi}(n_{i1}u_{i1}) \\
-\lambda \frac{\partial u_{i2}}{\partial \xi} + \frac{\partial \phi_2}{\partial \xi} &= -\frac{\partial u_{i1}}{\partial \tau} - u_{i1} \frac{\partial}{\partial \xi} u_{i1} \\
\phi_2 - n_{e2} &= \frac{1}{2} n_{e1}^2 - \frac{H_e^2}{4} \frac{\partial^2 n_{e1}}{\partial \xi^2} \\
pn_{e2} - n_{i2} &= \frac{\partial^2 \phi_1}{\partial \xi^2}
\end{aligned} \tag{6.27}$$

Solving the system of equations (6.26) and using (6.27), we obtain the following nonlinear KdV equation for QDIA (for negatively charged dust) solitary waves in one dimensional case

$$\frac{\partial \Phi}{\partial \tau} + A\Phi \frac{\partial \Phi}{\partial \xi} + B \frac{\partial^3 \Phi}{\partial \xi^3} = 0 \tag{6.28}$$

Here $\Phi \equiv \phi^{(1)}$, $A = \lambda(p\lambda^2 + 3/\lambda^2)/2$, and $B = \lambda^3(1 - pH_e^2/4)/2$, where A and B are the coefficients of nonlinearity and dispersion respectively.

6.6 KdVB Equation for Plane Geometry Case

We obtain KdVB equation for the quantum DIA shock waves using the reductive perturbation technique to solve Eqs. (6.20), (6.21), (6.23), and (6.24) [67]. The first order in ϵ yield the following result,

$$\begin{aligned}
n_{i1} &= \frac{1}{\lambda} u_{i1} \\
u_{i1} &= \frac{1}{\lambda} \phi_1 \\
n_{e1} &= \phi_1 \\
pn_{e1} &= n_{i1}
\end{aligned} \tag{6.29}$$

Solving for λ , we get

$$\lambda = \sqrt{p}$$

whereas the higher powers of ϵ yield the following set of equations

$$\begin{aligned}
-\lambda \frac{\partial n_{i2}}{\partial \xi} + \frac{\partial u_{i2}}{\partial \xi} &= -\frac{\partial n_{i1}}{\partial \tau} - \frac{\partial}{\partial \xi}(n_{i1}u_{i1}) \\
-\lambda \frac{\partial u_{i2}}{\partial \xi} + \frac{\partial \phi_2}{\partial \xi} &= -\frac{\partial u_{i1}}{\partial \tau} - u_{i1} \frac{\partial}{\partial \xi} u_{i1} + \eta_{i0} \frac{\partial^2 u_{i1}}{\partial \xi^2} \\
\phi_2 - n_{e2} &= \frac{1}{2} n_{e1}^2 - \frac{H_e^2}{4} \frac{\partial^2 n_{e1}}{\partial \xi^2} \\
pn_{e2} - n_{i2} &= \frac{\partial^2 \phi_1}{\partial \xi^2}
\end{aligned} \tag{6.30}$$

Solving the system of equations (6.29) and using (6.30), we obtain KdVB equation for 1-D quantum DIA shock waves for planar geometry case, by considering negatively charged dust particles

$$\frac{\partial \Phi}{\partial \tau} + A\Phi \frac{\partial \Phi}{\partial \xi} + B \frac{\partial^3 \Phi}{\partial \xi^3} - C \frac{\partial^2 \Phi}{\partial \xi^2} = 0 \tag{6.31}$$

where $\Phi \equiv \phi^{(1)}$, $\alpha = i, e$, $A = \lambda(p\lambda^2 + 3/\lambda^2)/2$, $B = \lambda^3(1 - pH_e^2/4)/2$ and $C = \eta_{i0}/2$. Here A is the nonlinearity coefficient, B is the dispersion coefficient and C is the dissipation coefficient. We obtain KdVB equation for DIA wave in 1-D case, by using the same procedure. Here A , B , and C coefficients for positively charged dust grains are given by

$$\begin{aligned}
A &= \frac{\lambda}{2} \left(\frac{3}{\lambda^2} + \frac{\lambda^2}{p} \right), \\
B &= \frac{\lambda^3}{2} \left(1 - \frac{H_e^2}{4p} \right), \\
C &= \frac{\eta_{i0}}{2}
\end{aligned} \tag{6.32}$$

For positively charged dust grains with majority of electrons, $p \equiv n_{i0}/n_{e0}$.

6.7 Model Equations for Nonplanar Geometry Case

The nonlinear dynamics of dust-ion-acoustic wave in dense quantum plasma is described by the following set of quantum hydrodynamic equations for nonplanar geometry [67]:

$$\frac{\partial n_i}{\partial t} + \frac{\nu}{r}(n_i u_i) + \frac{\partial}{\partial r}(n_i u_i) = 0 \quad (6.33)$$

$$\frac{\partial u_i}{\partial t} + u_i \frac{\partial u_i}{\partial r} = -\frac{\partial \phi}{\partial r} + \eta_i \frac{\partial^2 u_i}{\partial r^2} \quad (6.34)$$

$$0 = \frac{\partial \phi}{\partial r} - n_e \frac{\partial n_e}{\partial r} + \frac{H_e^2}{2} \frac{\partial}{\partial r} \left(\frac{1}{\sqrt{n_e}} \frac{\partial^2 \sqrt{n_e}}{\partial r^2} \right) \quad (6.35)$$

$$\frac{1}{r^\nu} \frac{\partial}{\partial r} (r^\nu \frac{\partial \phi}{\partial r}) = p n_e + (1 - p) n_d - n_i \quad (6.36)$$

The electron momentum equation yields the following result with the boundary conditions: at $\pm\infty$, $\phi = 0$ and $n_e = 1$,

$$\phi = -\frac{1}{2} + \frac{1}{2} n_e^2 - \frac{H_e^2}{2\sqrt{n_e}} \frac{1}{r^\nu} \frac{\partial}{\partial r} \left(r^\nu \frac{\partial \sqrt{n_e}}{\partial r} \right) \quad (6.37)$$

6.8 KdVB and KdV Equations for Nonplanar Geometry

We apply the reductive perturbation technique to solve Eqs. (6.33), (6.34), (6.36) and (6.37) to obtain KdVB equation in 1-D QDIA shock waves [67]. Since all the perturbed quantities are functions of r and t . Using the stretched variables: $\xi = \epsilon^{1/2}(x - \lambda t)$ and $\tau = \epsilon^{3/2}t$, where ϵ is an expansion parameter ($0 < \epsilon \leq 1$), Eqs. (6.33), (6.34), (6.36) and (6.37) yield the following type of KdVB equation, for quantum DIA shock wave for nonplanar geometry (for negative dust grains),

$$\frac{\partial \Phi}{\partial \tau} + A\Phi \frac{\partial \Phi}{\partial \xi} + B \frac{\partial^3 \Phi}{\partial \xi^3} - C \frac{\partial^2 \Phi}{\partial \xi^2} + \frac{\nu}{\tau} \Phi = 0 \quad (6.38)$$

where $\Phi \equiv \phi^{(1)}$, $A = \lambda (p\lambda^2 + 3/\lambda^2) / 2$, $B = \lambda^3 (1 - pH_e^2/4) / 2$ and $C = \eta_{i0}/2$.

Here, $\nu = 0, 1, 2$ corresponds to the KdVB equations for planar, cylindrical and spherical geometry cases. If we take $\nu = C = 0$, then we obtain the standard KdV type equation, whereas, for $\nu = B = 0$, Eq. (6.38) becomes Burger type equation. We obtain KdVB equation for DIA wave for planar case by using the same procedure as discussed earlier. The coefficients A , B , and C for positively charged dust would be

$$\begin{aligned} A &= \frac{\lambda}{2} \left(\frac{3}{\lambda^2} + \frac{\lambda^2}{p} \right), \\ B &= \frac{\lambda^3}{2} \left(1 - \frac{H_e^2}{4p} \right), \\ C &= \frac{\eta_{i0}}{2}. \end{aligned}$$

When the electrons are in majority, $p = n_{i0}/n_{e0}$ for positively charged dust grains.

Here new term ν/τ arises due to geometry factor. The geometry term which appears as a higher order contribution, which is of the order of $\epsilon^{7/2}$ and above; from the momentum equation. If we put the kinematic viscosity equal to zero in Eq. (6.34), then the algebraic manipulation of Eqs. (6.33), (6.34), (6.35) and (6.37) yield the following nonlinear KdV equation for 1-D quantum DIA solitary waves in the nonplanar geometry, for negatively charged dust

$$\frac{\partial \Phi}{\partial \tau} + A\Phi \frac{\partial \Phi}{\partial \xi} + B \frac{\partial^3 \Phi}{\partial \xi^3} + \frac{\nu}{\tau} \Phi = 0$$

where

$$\begin{aligned} A &= \frac{\lambda}{2} \left(\frac{3}{\lambda^2} + \frac{\lambda^2}{p} \right), \\ B &= \frac{\lambda^3}{2} \left(1 - \frac{H_e^2}{4p} \right), \end{aligned}$$

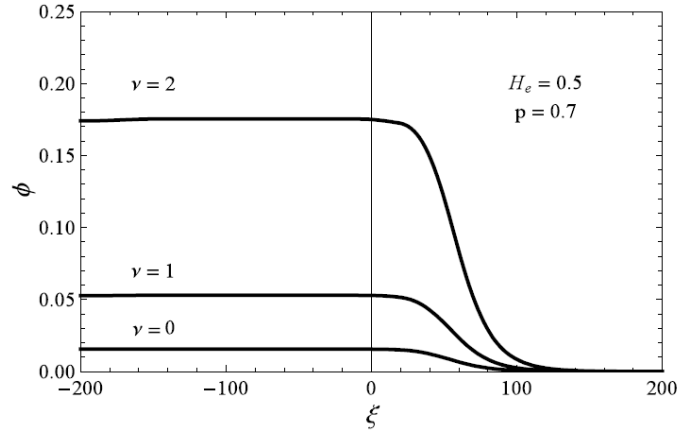


Figure 6-1: Numerical results by solving equation (6.38) for different values of ν , with $H_e = 0.5$, $p = 0.7$, and $\eta_0 = 0.5$.

6.9 Results

By employing two-level finite difference approximation method, we solve numerically the modified KdVB Eq. (6.38) for quantum DIA shock waves for nonplanar case. We use the tanh method [116, 117], to obtain the following exact solution of the planar KdVB equation, which was used as a initial profile in our numerical simulations:

$$\Phi = \frac{3}{25} \frac{C^2}{AB} \sec^2 h^2 [k(\xi - v\tau)] + \frac{6}{25} \frac{C^2}{AB} [1 - \tanh \{k(\xi - v\tau)\}], \quad (6.39)$$

where $k = C/10B$. It may be noted here that exact analytical solution of KdVB equation for planar case which contains dispersion and dissipative effects.

In order to find the evolution of nonplanar KdVB equation in time, we numerically solve equation (6.38) by varying positive dust concentration. The geometry effect on the quantum dust ion acoustic shock is shown in Fig. (6-1). It is evident from the graph that shock strength is maximum for spherical geometry, intermediate for cylindrical, and minimum for the planar geometry case. We consider first the spherical geometry case and investigate how the shock strength changes with plasma parameters (for $\nu = 2$ case).

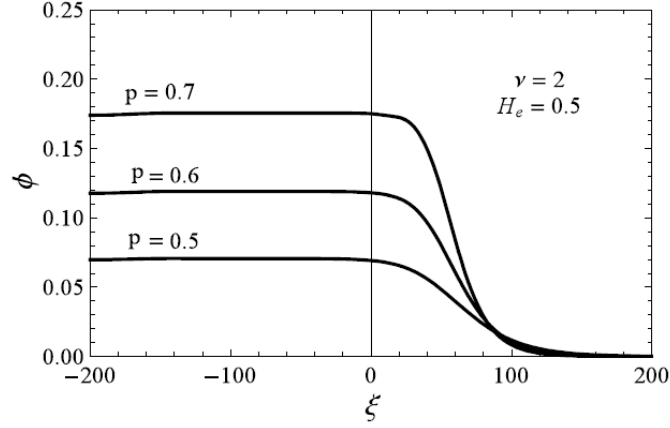


Figure 6-2: Solution of equation (6.38) numerically for different positron concentrations: $p = 0.5 - 0.7$, where $\nu = 2$, $H_e = 0.5$, and $\eta_0 = 0.5$.

Figure (6-2) shows the variation of shock structure with dust concentration. We found an increase of the strength of quantum dust ion acoustic shock by decreasing the concentration of dust. Similarly, we showed the effect of Bohm potential on the shock structure. We found that Bohm term increases the strength of shock. Figure (6-4) investigates The effect of kinematic viscosity η , on the shock structure is investigated and showed in Fig. (6-5). The strength of the shock decreases with increasing $|\tau|$. We also found that the shock strength increases with increase of η .

By ignoring the dissipative and dispersive coefficients, we have plotted the KdV and KdVB equations. By putting $C = 0$, the temporal evolution of the quantum DIA soliton in a spherical geometry is plotted and shown in Fig. (6-6). It is found that the amplitude of the DIA soliton increases with decreasing $|\tau|$. Figure (6-7) shows the time variation of quantum DIA Burger equation by taking $B = 0$ in equation (6.38). The shock strength decreases with the increase of $|\tau|$.

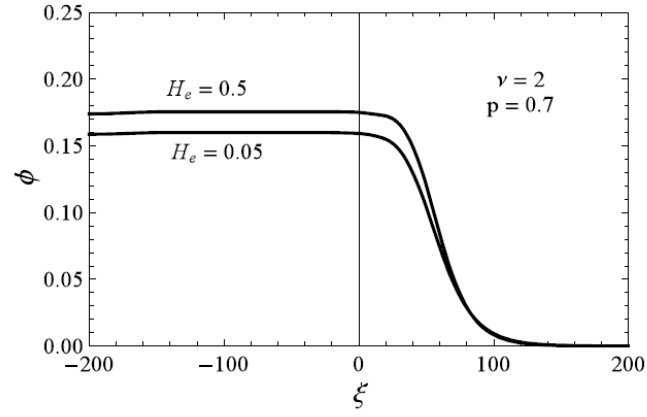


Figure 6-3: Numerical solution of (6.38) for various values of $H_e = 0.05$ and 0.5 , where $\nu = 2$, $p = 0.7$ and $\eta_0 = 0.5$.

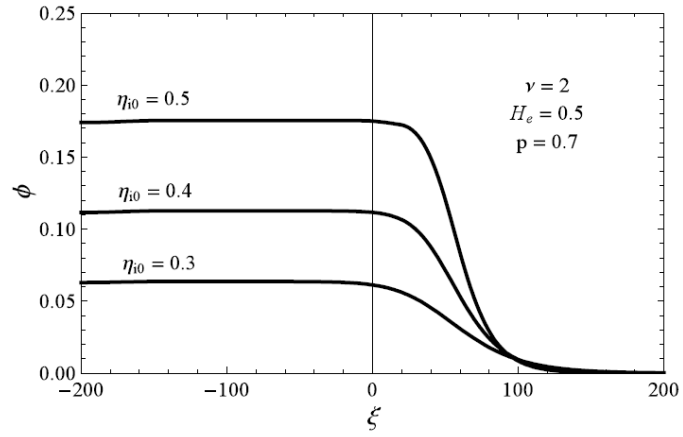


Figure 6-4: Solution of equation (6.38) numerically for various values of $H_e = 0.05$ and 0.5 , where $\nu = 2$, $p = 0.7$ and $\eta_0 = 0.5$.

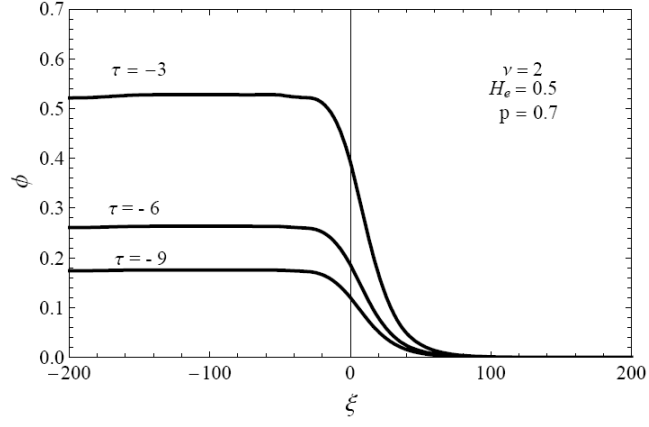


Figure 6-5: Solution of Eq. (6.38) for $\nu = 2$ and for various time scale $\tau = -9, -6, -3$, and $H_e = 0.5$, $p = 0.7$ with $\eta_0 = 0.5$.

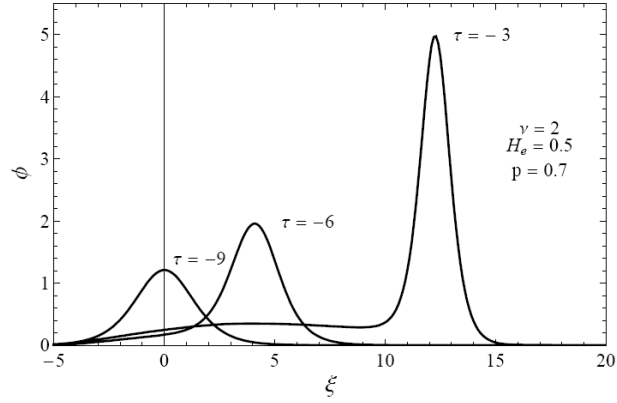


Figure 6-6: Formation of dust-ion-acoustic solitons for various time scale as a function of ξ for $\nu = 2$ by taking $C = 0$ in Eq. (6.38) for time $\tau = -9, -6, -3$, and $H_e = 0.5$, and $p = 0.7$.

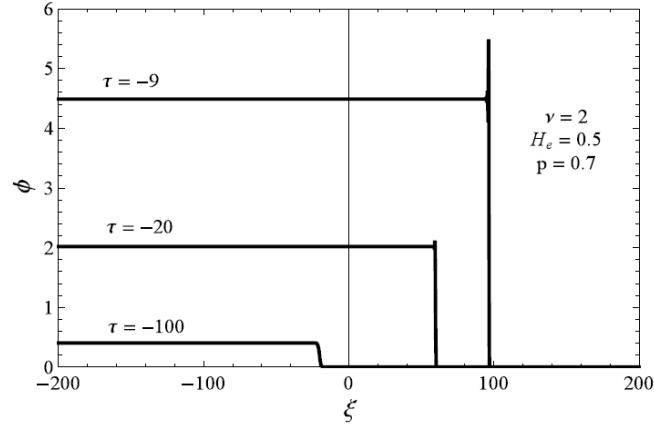


Figure 6-7: The solution of quantum DIA Burgers equation (6.38) for various time scale: $\tau = -9, -6, -3$ and by taking $B = 0$ in spherical case ($\nu = 2$), with $H_e = 0.5$, $p = 0.7$ and $\eta_0 = 0.5$.

6.10 Stability Condition of DIA Shocks

To find the stability condition of quantum DIA shock waves, we use a coordinate transformation which transform all independent variables ξ and τ into a new co-moving frame such that $\Psi = \xi - U_0\tau$. Here U_0 represents the speed of DIA wave. We finally obtain a third order ordinary differential equation of $\Phi(\Psi)$, which can solved and integrated once to give the following result,

$$B \frac{\partial^2 y}{\partial \Psi^2} + \frac{1}{2} A y^2 - C \frac{\partial y}{\partial \Psi} - U_0 y = 0 \quad (6.40)$$

where $y = \Phi$ and we have imposed the appropriate boundary conditions, namely $y \rightarrow 0$, $\frac{dy}{d\Psi} \rightarrow 0$, $\frac{d^2 y}{d\Psi^2} \rightarrow 0$ at $\Psi \rightarrow \infty$. We linearize equation (6.40) in y_1 and look for an asymptotic behavior and obtain the following equation [118],

$$B \frac{\partial^2 y_1}{\partial \Psi^2} - C \frac{\partial y_1}{\partial \Psi} + U_0 y_1 = 0 \quad (6.41)$$

The solutions of equation (6.41) are proportional to $\exp(W\Psi)$, where $W = C/2B \pm$

$\sqrt{C^2/4B^2 - U_0/B}$. The condition for a stable shock is $C > 2\sqrt{BU_0}$, whereas for $C \leq 2\sqrt{BU_0}$ we have an oscillatory quantum DIA shock. It may be noted here that quantum Bohm potential modifies the stability criteria through the dispersion coefficient B , in this model.

6.11 Summary

To summarize, in this section, we have investigated the effect of geometry (planar or nonplanar) on the propagation of DIA shock waves for 1-D case [67]. We assume that the dust charge state is fixed and the dust grains can be wither positive or negative, depending upon the background conditions of the plasma. Since the mass of dust grains is very large as compared to the electrons and ions, we consider both ions and electrons as inertialess. The kinematic viscosity term has been introduced so as to retain dissipation effects among the plasma constituents. The quantum hydrodynamic model has been used and using small amplitude approximation method, we obtain a KdVB equation to describe the propagation of quantum DIA shock waves in dusty plasma. We found that the strength of quantum DIA shock depends upon the geometry and it is maximum for spherical, intermediate for cylindrical, and minimum for the planar case. We have also investigated the effects of dust concentration as well as the quantum Bohm potential on the shock strength. We found that shock strength increases with an increase of quantum Bohm potential whereas it decreases with an increase of dust concentration. We have investigated the time evolution of quantum DIA shock in spherical geometry case. We found a decrease in the shock strength with an increase of $|\tau|$. We also found that with an increase of η the shock strength increases and the shock gets steeper. By neglecting the dissipation and dispersive coefficients, the time evolution of quantum DIA solitons and shocks are also investigated. We found that both the amplitude as well as the strength of shock decreases with an increase of $|\tau|$. We have also investigated the effect of quantum Bohm potential on the stability of the DIA shock. These results would

play very important role to understand various nonlinear processes occurring in quantum dusty plasmas which are relevant in microelectronic devices and in dense astrophysical plasmas.

Bibliography

- [1] A. Markowich, C. Ringhofer, and C. Schmeiser, *Semiconductor Equations* (Springer, Vienna 1990).
- [2] Y. D. Jung, Phys. Plasmas **8**, 3842 (2001).
- [3] M. Opher, L. O. Silva, D. E. Dauger, V. K. Decyk, and J. M. Dawson, Phys. Plasmas **8**, 2454 (2001).
- [4] A. K. Jonscher, British J. Appl. Phys., **15**, 365 (1964).
- [5] M. Marklund and P.K. Shukla, Rev. Mod. Phys. **78**, 591 (2006).
- [6] P. K. Shukla and S. Ali, Phys. Plasmas **12**, 114502 (2005).
- [7] S. A. Khan, A. Mushtaq, and W. Masood, Phys. Plasmas **15**, 013701 (2008).
- [8] G. Manfredi, Fields Inst. Commun. **46**, 263 (2005).
- [9] W. Masood and A. Mushtaq, Phys. Plasmas **15**, 022306 (2008).
- [10] P. K. Shukla and S. Ali, Phys. Plasmas **13**, 082101 (2006).
- [11] W. F. El-Taibany and Miki Wadati, Phys. Plasmas **14**, 42302 (2007).
- [12] L. Yu Kilontovich and V. P. Silin, Dokl. Akad. Nauk SSSR **82**, 361 (1952).
- [13] D. Bohm and D. Pines, Phys. Rev. **92**, 609 (1953).

- [14] D. Pines, J. Nucl. Energy C: Plasma Phys. **2**, 5 (1961).
- [15] V. M. Eleonski, P. S. Zyryanov and V. P. Silin, JETP **42**, 896 (1962).
- [16] P. S. Zyryanov, V. I. Okulov and V. P. Silin, JETP Lett. **9**, 283 (1969).
- [17] B. Bezzerides and D. F. DuBois, Ann. Phys. (New York) **70**, 10 (1972).
- [18] R. Hakim and J. Heyvaerts, Phys. Rev. A **18**, 1250 (1978).
- [19] D. B. Melrose, *Quantum Plasmadynamics: Unmagnetized Plasmas* (Springer, New-York, 2008).
- [20] F. Haas, L. G. Garcia and G. Manfredi, Phys. Plasmas **10**, 3858 (2003).
- [21] P. K. Shukla and B. Eliasson, Phys. Rev. Lett. **99**, 096401 (2007).
- [22] S. Ali, N. Shukla and P. K. Shukla, Europhys. Lett. **78**, 45001 (2007).
- [23] F. Haas, G. Manfredi and M. Geix, Phys. Rev. E **62**, 2763(2000).
- [24] F. Haas, Phys. Plasmas **12**, 062117 (2005).
- [25] P. K. Shukla and B. Eliasson, Phys. Rev. Lett. **96**, 245001 (2006).
- [26] R. Redmer, Phys. Reports **282**, 35 (1997).
- [27] H. M. Kim and Y. D. Jung, Europhys. Lett. **78**, 35001 (2007).
- [28] S. Sasabe and K. Tsuchiya, Phys. Lett. A, **372**, 381 (2008).
- [29] L. Landau, E. M. Lifshitz and M. Kvantovaya, *Quantum Mechanics: Non-Relativistic Theory* (Oxford University Press, Oxford, 1977) 3rd ed.
- [30] M. Marklund and G. Brodin, Phys. Rev. Lett. **98**, 025001 (2007).

- [31] G. Brodin and M. Marklund, *New Aspects of Plasma Physics; Proc. of the AS-ICTP Summer College on Plasma Physics*, Edited by P. K. Shukla, L. Stenflo and B. Eliasson (World Scientific, Singapore 2008) p.26.
- [32] G. Brodin, M. Marklund and G. Manfredi, Phys. Rev. Lett. **100**, 175001 (2008).
- [33] G. Manfredi, P. A. Hervieux, Y. Yin and N. Crouseilles, *Collective Electron Dynamics in Metallic and Semiconductor Nanostructures: Advances in the atomic-scale modeling of nanosystems and nanostructured materials* Edited by: C. Massobrio, H. Bulou and C. Goyenex (Springer, Heidelberg, 2009) p.1.
- [34] L. K. Ang, T. J. T. Kwan and Y. Y. Lau, Phys. Rev. Lett. **91**, 208303 (2003).
- [35] G. Agrawal, *Nonlinear Fiber Optics* (Academic Press, San Diego, 1995).
- [36] G. Manfredi and F. Haas, Phys. Rev. B, **64**, 075316 (2001).
- [37] S. Galam and J. P. Hansen, Phys. Rev. A, **12**(2) (1976).
- [38] H. E. Dewitt, J. de Physique, **39**(5), 173 (1978).
- [39] S. V. Adamjan, J. Ortner and I. M. Tkachenko, Europhys. Lett. **25** (1), 11 (1994).
- [40] P. K. Shukla and L. Stenflo, Phys. Lett. A **357**, 229 (2006).
- [41] Q. Haque and S. Mahmood, Phys. Plasmas **15**, 034501 (2008).
- [42] Q. Haque and H. Saleem, Phys. Plasmas **15**, 064504 (2008).
- [43] W. Masood, A. M. Mirza and S. Nargis, Phys. Plasmas **15**, 122305 (2008).
- [44] N. N. Rao, P. K. Shukla, and M. Y. Yu, Planet Space Sci. **38**, 543 (1990).
- [45] P. K. Shukla and V. P. Silin, Phys. Scripta **45**, 508 (1992).
- [46] A. Barkan, D'Angelo, and R. L. Merlino, Phys. Plasmas **2**, 231 (1995).

- [47] H. R. Prabhakara and V.I. Thana, Phys. Plasmas **3**, 231 (1996).
- [48] Y. Nakamura, H. Bailung, and P. K. Shukla, Phys. Rev. Lett. **83**, 1602 (1999).
- [49] J. B. Pieper and J. Goree, Phys. Rev. Lett. **77**, 3137 (1996).
- [50] S. Ali, W. M. Moslem, P. K. Shukla, and R. Schlickeiser, Phys. Plasmas **14**, 082307 (2007).
- [51] A. Mushtaq and S. A. Khan, Phys. Plasmas. **14**, 052307 (2007).
- [52] W. Masood, A. M. Mirza, and M. Hanif, Phys. Plasmas **15**, 072106 (2008).
- [53] W. Masood, A. M. Mirza, S. Nargis and M. Ayub, Phys. Plasmas **16**, 042308 (2009).
- [54] S. V. Vladimirov and K. Ostrikov, Phys. Rep. **393**, 175 (2004).
- [55] I. Levchenko, K. Ostrikov, A. E. Rider, E. Tam, S. V. Vladimirov and S. Xu, Phys. Plasmas **14**, 063502 (2007).
- [56] J. Winter, Plasma Phys. Contr. Fusion **40**, 1201 (1998).
- [57] H. Ikezi, Phys. Fluids **29**, 1764 (1986).
- [58] J. H. Chu and L. I, Phys. Rev. Lett. **72**, 4009 (1994).
- [59] H. Thomas and G. E. Morfill, Nature **379**, 806 (1996).
- [60] S. Ali and P. K. Shukla, Phys. Plasmas **13**, 022313 (2006).
- [61] W. Masood, A. M. Mirza and S. Nargis, Phys. Plasmas **15**, 103703 (2008).
- [62] W. Masood, A. M. Mirza and S. Nargis, J. Plasma Physics **76**, 547 (2010).
- [63] P. K. Shukla and R. K. Varma, Phys. Fluids B **5**, 236 (1993).

- [64] P. K. Shukla and A. A. Mamun, *Introduction to Dusty Plasma Physics* (Institute of Physics: Bristol, U. K., 2002).
- [65] B. Sahu and R. Roychoudhury, Phys. Plasmas **14**, 072310 (2007).
- [66] Ju-Kui Xue, Phys. Plasmas **10**, 4893 (2003).
- [67] W. Masood, M. Saddiq, S. Nargis and A. M. Mirza, Phys. Plasmas **16**, 013705 (2009).
- [68] L. Landau and E. M. Lifshitz, *Statistical Physics* (Oxford University Press, Oxford, 1980), Part 1, p. 167.
- [69] W. Horton, B. Hu, J. Q. Dong and P. Zhu, New J. Physics, **5**, 14 (2003).
- [70] J. G. Charney, Geophys. Public. Nors. Visenkamp. Akad. Oslo, **17**, 3 (1948).
- [71] A. Hasegawa and K. Mima, Phys. of Fluids, **21**, 87 (1978).
- [72] L. Stenflo, Phys. Lett. A **186**, 133 (1994).
- [73] P. K. Shukla, G. T. Birk and R. Bingham, Geophys. Res. Lett. **22**, 671 (1995).
- [74] V. D. Larichev and G. M. Resnik, Dokl. Akad Nauk SSSR, **231**, 1077 (1976).
- [75] M. Salimullah and P. K. Shukla, Phys. Plasmas **5**, 4502 (1998).
- [76] F. C. Michel, Rev. Mod. Phys. **54**, 1 (1982).
- [77] M. C. Begelman, R. D. Blandford and M. D. Rees, Rev. Mod. Phys. **56**, 255 (1984).
- [78] M. J. Rees, Nature **229**, 312 (1971).
- [79] T. Tajima and T. Taniuti, Phys. Rev. A, **42**, 3587 (1990).
- [80] M. E. Gedalin, J. G. Lominadze, L. Stenflo and V. N. Tsitovich, Astrophysics and Space Science **108**, 393 (1985).

- [81] V. I. Berezhiani, L. N. Tsintsadze and P. K. Shukla, J. Plasma Phys. **48**, 139 (1992).
- [82] J. Zhao, J. I. Sakai and K. Nishikawa, Phys. Plasmas **3**, 844 (1996).
- [83] C. M. Surko and T. Murphy. Phys. Fluids B **2**, 1372 (1990).
- [84] V. I. Berezhiani, D. D. Tskhakaya and P. K. Shukla, Phys. Rev. A, **46**, 6608 (1992).
- [85] G. S. Lakhina and B. Buti, Astrophysics and Space Science **79**, 25 (1981).
- [86] F. B. Rizzato, J. Plasma Phys. **40**, 289 (1988).
- [87] S. Hasegawa, S. Irie, S. Usami and Y. Ohsawa, Phys. Plasmas **9**, 2549 (2002).
- [88] M. Y. Yu, Astrophys. Space Sci. **177**, 203 (1985).
- [89] H. R. Mille and P. Witta, *Active Galactic Nuclei* (Springer, Berlin, 1987) p.202.
- [90] F. C. Michel, *Theory of Neutron Star Magnetosphere* (Chicago University Press, Chicago 1991).
- [91] V. Berezhiani, D. D. Tskhakaya, and P. K. Shukla, Phys. Rev. A **46**, 6608 (1992).
- [92] W. Misner, K. Thorne, and J. A. Wheeler, *Gravitation* (Freeman, San Francisco, 1973) p.763.
- [93] M. L. Burns, *Positron-Electron Pairs in Astrophysics*, Edited by M. L. Burns, A. K. Harding, and R. Ramaty (American Institute of Physics, Melville, NY, 1983).
- [94] G. Praburam and J. A. Goree, Astrophys. J. **441**, 830 (1995).
- [95] M. Horanyi and D. A. Mendis, Astrophys. J. **294**, 357 (1985).
- [96] C. K. Geortz, Rev. Geophys. **27**, 271 (1989).
- [97] D. A. Mendis, M. Rosenberg, IEEE Trans. Plasma Sci. **20**, 929 (1992).

- [98] F. Verheest, Space Sci. Rev. **77**, 267 (1996).
- [99] D. A. Mendis, W. H. Wong and M. R. Rosenberg, Phys. Scr., **T113**, 141(2004).
- [100] G. Nishimaru *et al.*, Diamond Relat. Mater. **12**, 374 (2003).
- [101] U. de Angelis, Phys. Plasmas **13**, 012514 (2006).
- [102] A. Barkan, D'Angelo and R. L. Merlino, Planet. Space Sci. **44**, 239 (1996).
- [103] F. MelandsØ, Phys. Plasmas **3**, 3890 (1996).
- [104] F. MelandsØ and P. K. Shukla, Planet. Space Sci. **43**, 635 (1995).
- [105] Q. Z. Luo, N. D'Angelo and R. L. Merlino, Phys. Plasmas **6**, 3455 (1999).
- [106] P. K. Shukla, Phys. Plasmas **8**, 1791 (2001).
- [107] A. P. Misra and A. Roychowdhury, Phys. Plasmas **13**, 062307 (2006).
- [108] M. Leontovich, Izv. Akad. Nauk SSR Ser. Fiz. Mat. Nauk **8**, 16 (1994).
- [109] J. S. Russell, *Report on Waves*, Proc. Royal Society Edinburgh, **319**, 20 (1844).
- [110] Korteweg and de Vries, Phil. Mag. **39**, 422 (1895).
- [111] N. J. Zabusky and M. D. Kruskal, Phys. Rev. Lett. **15**, 240 (1965).
- [112] R. Z. Sagdeev, *Review of Plasma Physics*, edited by M. A. Leontovich (Consultants Bureau, New York, 1966), vol. **4**, p.23.
- [113] H. Washimi and T. Taniuti, Phys. Rev. Lett. **17**, 996 (1966).
- [114] S. Maxon and J. Viecelli, Phys. Rev. Lett. **32**, 4 (1974).
- [115] J. X. Ma and J. Liu, Phys. of Plasmas, **4**, 253 (1997).
- [116] W. Malfliet, Am. J. Phys. **60**, 650 (1992).

- [117] W. Malfliet, J. Comput. Appl. Math. **164**, 529 (2004).
- [118] V. I. Karpman, *Nonlinear Waves in Dispersive Media* (Pergamon, Oxford, 1975).